SUBCELLULAR LOCALIZATION AND ROLE OF POTATO VIRUS X (PVX) TGBp2 AND TGBp3 IN VIRUS MOVEMENT

By

HO-JONG JU

Bachelor of Science in Agronomy
Kon-Kuk University
Seoul, Republic of Korea
1995

Master of Science in Agronomy
University of Georgia
Athens, Georgia
2003

Submitted to the Faculty of the
Graduate College of the
Oklahoma State University
in partial fulfillment of
the requirements for
the Degree of
DOCTOR OF PHILOSOPHY
May, 2007

SUBCELLULAR LOCALIZATION AND ROLE OF POTATO VIRUS X (PVX) TGBp2 AND TGBp3 IN VIRUS MOVEMENT

Dissertation Approved:

Dr. Jeanmarie Verchot-Lubicz

Dissertation Adviser

Dr. Jacqueline Fletcher

Dr. Stephen Marek

Dr. Ulrich Melcher

A. Gordon Emslie

Dean of the Graduate College

ACKNOWLEDGEMENTS

Many people have contributed to my education through their guidance and support throughout my graduate school years. I would like to thank to all those who assisted me through my degree program. I especially want to express my gratitude to my major professor, Dr. Jeanmarie Verchot-Lubicz, who accepted me into her laboratory and supported my scientific endeavors. I appreciate her vast knowledge and her assistance in writing thesis. I also thank toward my committee members Dr. Jacqueline Fletcher, Dr. Stephen Mareck and Dr. Ulrich Melcher, for the advice and time given me. To my lab-mates, Dr. ChangMing Ye, Dr. Timmy Samuel, Teferra Mekuria, and Devinca, thanks for the fun and help. I appreciate Dr. Charlotte Ownby and Terry Coburn. I would like to thank my father (Jaenam Ju) and mother (Soonduck Kim) for the support they provided me through my entire life. I am sorry spending little time with my lovely kids, Seoyeon, Seungyeon, and Chungyeon. In particular, I must acknowledge my wife, Soogyeong Oh If there is no her love and encouragement, I would not have finished this dissertation.

TABLE OF CONTENTS

Chapter Page

I. INTRODUCTION AND REVIEW OF LITERATURE

Potato Virus X (PVX) Taxonomy and Genome Architecture 1

Structure and Function of PD 4

Selective Transport of Proteins and Macromolecules through PD.....6

Tobacco mosaic virus (TMV) Model for Virus Movement across PD 8

Cell-to-Cell Movement of Potexviruses 9

Research Objectives.....15

Literature Cited 17

II. THE POTATO VIRUS X TGBp2 MOVEMENT PROTEIN ASSOCIATES WITH ENDOPLASMIC RETICULUM-DERIVED VESICLES DURING VIRUS INFECTION

Abstract.....25

Introduction.....26

Results.....28

Discussion.....47

Materals and methods 56

Acknowledements.....61

Literature Cited 62

III. MUTATIONS IN THE CENTRAL DOMAIN OF POTATO VIRUS X TGBP2ELIMINATE GRANULAR VESICLES AND VIRUS CELL-TO-CELL TRAFFICKING

Abstract.....71

Introduction.....72

Results.....75

Discussion 100

Materals and methods 105

Acknowledements.....111

Literature Cited 112

IV. MUTATIONS IN TGBP3 DELAY VIRUS CELL-TO-CELL MOVEMENT AND INHIBIT VASCULAR TRANSPORTTRAFFICKING

Abstract 121

Introduction 122

Results 125

Discussion 144

Materals and methods 151

Acknowledements 156

Literature Cited 156

LIST OF TABLES

Table Page

CHAPTER II.

I. Subcellular accumulation of fluorescence in transiently transfected protoplast…….44

CHAPTER III.

I. Oligouncleotide used for mutagenesis of pRTL2-GFP:TGBp2 plasmids.....79

II. Tobacco plants that are systemically infected with modified PVX viruses.....99

CHAPTER IV.

I. Number of plants showing systemic and cell-to-cell movement of recombinant PVX viruses 133

LIST OF FIGURES

Figure Page

CHAPTER I

1. Diagrammatic representation of the PVX genome 2

2. Schematic representations of plant PD 5

3. Models for cell-to-cell movement of TMV and *Potexvirus*.....13

4. Model for *Potexvirus* movement describing sequential events 14

CHAPTER II.

1. Schematic representation of plasmids used in this study.....29

2. Confocal images of protoplasts infected with PVX-GFP:TGBp2 and PVX-GFP 32

3. Confocal images of PVX-GFP and PVX-GFP:TGBp2-infected *N. benthamiana* leaf epidermal cells.....36

4. Fluorometric assays measuring GFP fluorescence in BY-2 protoplasts.....41

5. Confocal images showing subcellular accumulation of fluorescent proteins expressed transiently in BY-2 protoplasts and *N. benthamiana* leaves.....45

6. Model linking the ER stress response with virus movement.....54

Figure Page

CHAPTER III.

1. Diagrammatic representation of plasmids used in this work 76

2. Confocal images of PVX infected tobacco leaves 80

3. Confocal images show fluorescence patterns in virus infected protoplasts.....84

4. Confocal images of tobacco leaf epidermal cells bombarded with pRTL2-GFP:TGBp2 or –GFP:TGBp2m2 and treated with FM4-64 dye……87

5. Confocal images of protoplasts taken between 18 and 24 h post transfection with pRTL2 plasmids 90

6. Bar graphs depict the percentage of protoplasts containing fluorescence in the ER network, granular vesicles, and enlarged vesicles following transfection with pRTL2 plasmids 92

7. Average fluorometric values in a time course analysis of BY-2 protoplasts transfected with pRTL2 plasmids 94

8. Confocal images show protoplasts transfected with mutant pRTL2-GFP:TGBp2 plasmids at 24 h post transfection.....97

CHAPTER IV.

1. Diagrammatic representation of PVX infectious clones and other plasmids used in this study 126

2. Confocal images of tobacco leaf epidermal cells showing subcellular accumulation of TGBp3:GFP 130

3. Confocal images of infection foci on tobacco leaves 137

Figure Page

4. Fluorometric values of the GFP fluorescence in BY-2 …….....141

ABBRIVIATIONIONS

A .....Alanine

ARFs ..... ADP-ribosylation factors

BaMV.....*Bamboo mosaic virus*

BMV .....*Brome mosaic virus*

BSMV ..... *Barley stripe mosaic virus*

CaMV..... *Cauliflower mosaic virus*

CMV .....*Cucumber mosaic virus*

CP .....Coat potein

CPMV ..... *Cowpea mosaic virus*

CS ..... Cytoplasmic sleeve

CW .....Cell wall

D ..... Aspartate

DAPI ..... 4',6-diamino-phenylindole

DDT ..... Dichloro-diphenyl-trichloroethane

Dpi.....Days post inoculation

DsRedST .....DSRed sialyl transferase

DT ..... Desmotubule

E .....Glutamate

EDTA..... Ethylene diamine tetraacetic acid

EGTA ..... Ethylene glycol tetraacetic acid

ER ..... Endoplasmic reticulum

FITC .....fluorescein isothiocyanate

FM4-64 .....(N-(3-triethylammoniumpropyl)-4-(*p*-diethylaminophenylhexatrienyl)-pyridinium dibromide

G .....Glycine

GC .....Gate Closed

GFP .....green fluorescent protein

GLU β-1,3-glucanase

GO ..... Gate Open

GR .....Gating receptor

H .....Histidine

Hpi..... Hours postinoculation

I ..... Isoleucine

K .....Lysine

kDa .....kilo Daltons

KN1 .....KNOTTED1

L .....Leucine

MP ..... Movement protein

NCAP ..... Non-cell-autonomous protein

NtNCAPP1 ..... *N. tabacum* non-cell-autonomous pathway protein 1

NTR..... Nontranslated regions

nts ..... nucleotides

ORF.....Open reading frame

PBS.....Phosphate-buffered saline

PCV..... *Peanut clump virus*

PD.....Plasmodesmata

PM..... Plasma membrane

PMTV..... *Potato mop top virus*

PSLV..... *Poa semilatent virus*

PV..... *Poliovirus*

PVX..... *Potato Virus X*

R..... Alginine

RClNM..... *Red clover necrotic mosaic virus*

RdRp.....RNA dependent RNA polymerase

RER..... Rough endoplasmic reticulum

RNP.....Ribonucleoprotein complex

S..... Serine

sgRNAs.....Subgenomic RNAs

SLE.....Spoke-like extension

ST..... sialyl transferase

T..... Threonine

TEV..... *Tobacco etch virus*

TGB..... Triple gene block

TIP1.....TGBp2 interacting protein 1

TMV..... Tobacco mosaic virus

TYMV ..... *Turnip yellow mosaic v*irus

UV ..... Ultra violet

VRCs ..... Virus replication complexes

VV ..... *Vaccinia virus*

WClMV ..... *White clover mosaic virus*

Y ..... Tyrosine

CHAPTER I

INTRODUCTION AND REVIEW OF LITERATURE

Potato Virus X (PVX) Taxonomy and Genome Architecture

PVX is a member of the genus *Potexvirus* and has a flexuous rod-shaped virion that is 550 nm in length and 11-18 nm in width (Huisman et al., 1988; Adams et al., 2004). PVX virions consist of positive sense, single strand RNA moleculeS of 2.1 X 10^6 M_r and coat protein (CP) (Koeing, 1989). PVX particles aggregate in the cytoplasm of infected cells either in interwoven masses (Kikumoto and Matsui, 1961) or in inclusion bodies, known as X-bodies (Kikumoto and Matsui, 1961; Kozar and Sheludko, 1969). X-bodies contain dense masses of rough endoplasmic reticulum (RER), ribosome-like particles and virus particles (Kozar and Sheludko, 1969).

The PVX genome is approximately 7000 nucleotides (nts) in length, has a methyl-guanosine cap at the 5' end and a poly (A) tail at the 3' end (Huisman et al., 1988); (Skryabin et al., 1988) (Fig. 1). There is a 5' nontranslated region (NTR) that is 84 nts in length and a 3' NTR that is 76 nts in length (Batten et al., 2003). The 5' NTR is involved in regulating genomic and subgenomic RNA (sgRNA) synthesis (Kim and Hemenway, 1996). The 3' NTR interacts with RNA-dependent RNA polymerase at stem-loop D and the poly(A) tail (Huang et al., 2001), suggesting that the 3' NTR is important for viral RNA replication (Cheng and Tsai, 1999; Tsai et al., 1999a; Chen et al., 2005).

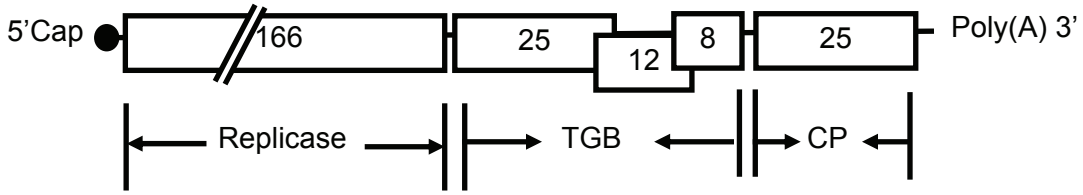

Figure 1. Diagrammatic representation of the PVX genome. The black circle on the left represents the methyl guanosine cap at the 5' end of the PVX genome. The double lines through the replicase indicate that the open reading frame is drawn shorter than to scale. The lines, on each side of the open boxes, indicate non translated nucleotide sequence of the PVX genome. Open boxes indicate each PVX coding region. The molecular weight (in kilo Daltons (kDa)) for each PVX protein is indicated inside each box. The first open reading frame (ORF) encodes the viral replicase. The triple gene block (TGB) consists of three overlapping ORFs named TGBp1, TGBp2, and TGBp3. The last ORF encodes the viral CP.

The PVX genome contains five ORFs (Huisman et al., 1988; Skryabin et al., 1988; Batten et al., 2003). The first ORF encodes a 166 kDa protein that is the viral replicase (Huisman et al., 1988). The replicase protein of *Potexvirus* contains three functional domains (Batten et al., 2003): 1) an N-terminal domain with GTP methyltransferase and guanylyltransferase activities, responsible for addition of the methylguanosine cap at the 5' end of progeny viral genomes (Li et al., 2001a; Huang et al., 2004); 2) an RNA helicase domain that has a G-K-S motif required for ATP hydrolysis (Davenport and Baulcombe, 1997); and 3) C-terminal RNA-dependent RNA polymerase (RdRp) domain that has a G-D-D tripeptide (Li et al., 1998; Brennan et al., 1999). The helicase domain participates in formation of the RNA 5' cap structure and is presumed to contribute to unwinding duplex RNA during the elongation phase of RNA synthesis (Li et al., 2001b). Mutations replacing either the G-D-D or the G-K-S motifs within the replicase eliminate virus replication (Davenport and Baulcombe, 1997; Brennan et al., 1999).

Adjacent to the replicase is TGB, which consists of three overlapping ORFs encoding three viral movement proteins (MPs) (reviewed in Morozov and Solovyev, 2003; Verchot-Lubicz, 2005). The TGB is conserved among viruses belonging to the genera *Potex-, Fovea-, Carla-, Allexi-, Beny-, Hordei-, Peclu-,* and *Pomovirus* (Morozov and Solovyev, 2003). The PVX TGB proteins are named TGBp1, TGBp2, and TGBp3 and have molecular masses of 25 kDa, 12 kDa, and 8 kDa, respectively (Huisman et al., 1988). The PVX TGB proteins are translated from two subgenomic RNAs (sgRNAs) (Verchot et al., 1998). PVX TGBp1 is expressed from the monocistronic sgRNA1, while PVX TGBp2 and TGBp3 are expressed from the bicistronic sgRNA2 (Verchot et al.,

1998). The final PVX ORF encodes a 25 kDa viral CP, which is expressed from sgRNA3 (Rozanov et al., 1990).

Structure and Function of PD

Plant cells communicate with each other through plasmodesmata (PD). PD are specialized intercellular channels that function for the exchange of various molecules including sugars, ribonucleoprotein complexes, transcription factors, and mRNA (reviewed in Zambryski and Crawford, 2000). Electron microscopic studies showed that the plasma membrane (PM), endoplasmic reticulum (ER), and cytoplasm are continuous between cells through the PD (Tilney et al., 1991; Ding et al., 1992b)(Fig. 2). The central structure of PD is the desmotubule (DT) which consists of the ER surrounded by globular proteins (Tilney et al., 1991; Ding et al., 1992b). Globular proteins also line the PM. Spoke-like extension (SLE) extend from the DT to either the PM or globular proteins lining the PM (Tilney et al., 1991; Ding et al., 1992b) (Fig. 2). The cytoplasmic sleeve (CS) is the space between the PM and the DT and its diameter is estimated to be 2.5 nm in the neck region of the PD. Molecules are exchanged between cells by moving through the CS (Ding et al., 1992b) (Fig. 2). The neck region, located at the entrance of the PD, is slightly constricted (Oleson et al., 1979). Several researchers proposed that constriction or expansion of the neck region could regulate transport of molecules between cells (Robards and Lucas, 1990; Citovsky and Zambryski, 1991).

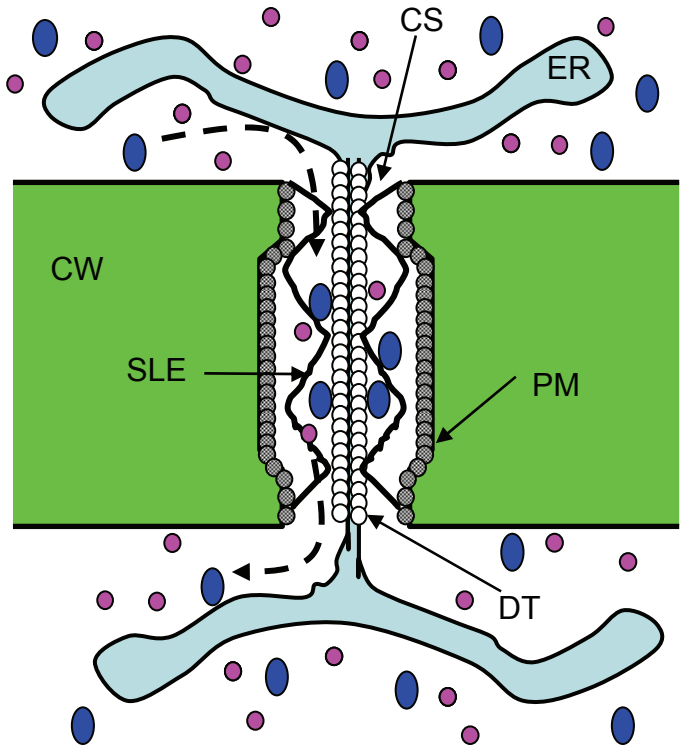

Figure 2. Schematic representations of plant PD. Green boxes represent cell wall (CW). Black lines around the green box represent the PM. The DT is represented by the white balls along the black line in the center of the PD. The white balls represent globular proteins in the DT that have not yet been characterized. The black line within the DT represents the appressed ER. The bent line, which zigzags through the PD, represents the SLE which creates microchannels through the CS. There are speculations that the SLE might control expansion and contraction of the PD. The gray balls along the PM represent globular proteins whose functions are not known. The light blue shape surrounded by the black line represents the ER in adjacent cells. The ER extends into the PD. The dark blue ovals represent macromolecules and pink balls represent low molecular weight molecules. Movement of the molecules through the PD occurs along the CS and is represented by the dashed arrow extending through the PD.

This was recently described as the Gate Open /Gate Closed (GO/GC) pathway (Lucas and Lee, 2004). Specific factors controlling expansion and contraction of the neck region are unknown.

Selective Transport of Proteins and Macromolecules through PD

A number of host proteins that move across PD control plant development. These are termed non-cell-autonomous proteins (NCAPs)(Lucas et al., 1995). In a recent review Lucas and Lee (2004) describe multiple pathways for moving NCAPS across PD. The GO/GC pathway controls movement of molecules based on their molecular weight and dimensions. In this model, large molecules require the GO pathway to diffuse between cells. A GO PD allows molecules of up to 40 kDa in size to diffuse between cells. A GC PD allows molecules of less than 1 kDa to diffuse between cells. This model best explains changes in protein diffusion seen during plant development. Diffusion of large molecules between cells occurs more often in young developing leaves than in mature leaves. For example, Oparka et al. (1999) and Krishnamurthy et al. (2002) showed that during development, young tobacco leaves, which represent photosynthetic sinks, allow diffusion of green fluorescent protein (GFP) between cells, while GFP diffusion is restricted in mature leaves, which are defined as photosynthetic source leaves. GFP, which is approximately 27 kDa in size, is expressed in the cytosol and is free to move across the GO PD, but is restricted from moving across a GC PD. These data led researchers to suggest that PD in young tissues may be dilated, representing the GO pathway, which allows large molecules to move through PD without a specific PD targeting mechanism (Lucas and Lee, 2004).

Another pathway that has been described is the NCAP pathway. The NCAP pathway is similar to the GO pathway in that the PD dilates to allow movement of macromolecules between cells (Lucas and Lee, 2004). The NCAP pathway differs from the GO pathway in that it requires specific proteins to interact with the PD to trigger dilation of the pore. There are two modes of action in the NCAP pathway. In the first mode, a cellular factor (called a GO factor) binds to a gating receptor (GR) at the mouth of the PD. This forms a gating complex which triggers dilation of the PD and allows NCAPs to traffic between cells. Some macromolecules (NCAPs) may be anchored to cellular membranes or targeted to specific sites within the cell. A releasing factor (which has not yet been identified) may dislodge the anchored NCAP, causing the NCAP to become cytosolic and thereby allowing it to diffuse across the PD. In other words, NCAPs normally targeted to a specific subcellular domain, such as the ER, can move across the plasmodesmata when they are exported into the cytoplasm. When the GO/GR complex is formed and the pore is dilated, other cytosolic macromolecules may pass through the PD (Lucas and Lee, 2004).

The second mode of action for the NCAP pathway is determined by the NCAP itself. The NCAP may bind to a carrier protein which then binds to a docking complex at the PD (Lucas and Lee, 2004). Binding of the NCAP/carrier to the docking complex triggers PD dilation. The cargo then is released from the carrier and moves across the PD. The cargo, in this case can be proteins or RNA-protein complexes which interact with the docking complex. Other macromolecules present in the cytoplasm can also diffuse across the PD.

Tobacco mosaic virus (TMV) Model for Virus Movement across PD

TMV encodes a single MP that is 30 kDa in size. This is the best studied movement protein (MP) and has been used as a model to describe cell-to-cell movement of a wide range of plant viruses. The TMV MP cooperatively binds single strand RNA (Citovsky et al., 1992). The TMV MP also dilates PD and traffics the viral RNA into neighboring cells (Deom et al., 1987; Wolf et al., 1989; Wolf et al., 1991). The TMV MP was reported to interact with the actin network and may traffic along actin filaments to reach the plasmodesmata (McLean et al., 1995) The TMV MP also interacts with the ER and colocalizes with the viral replicase and vRNA early in virus infection (Heinlein et al., 1998; Mas and Beachy, 1999; Hirashima and Watanabe, 2003). There are models for TM movement.

First is the TMV MP/NCAP model (Lucas, 2006). In this model the MP/vRNA, ribonucleoprotein complex (RNP) interacts with a cellular carrier which then interacts with the docking complex at the PD (Lucas, 2006). Binding of the MP/vRNA/carrier to the docking complex triggers PD dilation and then the MP/vRNA/carrier complex moves across the PD to adjacent cells. In the receiving cell the carrier protein dissociates from the MP/vRNA/carrier complex. The viral RNA is then translated in the receiving cell, initiating virus infection in that cell (Lucas, 2006).

The role of the TMV replicase, ER and actin networks in virus movement are not explained by the NCAP model. The NCAP model indicates that the MP/vRNA complex moves through the cytoplasm and across the PD. However evidence indicates that the helicase domain of the TMV replicase is required for TMV cell-to-cell movement (Hirashima and Watanabe, 2003), suggesting that it may also be an important component

of the complex that is transported between cells. Immunofluorescence labeling also showed that the TMV replicase and MP colocalize in granular bodies in tobacco protoplasts and leaves. Mutations in the TMV replicase seemed to alter the subcellular accumulation pattern of the TMV MP, suggesting that the subcellular targeting of the TMV MP is affected by the TMV replicase (Liu et al., 2005). Granular bodies containing the TMV replicase, MP, and viral RNA were suggested to move from the perinuclear region to the PD along actin filaments (Kawakami et al., 2004; Liu et al., 2005). In addition, chemical inhibitors disrupting the actin networks also inhibited intracellular movement of these granular bodies as well as TMV cell-to-cell movement (Kawakami et al., 2004; Liu et al., 2005).

Two models were proposed to explain these observations. The first model suggests that membrane bound virus replication complexes (VRCs) containing the TMV MP move along the actin network toward and through the PD (Fig 3A) (Kawakami et al., 2004). Here the VRCs resemble membrane rich bodies budding from the ER (Kawakami et al., 2004). The second model suggests that the VRCs move along the actin network and dock at the PD (Liu et al., 2005). The VRCs in this model are ribonucleoprotien complex (RNP), which remain associated with the ER network as they move through the plasmodesmata (Liu et al., 2005).

Cell-to-Cell Movement of Potexviruses

Potexviruses require three movement proteins (TGBp1, TGBp2, TGBp3) and the viral CP for cell-to-cell movement. TGBp1 is a multifunctional protein. TGBp1 is an RNA helicase and has two canonical ATPase motifs that are G-K-S and D-E-Y

tripeptides. Both motifs are necessary to provide ATP hydrolysis essential to unwind double stranded RNA (Kalinina et al., 1996; Kalinina et al., 2002; Leshchiner et al., 2006). TGBp1 destabilizes PVX virions and promotes translation of virion derived RNA. While PVX virions are not translatable in vitro in the presence of wheat germ extracts, addition of TGBp1 stimulates translation of virion derived RNA (Atabekov et al., 2000; Kiselyova et al., 2003; Rodionova et al., 2003; Karpova et al., 2006). TGBp1 ATPase activity and helicase activity may contribute to unwinding virions for translation; however there is no data yet to indicate this is an in vivo mechanism for translation of virions. Since TGBp1 is not present at the beginning of infection, it was suggested that TGBp1 might act after the virus has moved into neighboring cells as a factor promoting translation of virion derived RNAs (Atabekov et al., 2000; Kiselyova et al., 2003; Rodionova et al., 2003; Karpova et al., 2006). Microinjection and bombardment experiments showed that TGBp1 has the ability to increase plasmodesmal permeability necessary for virus transport through the PD (Angell et al., 1996; Yang et al., 2000; Howard et al., 2004). TGBp1 was shown to suppress RNA silencing. Mutations inhibiting silencing suppressor activity also block virus cell-to-cell movement suggesting that silencing suppression is linked to virus transport (Voinnet et al., 2000; Bayne et al., 2005). Further research is needed to understand how TGBp1 RNA helicase activity, silencing suppression, and virus movement are linked.

The PVX CP was shown using electron microscopy to reside inside plasmodesmata, but it does not trigger dilation of the PD (Oparka et al., 1996). Fibrillar material containing PVX CP was seen using electron microscopy near the mouth of the plasmodesmata, leading some researchers to suggest that either the PVX virion, or an

intermediate form, contributes to virus cell-to-cell movement (Oparka et al., 1996). The 5' NTR of the PVX genome contains a sequence motif recognized by the CP and is required for transport of viral RNA across PD. Lough et al., (2006) proposed that the CP first binds to this sequence motif and recruits TGBp1 to the viral RNA forming the TGBp1/CP/vRNA complex. In vitro RNA binding assays also indicated that TGBp1, CP, and vRNA can form a complex (Lough et al., 1998). Furthermore, mutations in the potexvirus CP that disrupt virion formation have no impact on the ability of the virus to move from cell-to-cell (Lough et al., 2000), lending further support to the hypothesis that TGBp1/CP/vRNA is a ribonucleoprotein (RNP) complex that traffics through PD.

Deleting TGBp2 or TGBp3 from the potexvirus PVX genome restricted virus movement, indicating that these factors contribute to virus export from the cell (Lough et al 2000). Microinjection experiments delivering large fluorescent dextrans or FITC-labeled TGBp1 proteins to transgenic plants expressing TGBp2 and TGBp3 showed that TGBp2 and TGBp3 promote cell-to-cell movement of TGBp1 but do not directly act to increase PD SLE (Lough et al., 1998). These data suggested that TGBp2 and TGBp3 play a role in promoting virus transport to the PD rather than across the PD (Lough et al., 1998). Further experiments showed that the PVX TGBp2 and TGBp3 proteins associate with ER (Krishnamurthy et al., 2003; Mitra et al., 2003). PVX TGBp2 has two transmembrane domains while the PVX TGBp3 has one transmembrane domain (Krishnamurthy et al., 2003; Mitra et al., 2003). Mutations disrupting ER association of TGBp2 or TGBp3 also inhibit virus movement, suggesting that ER association is essential for PVX cell-to-cell transport (Krishnamurthy et al., 2003; Mitra et al., 2003). TGBp2 interacts with a host factor named TIP1 (TGBp2 interacting protein 1), which

regulates activity of β-1,3-glucanase (GLU), which is a key enzyme involved in callose degradation (Fridborg et al., 2003). GLU expression facilitates TMV systemic movement (Bucher et al., 2001). A GLU-deficient mutant showed more callose deposition, inhibiting movement of TMV, PVX and *Cucumber mosaic virus* (CMV) 3a protein (Iglesias and Meins, 2000).

These data led to two models describing potexvirus movement. The first model resembles the NCAP pathway (Fig. 3B). In this model a viral RNP complex consisting of TGBp1, CP, and vRNA moves across PD. The RNP complex interacts with TGBp2 and TGBp3. TGBp2 and TGBp3 associate with a cellular carrier which moves along actin filament carrying the RNP complex to the docking complex at the PD (Lucas, 2006). The RNP complex then dissociates from entire complex and interacts with the docking complex at the PD, triggering PD dilation, thereby allowing the RNP complex to move across the PD into neighboring cells. After movement of the RNP complex across the PD the viral RNA is then translated in the receiving cell, initiating virus replication for the further infection (Lucas, 2006).

The second model was proposed by Verchot-Lubicz (2005) (Fig. 4). In this model the multiple functions of the PVX TGBp1 protein are incorporated in sequential events, early, middle and late events. RNA silencing is a plant anti-viral defense mechanism that inhibits further virus infection. Since PVX TGBp1 has the ability to suppress the anti-viral RNA silencing pathway (Voinnet et al., 2000), TGBp1 might gate

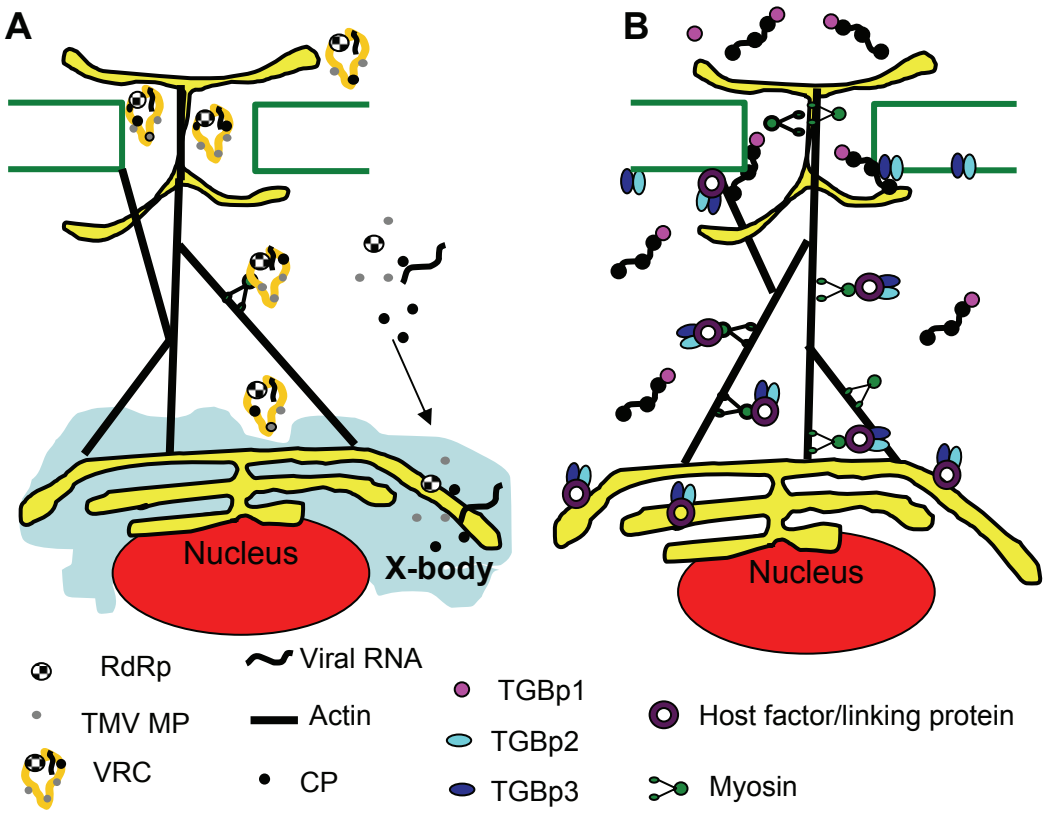

Figure 3. Models for cell-to-cell movement of TMV and *Potexvirus*. A, Model describing the TMV cell-to-cell movement (Kawakami et al., 2004). RdRp, MP viral RNA, and CP are evidenced in the early TMV infection. TMV replication occurs in X-bodies. VRC vesicles are containing the ER membrane, the vRNA, the MP, the replicase, and the CP bud from the X-bodies. These VRCs move along actin filament and across the PD. The irregular blue shape around the nucleus indicates an X-body. B, Model describing *Potexvirus* movement. The CP and the TGBp1 bind to the viral RNA, forming the RNP complex, and move to the PD. Both the TGBp2 and the TGBp3 are associated with ER and move along actin filament to the PD. The RNP complex may not bind to TGBp2 and TGBp3 complex. Both the RNP complex and the TGBp2 and TGBp3 complex move independently to the PD. The RNP complex moves across the PD but the TGBp2 and TGBp3 complex may not move to the adjacent cells (Lucas, 2006).

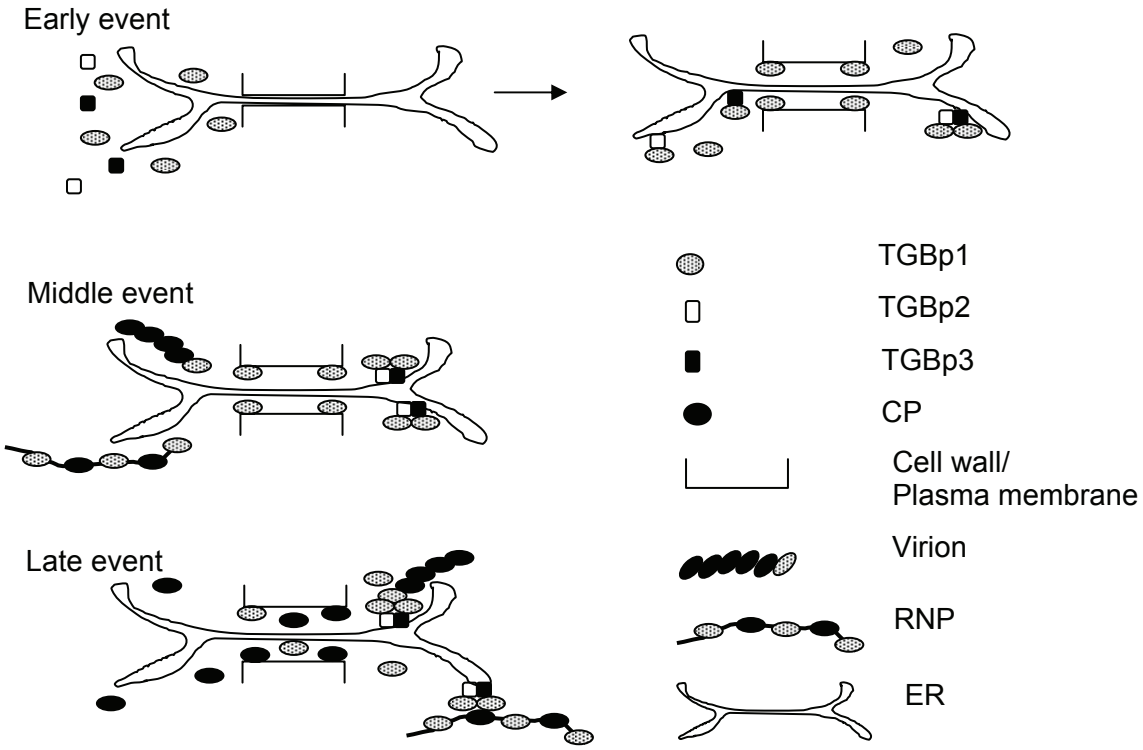

Figure 4. Model for *Potexvirus* movement describing sequential events. The process of virus movement has early, middle, and late events. In early events, TGBp1 increases plasmodesmal permeability due to the presence of TGBp1 inside the PD. Some TGBp1 molecules bind either TGBp2 or TGBp3, and these separate complexes move through the PD. In the middle events, the RNP complexes or the PVX virions move across the PD. In the late event, TGBp1 proteins in the PD dislodge and are replaced by CPs, restoring PD to an undilated state (Verchot-Lubicz, 2005).

plasmodesmata and move from cell-to-cell ahead of virus infection, suppressing the plant anti-viral defense. Thus, suppression of RNA silencing may be linked to promoting virus plasmodesmata transport (Bayne et al., 2005). In the early event, some populations of TGBp1 reside inside the PD to keep it dilated. In the middle events, the RNP complexes or the PVX virions move across the PD. In the late event, TGBp1 proteins in the PD dislodge and are replaced by CPs restoring PD to an undilated state. TGBp1 might function topromote translation of viral RNA present in the RNP complex or virions in the receiving cell (Verchot-Lubicz, 2005).

Research Objectives

When I began this study Krishnamurthy et al (2003) and Mitra et al. (2003), in our laboratory, had shown that the PVX TGBp2 and TGBp3 proteins associate with the ER. In these studies GFP was fused to TGBp2 and TGBp3 and was expressed from the CaMV 35S promoter in tobacco plants. Plasmids were bombarded to tobacco leaves and confocal microscopy was used to study protein accumulation. In addition the GFP:TGBp2 and GFP:TGBp3 fusions were expressed in transgenic tobacco for similar confocal microscopy studies. Krishnamurthy et al (2003) and Mitra et al. (2003) also showed that mutations eliminating ER association of TGBp2 and TGBp3 inhibit virus movement, indicating that the ER is required for PVX movement. The goal of my research was to explore the subcellular accumulation patterns of these proteins during virus infection and to contrast this with prior studies conducted in the absence of virus infection.

The initial objectives of this study were to characterize interactions between the TGB proteins during PVX infection. However during the course of this research, I found that TGBp2 accumulates in novel vesicles that are important for virus cell-to-cell movement. The following chapters of this thesis represent novel findings relating to the PVX TGBp2 and TGBp3 proteins. The chapters are entitled:

1. The PVX TGBp2 movement protein induces vesicles from the endoplasmic reticulum.
2. A central conserved amino acid sequence of PVX TGBp2 is necessary for vesicle formation and virus movement in plants.
3. Mutations in TGBp3 delay virus cell-to-cell movement and inhibit vascular transport.

During the course of this thesis I established BY-2 tobacco suspension cells as a system for studying PVX infection. I also developed an assay using GFP fluorescence to quantitate protein turnover. During the course of my studies we defined novel vesicles induced from ER by the PVX TGBp2 protein. GFP:TGBp2 fusion proteins expressed in ths presence of virus have shorter half-lives than those expressed in the absence of virus. These data suggest that PVX infection triggers the cellular protein degradation machinery that targets GFP:TGBp2. I proposed a model in chapter II to explain the potential link between protein degradation and virus cell-to-cell movement. In chapter III I identified a conserved sequence in TGBp2 that modulates the nature of TGBp2 containing vesicles. Mutations in this conserved sequence changed the vesicle phenotype and inhibited virus movement, indicating that these TGBp2-related vesicles are necessary for virus transport. These observations led to a new model, suggesting that TGBp2 induces novel vesicles required for virus cell-to-cell trafficking. Finally in chapter IV, I present evidence that mutations in the transmembrane domain of TGBp3, which govern TGBp3-ER

association, have a greater effect on virus movement than do mutations in the cytosolic domain of TGBp3, indicating that ER association of TGBp3 is important for virus cell-to-cell movement. Mutations in the C-terminal domain of TGBp3 increase protein turnover but do not hamper virus cell-to-cell movement. Thus, changes in protein stability are not directly related to changes in virus cell-to-cell movement.

LITERATURE CITED

Adams MJ, Antoniw JF, Bar-Joseph M, Brunt AA, Candresse T, Foster GD, Martelli GP, Milne RG, Zavriev SK, Fauquet CM (2004) The new plant virus family *Flexiviridae* and assessment of molecular criteria for species demarcation. Arch Virol **149:** 1045-1060

Angell SM, Davies C, Baulcombe DC (1996) Cell-to-cell movement of *Potato virus X* is associated with a change in the size-exclusion limit of plasmodesmata in trichome cells of *Nicotiana clevelandii*. Virology **216:** 197-201

Atabekov JG, Rodionova NP, Karpova OV, Kozlovsky SV, Poljakov VY (2000) The movement protein-triggered in situ conversion of *Potato virus X* virion RNA from a nontranslatable into a translatable form. Virology **271:** 259-263

Batten JS, Yoshinar S, Hemenway C (2003) *Potato virus X*: a model system for virus replication, movement, and gene expression. Mol Plant Pathol **4:** 125-131

Bayne EH, Rakitina DV, Morozov SY, Baulcombe DC (2005) Cell-to-cell movement of *Potato potexvirus X* is dependent on suppression of RNA silencing. Plant J **44:** 471-482

Brennan FR, Jones TD, Longstaff M, Chapman S, Bellaby T, Smith H, Xu F, Hamilton WD, Flock JI (1999) Immunogenicity of peptides derived from a fibronectin-binding protein of *S. aureu*s expressed on two different plant viruses. Vaccine **17:** 1846-1857

Bucher GL, Tarina C, Heinlein M, Di Serio F, Meins F, Jr., Iglesias VA (2001) Local expression of enzymatically active class I beta-1, 3-glucanase enhances symptoms of TMV infection in tobacco. Plant J **28:** 361-369

Chen IH, Chou WJ, Lee PY, Hsu YH, Tsai CH (2005) The AAUAAA motif of bamboo mosaic virus RNA is involved in minus-strand RNA synthesis and plus-strand RNA polyadenylation. J Virol **79:** 14555-14561

Cheng CP, Tsai CH (1999) Structural and functional analysis of the 3' untranslated region of *Bamboo mosaic potexvirus* genomic RNA. J Mol Biol **288:** 555-565

Citovsky V, Wong ML, Shaw AL, Prasad BV, Zambryski P (1992) Visualization and characterization of *Tobacco mosaic virus* movement protein binding to single-stranded nucleic acids. Plant Cell **4:** 397-411

Citovsky V, Zambryski P (1991) How do plant virus nucleic acids move through intercellular connections? Bioessays **13:** 373-379

Davenport GF, Baulcombe DC (1997) Mutation of the GKS motif of the RNA-dependent RNA polymerase from *Potato virus X* disables or eliminates virus replication. J Gen Virol **78:** 1247-1251

Deom CM, Oiver MJ, Beachy RN (1987) The 30-kilodalton gene product of *Tobacco mosaic virus* potentiates virus movement. Science **237:** 384-389

Ding B, Turgeon R, Parthasarathy MV (1992b) Substructure of freeze-substituted plasmodesmata. Protoplasma **169:** 28-41

Fridborg I, Grainger J, Page A, Coleman M, Findlay K, Angell S (2003) TIP, a novel host factor linking callose degradation with the cell-to-cell movement of P*otato virus X*. Mol Plant Microbe Interact **16:** 132-140

Heinlein M, Padgett HS, Gens JS, Pickard BG, Casper SJ, Epel BL, Beachy RN (1998) Changing patterns of localization of the T*obacco mosaic virus* movement protein and replicase to the endoplasmic reticulum and microtubules during infection. Plant Cell **10:** 1107-1120

Hirashima K, Watanabe Y (2003) RNA helicase domain of *tobamovirus* replicase executes cell-to-cell movement possibly through collaboration with its nonconserved region. J Virol **77:** 12357-12362

Howard AR, Heppler ML, Ju H-J, Krishnamurthy K, Payton ME, Verchot-Lubicz J (2004) *Potato virus X* TGBp1 induces plasmodesmata gating and moves between cells in several host species whereas CP moves only in *N. benthamiana* leaves. Virology **328:** 185-197

Huang CY, Huang YL, Meng M, Hsu YH, Tsai CH (2001) Sequences at the 3' untranslated region of *Bamboo mosaic potexvirus* RNA interact with the viral RNA-dependent RNA polymerase. J Virol **75:** 2818-2824

Huang YL, Han YT, Chang YT, Hsu YH, Meng M (2004) Critical residues for GTP methylation and formation of the covalent m7GMP-enzyme intermediate in the capping enzyme domain of *Bamboo mosaic virus*. J Virol **78:** 1271-1280

Huisman MJ, Linthorst HJ, Bol JF, Cornelissen JC (1988) The complete nucleotide sequence of *Potato virus X* and its homologies at the amino acid level with various plus-stranded RNA viruses. J Gen Virol **69:** 1789-1798

Iglesias VA, Meins F, Jr. (2000) Movement of plant viruses is delayed in a beta-1,3-glucanase-deficient mutant showing a reduced plasmodesmatal size exclusion limit and enhanced callose deposition. Plant J **21:** 157-166

Kalinina NO, Fedorkin ON, Samuilova OV, Maiss E, Korpela T, Morozov S, Atabekov JG (1996) Expression and biochemical analyses of the recombinant *Potato virus X* 25K movement protein. FEBS Lett **397:** 75-78

Kalinina NO, Rakitina DV, Solovyev AG, Schiemann J, Morozov SY (2002) RNA helicase activity of the plant virus movement proteins encoded by the first gene of the triple gene block. Virology **296:** 321-329

Karpova OV, Zayakina OV, Arkhipenko MV, Sheval EV, Kiselyova OI, Poljakov VY, Yaminsky IV, Rodionova NP, Atabekov JG (2006) *Potato virus X* RNA-mediated assembly of single-tailed ternary 'coat protein-RNA-movement protein' complexes. J Gen Virol **87:** 2731-2740

Kawakami S, Watanabe Y, Beachy RN (2004) Tobacco mosaic virus infection spreads cell to cell as intact replication complexes. Proc Natl Acad Sci U S A **101:** 6291-6296

Kikumoto T, Matsui C (1961) Electron microscopy of intracellular *Potato virus X*. Virology **13:** 294-299

Kim KH, Hemenway C (1996) The 5' nontranslated region of *Potato virus X* RNA affects both genomic and subgenomic RNA synthesis. J Virol **70:** 5533-5540

Kiselyova OI, Yaminsky IV, Karpova OV, Rodionova NP, Kozlovsky SV, Arkhipenko MV, Atabekov JG (2003) AFM Study of *Potato Virus X* Disassembly induced by movement protein. J Mol Biol **332:** 321-325

Koeing RaL, D.E. (1989) *Potato virus X In* AAB descriptions of plant viuses., Vol No. 354

Kozar FE, Sheludko YM (1969) Ultrastructure of potato and *Datura stramonium* plant cells infected with *Potato virus X*. Virology **38:** 220-229

Krishnamurthy K, Heppler M, Mitra R, Blancaflor E, Payton M, Nelson RS, Verchot-Lubicz J (2003) The *Potato virus X* TGBp3 protein associates with the ER network for virus cell-to-cell movement. Virology **309:** 135-151

Leshchiner AD, Solovyev AG, Morozov SY, Kalinina NO (2006) A minimal region in the NTPase/helicase domain of the TGBp1 plant virus movement protein is responsible for ATPase activity and cooperative RNA binding. J Gen Virol **87:** 3087-3095

Li YI, Chen YJ, Hsu YH, Meng M (2001a) Characterization of the AdoMet-dependent guanylyltransferase activity that is associated with the N terminus of *Bamboo mosaic virus* replicase. J Virol **75:** 782-788

Li YI, Cheng YM, Huang YL, Tsai CH, Hsu YH, Meng M (1998) Identification and characterization of the *Escherichia coli*-expressed RNA-dependent RNA polymerase of bamboo mosaic virus. J Virol **72:** 10093-10099

Li YI, Shih TW, Hsu YH, Han YT, Huang YL, Meng M (2001b) The helicase-like domain of plant *potexvirus* replicase participates in formation of RNA 5' cap structure by exhibiting RNA 5'-triphosphatase activity. J Virol **75:** 12114-12120

Liu JZ, Blancaflor EB, Nelson RS (2005) The *Tobacco mosaic virus* 126-kilodalton protein, a constituent of the virus replication complex, alone or within the complex aligns with and traffics along microfilaments. Plant Physiol **138:** 1853-1865

Lucas WJ (2006) Plant viral movement proteins: Agents for cell-to-cell trafficking of viral genomes. Virology **344:** 169-184

Lucas WJ, Bouche-Pillon S, Jackson DP, Nguyen L, Baker L, Ding B, Hake S (1995) Selective trafficking of KNOTTED1 homeodomain protein and its mRNA through plasmodesmata. Science **270:** 1980-1983

Lucas WJ, Lee JY (2004) Plasmodesmata as a supracellular control network in plants. Nat Rev Mol Cell Biol **5:** 712-726

Mas P, Beachy RN (1999) Replication of *Tobacco mosaic virus* on endoplasmic reticulum and role of the cytoskeleton and virus movement protein in intracellular distribution of viral RNA. J Cell Biol **147:** 945-958

McLean BG, Zupan J, Zambryski PC (1995) *Tobacco mosaic virus* movement protein associates with the cytoskeleton in tobacco cells. Plant Cell **7:** 2101-2114

Mitra R, Krishnamurthy K, Blancaflor E, Payton M, Nelson RS, Verchot-Lubicz J (2003) The *Potato virus X* TGBp2 protein association with the endoplasmic reticulum plays a role in but is not sufficient for viral cell-to-cell movement. Virology **312:** 35-48

Morozov SY, Solovyev AG (2003) Triple gene block: modular design of a multifunctional machine for plant virus movement. J Gen Virol **84:** 1351-1366

Oparka KJ, Roberts AG, Roberts IM, Prior DAM, SantaCruz S (1996) Viral coat protein is targeted to, but does not gate, plasmodesmata during cell-to-cell movement of *Potato virus X*. Plant J **10:** 805-813

Oparka KJ, Roberts AG, Boevink P, Santa Cruz S, Roberts I, Pradel KS, Imlau A, Kotlizky G, Sauer N, Epel B (1999) Simple, but not branched, plasmodesmata allow the nonspecific trafficking of proteins in developing tobacco leaves. Cell **97:** 743–754

Robards AW, Lucas WJ (1990) Plasmodesmata. Annu. Rev. Plant Physiol. Plant Mol. Biol. **41:** 369-419

Rodionova NP, Karpova OV, Kozlovsky SV, Zayakina OV, Arkhipenko MV, Atabekov JG (2003) Linear remodeling of helical virus by movement protein binding. J Mol Biol **333:** 565-572

Rozanov MN, Morozov SY, Skryabin KG (1990) Unexpected close relationship between the large nonvirion proteins of filamentous potexviruses and spherical tymoviruses. Virus Genes **3:** 373-379

Skryabin KG, Kraev AS, Morozov S, Rozanov MN, Chernov BK, Lukasheva LI, Atabekov JG (1988) The nucleotide sequence of *Potato virus X* RNA. Nucleic Acids Res **16:** 10929-10930

Tilney LG, Cooke TJ, Connelly PS, Tilney MS (1991) The structure of plasmodesmata as revealed by plasmolysis, detergent extraction, and protease digestion. J Cell Biol **112:** 739-747

Tsai CH, Cheng CP, Peng CW, Lin BY, Lin NS, Hsu YH (1999a) Sufficient length of a poly(A) tail for the formation of a potential pseudoknot is required for efficient replication of bamboo mosaic potexvirus RNA. J Virol **73:** 2703-2709

Verchot-Lubicz J (2005) A new cell-to-cell transport model for *Potexviruses*. Mol Plant Microbe Interact **18:** 283-290

Verchot J, Angell SM, Baulcombe DC (1998) In vivo translation of the triple gene block of *Potato virus X* requires two subgenomic mRNAs. J Virol **72:** 8316-8320

Voinnet O, Lederer C, Baulcombe DC (2000) A viral movement protein prevents spread of the gene silencing signal in *Nicotiana benthamiana*. Cell **103:** 157-167

Wolf S, Deom CM, Beachy R, Lucas WJ (1991) Plasmodesmatal function is probed using transgenic tobacco plants that express a virus movement protein. Plant Cell **3:** 593-604

Wolf S, Deom CM, Beachy RN, Lucas WJ (1989) Movement protein of *Tobacco mosaic virus* modifies plasmodesmatal size exclusion limit. Science **246:** 377-379

Yang Y, Ding B, Baulcombe DC, Verchot J (2000) Cell-to-cell movement of the 25K protein of *Potato virus X* is regulated by three other viral proteins. Mol Plant Microbe Interact **13:** 599-605

CHAPTER II

THE POTATO VIRUS X TGBp2 MOVEMENT PROTEIN ASSOCIATES WITH ENDOPLASMIC RETICULUM-DERIVED VESICLES DURING VIRUS INFECTION

Published in 2005, Aug Plant Physiology

ABSTRACT

The green fluorescent protein (GFP) gene was fused to the *Potato virus X* (PVX) TGBp2 gene, inserted into either the PVX infectious clone or pRTL2 plasmids, and used to study protein subcellular targeting. In plants and protoplasts inoculated with PVX-GFP:TGBp2 or transfected with pRTL2-GFP:TGBp2, fluorescence was mainly in vesicles and the endoplasmic reticulum (ER). For comparison, plasmids expressing GFP fused to TGBp3 were transfected to protoplasts, bombarded to tobacco leaves, and studied in transgenic leaves. The GFP:TGBp3 proteins were associated mainly with the ER and did not cause obvious changes in the endomembrane architecture, suggesting that the vesicles reported in GFP:TGBp2 studies were induced by the PVX TGBp2 protein. During late stages of virus infection, fluorescence became increasingly cytosolic and nuclear. Protoplasts transfected with PVX-GFP:TGBp2 or pRTL2-GFP:TGBp2 were treated with cycloheximide and the decline of GFP fluorescence was greater in virus-infected protoplasts than in pRTL2-GFP:TGBp2-transfected protoplasts. Thus, protein

instability is enhanced in virus-infected protoplasts, which may account for the cytosolic and nuclear fluorescence during late stages of infection. Supporting experiments using electron and confocal microscopy showed that the label was associated with the ER and vesicles, but not the Golgi apparatus. The TGBp2-induced vesicles appeared to be ER derived and associated with actin filaments. We propose a model in which reorganization of the ER and increased protein degradation is linked to plasmodesmata gating.

INTRODUCTION

Plant viruses use the cellular endomembrane system to support virus replication (Schaad et al., 1997; Reichel and Beachy, 1998; Carette et al., 2002a, 2002b; Schwartz et al., 2002). Among positive-strand RNA viruses, the viral replicase is typically anchored to membranes associated with the endoplasmic reticulum (ER), the endocytic pathway, or cellular organelles (Rubino and Russo, 1998; Mas and Beachy, 1999; Rubino et al., 2001; Schwartz et al., 2002, 2004). Many viral replication-associated proteins cause reorganization of cellular membranes with the purpose of creating centers that protect the viral replication complexes (VRCs) from cellular nucleases and host defenses (Schwartz et al., 2002, 2004; Ding et al., 2004). Specifically, the replication complexes of plant viruses belonging to the genera *Potyvirus, Comovirus, Dianthovirus, Pecluviru*s, and *Bromovirus* cause proliferation and vesiculation of either the perinuclear or the cortical ER (Schaad et al., 1997; Dunoyer et al., 2002; Lee and Ahlquist, 2003). The replicases of *Cowpea mosaic virus* and *Red clover necrotic mosaic virus* induce ER proliferation (Carette et al., 2002a, 2002b; Turner et al., 2004). The best-studied example is the *Brome*

mosaic virus (BMV) 1a replicase, which localizes to the ER and induces membrane invaginations to form spherules (Lee and Ahlquist, 2003). These invaginations, or spherules, are centers for virus replication and contain the BMV 2a protein and viral RNA (Schwartz et al., 2004). It was suggested that the BMV-induced spherules resemble budding retrovirus cores and that these membrane invaginations containing VRCs have a place in virus evolution (Schwartz et al., 2002, 2004).

Recent information supports the involvement of the endomembrane system in virus intracellular and intercellular movement (for review, see Reichel and Beachy, 1998, 2000; Morozov and Solovyev, 2003; Nelson, 2005; Verchot-Lubicz, 2005). For example, the tobacco mosaic virus (TMV) membrane-bound replication complexes were reported to traffic along the microfilament network with the cell (Liu et al., 2005) and then move from cell to cell through the plasmodesmata (Kawakami et al., 2004). The 126- and 183-kD proteins of TMV aid in forming, and are present in, the ER-derived VRCs (Heinlein et al., 1998; Szecsi et al., 1999; Kawakami et al., 2004; Liu et al., 2005). The TMV movement protein associates with the VRCs and is required to transport the VRCs across plasmodesmata (Heinlein et al., 1998; Mas and Beachy, 1999; Szecsi et al., 1999; Liu et al., 2005).

Potato virus X (PVX) encodes three movement proteins from a genetic module of three overlapping open reading frames (ORFs), termed the triple gene block. These triple gene block proteins, named TGBp1, TGBp2, and TGBp3, have molecular masses of roughly 25, 12, and 8 kD (Huisman et al., 1988). The PVX TGBp1 protein is a suppressor of gene silencing, an RNA helicase, and gates plasmodesmata (Rouleau et al., 1994; Brigneti et al., 1998; Howard et al., 2004). The TGBp2 and TGBp3 proteins

associate with the ER. The results of mutational analyses showed that the association of TGBp2 and TGBp3 proteins with the ER is important for virus infection (Krishnamurthy et al., 2003; Mitra et al., 2003). The PVX coat protein also plays a role in virus movement (Spillane et al., 1997).

In this study, the green fluorescent protein (GFP) gene was fused to the PVX TGBp2 gene to study protein subcellular targeting during virus infection. Time-course experiments were conducted in tobacco protoplasts and leaves to examine the association of the GFP:TGBp2 protein with the ER network during the course of virus infection. We present evidence that the PVX TGBp2 protein, similar to many viral membrane-associated proteins, induces formation of vesicles from the ER. In addition, the PVX TGBp3 protein also associates with the ER. Last, we present evidence that TGBp2-induced vesicles associate with the actin network and are unrelated to the Golgi apparatus.

RESULTS

GFP:TGBp2 Associates with Cellular Membranes during Virus Infection in Protoplasts

The PVX-GFP infectious clone (Fig. 1) expresses the GFP gene from a duplicated coat protein subgenomic promoter. GFP is used as a visual marker to follow virus infection over time. The GFP:TGBp2 fused genes were inserted into the PVX genome in place of the GFP gene to study TGBp2 protein subcellular targeting during virus infection (Fig. 1). Most of the endogenous TGBp2 gene was deleted from the PVX-GFP:TGBp2 infectious clone (Verchot et al., 1998; Fig. 1), and the GFP:TGBp2 fusion provides a functional replacement for the deleted gene.

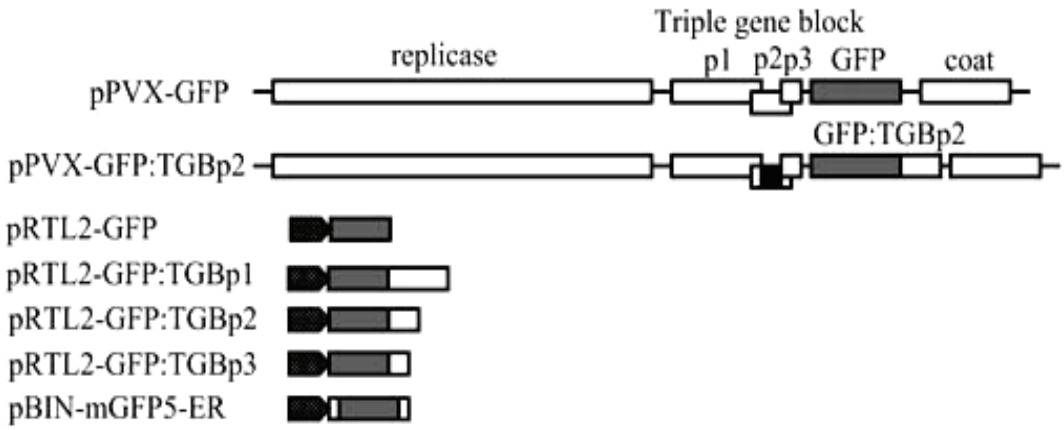

Figure 1. Schematic representation of plasmids used in this study. The pPVX-GFP and pPVX-GFP:TGBp2 plasmids contain the entire PVX genome. The white boxes in these schematics represent the PVX ORFs or subcellular targeting signals, and the lines represent noncoding regions. The names for each PVX gene are indicated above the boxes. The GFP gene (gray box) or GFP:TGBp2-fused genes were inserted into the PVX genome. In the pPVX-GFP:TGBp2 plasmid, a large portion of the endogenous TGBp2 coding sequence was deleted from the PVX genome (indicated by a black box). Four pRTL2 plasmids expressed GFP alone (gray box) or fused to the 5'-end of the PVX TGBp1, TGBp2, or TGBp3 genes (white boxes). The pBIN-mGFP5-ER has sequences encoding ER-targeting and retention signals fused to the 5'- and 3'-ends of the GFP gene. All pRTL2, pBIN, and pCambia1300 plasmids contain a CaMV 35S promoter (black spotted arrows).

Infectious PVX-GFP and PVX-GFP:TGBp2 transcripts were inoculated to BY-2 protoplasts, and the subcellular distribution of fluorescence was studied at 18, 24, 36, 48, and 72 h postinoculation (hpi) using confocal microscopy. In PVX-GFP-inoculated protoplasts, fluorescence was mainly cytosolic and nuclear, with no obvious change in the

We quantified the patterns of GFP:TGBp2 protein fluorescence to determine whether the subcellular distribution of GFP:TGBp2 fluorescence changes over time. Thirty protoplasts were scored at each time point for fluorescence associated with the vesicles, nucleus, and/or cytosol (Fig. 2J). The proportion of protoplasts containing GFP:TGBp2 fluorescence in vesicles was 80% at 18 hpi and declined to 27% by 48 hpi. This level was maintained through 72 hpi (Fig. 2J). The proportions of protoplasts containing GFP:TGBp2 fluorescence in the cytosol and nucleus were 40% at 18 hpi and increased to 80% and 90% at 48 and 72 hpi, respectively (Fig. 2J). Thus, GFP:TGBp2 fluorescence associates mainly with vesicles early in virus infection, but increasingly with the cytosol and nucleus as infection progresses (Fig. 2J).

Statistical analyses were performed by Dr. Mark Payton (Statistics Department, OSU) using the data represented in Figure 2 J and K, to determine whether the subcellular distribution of fluorescence in PVX-GFP:TGBp2- and PVX-GFP-infected protoplasts is regulated over time. Time is a likely variable in studying protein subcellular trafficking. If the TGBp2 proteins traffic from one location to another in the cell, then changes in the distribution of GFP:TGBp2 fluorescence within the cell over time would not be random. For example, movement of the GFP:TGBp2 proteins from vesicles into the cytosol may be regulated by the host degradation machinery. Since GFP:TGBp2 is an ER-associated

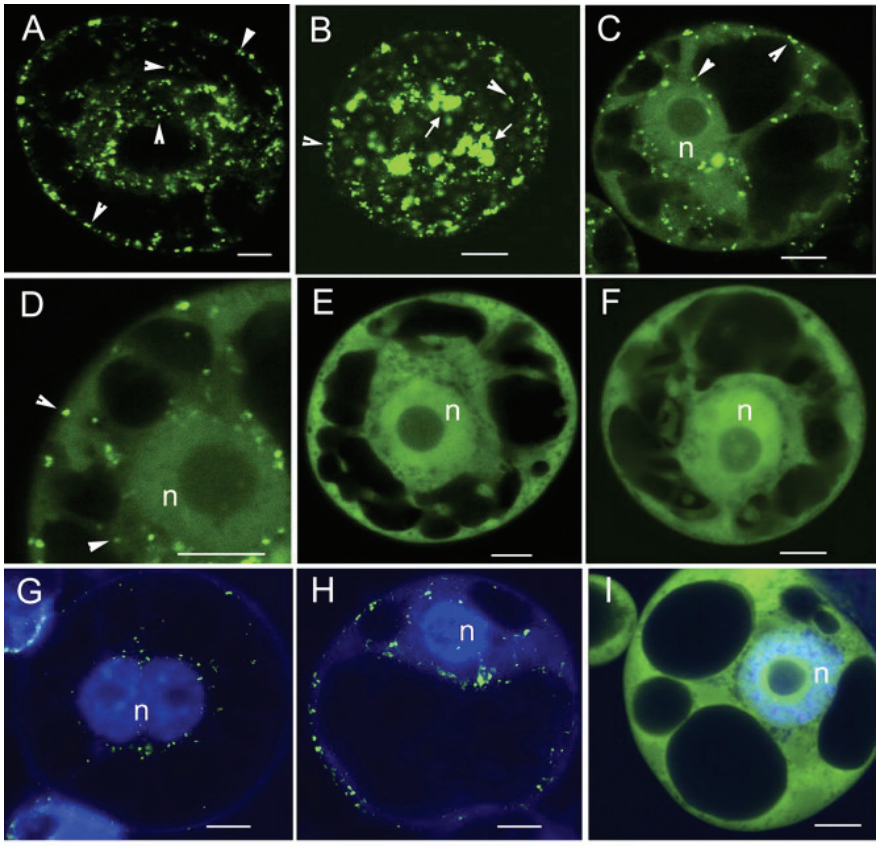
A
B
C
D
E
F
G
H
I
n

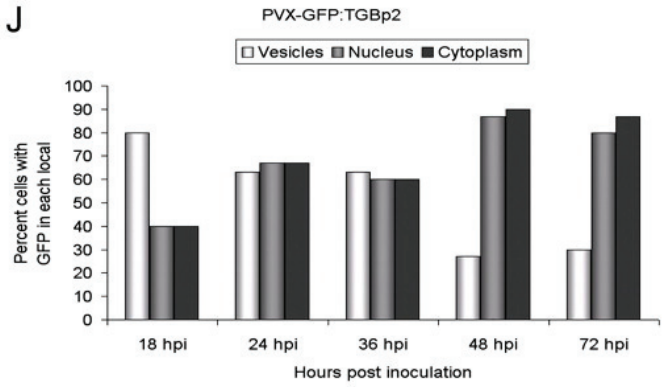
J
PVX-GFP:TGBp2
Vesicles
Nucleus
Cytoplasm
Percent cells with GFP in each local
100
90
80
70
60
50
40
30
20
10
0
18 hpi
24 hpi
36 hpi
48 hpi
72 hpi
Hours post inoculation

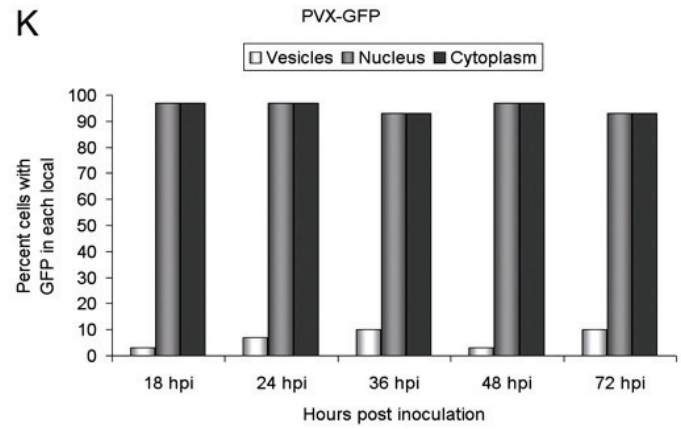
K
PVX-GFP
Vesicles
Nucleus
Cytoplasm
Percent cells with GFP in each local
100
90
80
70
60
50
40
30
20
10
0
18 hpi
24 hpi
36 hpi
48 hpi
72 hpi
Hours post inoculation

Figure 2. Confocal images of protoplasts infected with PVX-GFP:TGBp2 and PVX-GFP. A to C, PVX-GFP:TGBp2-infected protoplasts show fluorescence in vesicles (A); vesicles and aggregates of vesicles (B); and vesicles, nucleus (n), and cytoplasm (C). D, A magnified portion of the protoplast presented in C. Vesicles appear along the plasma membrane and surrounding the nucleus. E and F, PVX-GFP:TGBp2 (E) and PVX-GFP-infected protoplast (F) show nuclear and cytoplasmic fluorescence. G to I, DAPI-stained protoplasts infected with PVX-GFP:TGBp2. G, Dividing protoplasts have two adjacent nuclei stained with DAPI. GFP fluorescent vesicles surround the nuclei in G and H. I, DAPI-stained cell shows GFP:TGBp2 in the nucleus and cytoplasm. Bars in each photograph represent 10 μm. J, Thirty protoplasts were scored for the presence of fluorescence in vesicles, nucleus, and cytoplasm in PVX-GFP:TGBp2-infected protoplasts at 18, 24, 36, 48, and 72 hpi. K, thirty protoplasts were scored for the presence of fluorescence in vesicles, nucleus, and cytoplasm in PVX-GFP-infected protoplasts at 18, 24, 36, 48, and 72 hpi. Bars represent the percentage of protoplasts having fluorescence in each subcellular compartment at each time point. Between 1% and 10% of protoplasts at each time point contained GFP in vesicles resembling those seen in the PVX-GFP:TGBp2-infected cells. Logistic regressions were conducted using data in J and K and reported in "Results."

protein, it is possible that ER stress stimulates export of the GFP:TGBp2 proteins to the cytosol for degradation by the 26S proteasome. It is also possible that movement of the GFP:TGBp2 proteins would be regulated and not random if it is controlled by interactions with other PVX proteins.

Therefore, Dr. Mark Payton (Statistics Department, OSU) employed a logistic regression to test whether time is a variable in the subcellular accumulation patterns of GFP:TGBp2 and GFP fluorescence. The presence/absence of fluorescence in each subcellular address (vesicle, nucleus, and cytoplasm; dependent variable) were compared over time (independent variable). We hypothesized that the observed changes in the distribution of GFP:TGBp2 proteins over time would indicate subcellular trafficking of the fusion protein. If time is not a variable controlling the distribution of fluorescence within the cell, then statistical analyses would indicate that the distribution of protein in each subcellular address is independent of time (i.e. random) and no correlation would exist. Slope estimates and *P* values were determined. A nonsignificant slope (i.e. large *P* value) indicates no relationship to time. Conversely, a significant slope (i.e. small *P* value) indicates the response is affected by time. A negative slope indicates a decreased presence of fluorescence in each address over time, and a positive slope indicates an increase of fluorescence in each address over time. For PVX-GFP:TGBp2, the slope values for vesicles, nucleus, and cytoplasm were –0.0367, 0.0313, and 0.0463, respectively. The *P* values were 0.0001, 0.0014, and 0.0001, respectively. The negative slope for PVX-GFP:TGBp2 in vesicles indicates that fluorescence decreased in these locations over time. The positive slope for PVX-GFP:TGBp2 in the cytoplasm and nucleus indicates fluorescence increased in these locations over time. The extremely low

P values indicate that changes in subcellular targeting of GFP:TGBp2 proteins over time were significant. For PVX-GFP, the slope values for vesicles, nucleus, and cytoplasm were 0.0145, –0.0155, and –0.0155, respectively. The *P* values were 0.3631, 0.4009, and 0.4009, respectively. The nonsignificant slopes and high *P* values for PVX-GFP indicate that the change in fluorescence at each subcellular address had no relationship to time and was random. Thus, statistical analysis supports the hypothesis that GFP:TGBp2 proteins first resided in vesicles and over time became increasingly cytosolic and nuclear.

Subcellular Targeting of GFP:TGBp2 during Virus Infection of Tobacco Leaves

PVX-GFP and PVX-GFP:TGBp2 transcripts were inoculated to tobacco leaves and fluorescence was examined between 2 and 5 d post inoculation (dpi) to determine whether the pattern of fluorescence observed in tobacco leaves resembles the pattern reported in protoplasts. Within a single infection focus, cells were viewed early and late during virus infection. The intracellular fluorescence patterns located at the leading edge and at the center of infection foci were compared to determine whether the subcellular distribution of fluorescence changed as infections developed. Since tobacco leaf cells are not synchronously infected, we could not use statistical methods to assess changes in the distribution of GFP or GFP:TGBp2 proteins over time.

In PVX-GFP-inoculated leaves, the patterns of fluorescence at the leading edge and at the center of the infection foci were similar. Fluorescence was observed in the cytosol, nucleus, and perinuclear inclusion bodies (Fig. 3, A and B). Sometimes it was difficult to discriminate between GFP fluorescence inside the nucleus and perinuclear inclusion bodies. These inclusion bodies are likely X-bodies described in early literature

as masses containing virus particles, ER, and ribosomes (Kikumoto and Matsui, 1961; Kozar and Sheludko, 1969; Allison and Shalla, 1973). Based on previous reports describing formation of X-bodies (Kikumoto and Matsui, 1961; Kozar and Sheludko, 1969; Allison and Shalla, 1973; Espinoza et al., 1991), we postulate the strands extending from these X-bodies to the plasma membrane (Fig. 3, A and B) to be ER derived.

PVX-GFP:TGBp2 infection foci were observed from 2 to 5 dpi. Fluorescence was associated with the ER network and vesicles in all infected cells. Perinuclear inclusion bodies were observed in all infected cells (Fig. 3, C–E). Vesicles appeared to move along the ER strands in tobacco epidermal cells (data not shown). A thick band of cytosolic fluorescence was evident in cells located at the center of infection, but was less obvious at the leading edge of infection. Although the intensity of fluorescence was weaker at the leading edge of infection, the patterns of fluorescence in the ER network and vesicles at this location were similar to those observed in cells at the center of the infection foci (Fig. 3, C–F). Single optical cross-sections taken through the middle of infected cells revealed vesicles lining the cell wall (Fig. 3, E and F). These vesicles were sometimes twin structures along the walls of adjacent cells and resemble the peripheral bodies reported to occur in *Beet necrotic yellow vein virus* (BNYVV; a benyvirus), *Potato mop top* (PMTV; a pomovirus) or the *Poa semilatent virus* (PSLV; a hordeivirus; Erhardt et al., 2000; Solovyev et al., 2000; Gorshkova et al., 2003; Zamyatnin et al., 2004; Haupt et al., 2005) infected cells.

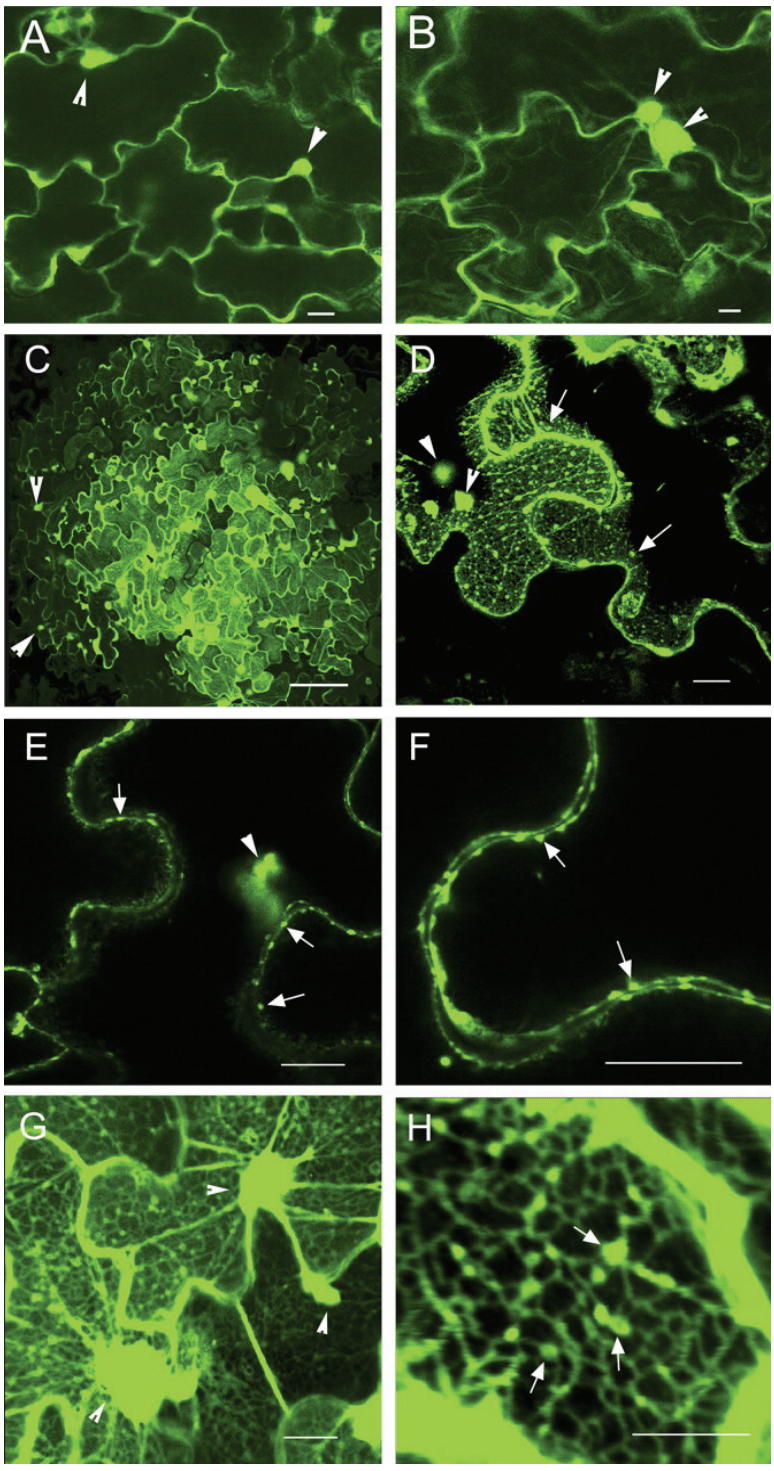

Figure 3. Confocal images of PVX-GFP and PVX-GFP:TGBp2-infected *N. benthamiana* leaf epidermal cells. A and B, PVX-GFP-infected cells at 2 and 6 dpi, respectively. Green fluorescence is present in the cytoplasm and nucleus. There were also

perinuclear inclusion bodies that, on occasion, seemed to surround the nucleus. Since the perinuclear inclusions often overlap the nucleus, single arrowheads point to both structures in all images. C to G, PVX-GFP:TGBp2-infected cells at 2 or 4 dpi. Single arrowheads point to inclusion bodies and arrows point to vesicles. C, Image of a PVX-GFP:TGBp2 infection focus taken at low magnification at 4 dpi. D, Image of cells located at the front of an infection focus. Fluorescence was evident in the ER network, vesicles, and inclusion bodies. E and F, Single optical cross-sections through the middle of the cell located at the front of an infection focus. The vesicles appear as twin structures along the walls of opposing cells. G and H, Images of cells located in the center of an infection focus at 4 dpi. These images show fluorescence in a thick layer of cytoplasm around the cell, the ER, and vesicles. The nuclear fluorescence is either due to GFP:TGBp2 accumulating inside the nucleus, perinuclear X-bodies that overwhelm the nucleus (Kikumoto and Matsui, 1961; Kozar and Sheludko, 1969; Allison and Shalla, 1973), or both. Bars in all images, except C, represent 20 μm; bar in C represents 200 μm.

Data obtained in inoculated plants confirmed observations in protoplasts. In early infected cells and protoplasts, the GFP:TGBp2 proteins accumulated mainly in vesicles. In cells and protoplasts infected for a long period of time, we observed an increase in cytosolic fluorescence. In plants, GFP:TGBp2 proteins were found simultaneously in the ER as well as in vesicles. We never obtained evidence that the GFP:TGBp2 proteins move from the ER into vesicles, or from vesicles into the ER. Rather, the data indicate that GFP:TGBp2 proteins are either simultaneously targeted to the ER and cellular vesicles or that the GFP:TGBp2 proteins induce reorganization of the ER soon after translation.

Fluorescence Declines in PVX-Infected Protoplasts following Cycloheximide Treatment

In PVX-GFP:TGBp2-infected plants, we observed GFP:TGBp2 fluorescence in the ER as well as in vesicles, suggesting that the vesicles may be invaginations of the ER network. In protoplasts inoculated with PVX-GFP:TGBp2, fluorescence was redistributed from the vesicles into the cytosol. It is therefore reasonable to consider that ER retention of viral proteins and/or ER reorganization by the TGBp2 protein triggers ER-associated protein degradation as a result of ER stress (Brandizzi et al., 2003; Martinez and Chrispeels, 2003; Smalle and Vierstra, 2004; Kirst et al., 2005). It is also possible that the TGBp2 protein itself is unstable, causing the fusion protein to be targeted to the cytosol for degradation.

Fluorometric assays were used to quantify GFP expression over time as a measure of both protein accumulation and degradation in BY-2 protoplasts. We then compared

the rates of protein turnover in protoplasts inoculated with the PVX viruses with the rates of protein turnover in protoplasts transfected with the pRTL2 plasmids. Inoculated and transfected protoplasts were chased at 24 h with cycloheximide to halt protein synthesis. Fluorometric values were obtained at 0, 4, 8, and 12 h following treatment with cycloheximide and the protein half-lives were calculated. The fluorometric values were normalized to a time 0 measurement. The data were plotted and a linear regression was used to calculate protein half-lives.

We predicted that if protein turnover was stimulated as the result of virus infection, then fluorescence would decline more rapidly in virus-infected protoplasts than in pRTL2-transfected protoplasts. On the other hand, if TGBp2 contained a degradation signal, then we would expect greater turnover of GFP:TGBp2 than GFP proteins in both PVX-inoculated and pRTL2-transfected protoplasts.

In protoplasts transfected with PVX-GFP or PVX-GFP:TGBp2 transcripts, there was a linear increase in fluorescence between 12 and 48 hpi (Fig. 4A). The fluorescence values obtained at 48 hpi were between 8- and 12-fold higher than the values obtained at 12 hpi. The plotted fluorometric values for PVX-GFP:TGBp2- and PVX-GFP-infected protoplasts were almost identical to each other during most of the time course (Fig. 4A). Since the decrease in GFP and GFP:TGBp2 fluorescence had similar rates, the stability of GFP is not altered by fusion to the TGBp2 protein (Fig. 4B). The half-lives of GFP and GFP:TGBp2 proteins were similar, 8.9 and 8.6 h, respectively.

In protoplasts transfected with pRTL2-GFP or -GFP:TGBp2 plasmids, fluorescence did not show the same linear increase between 12 and 48 h post-transfection

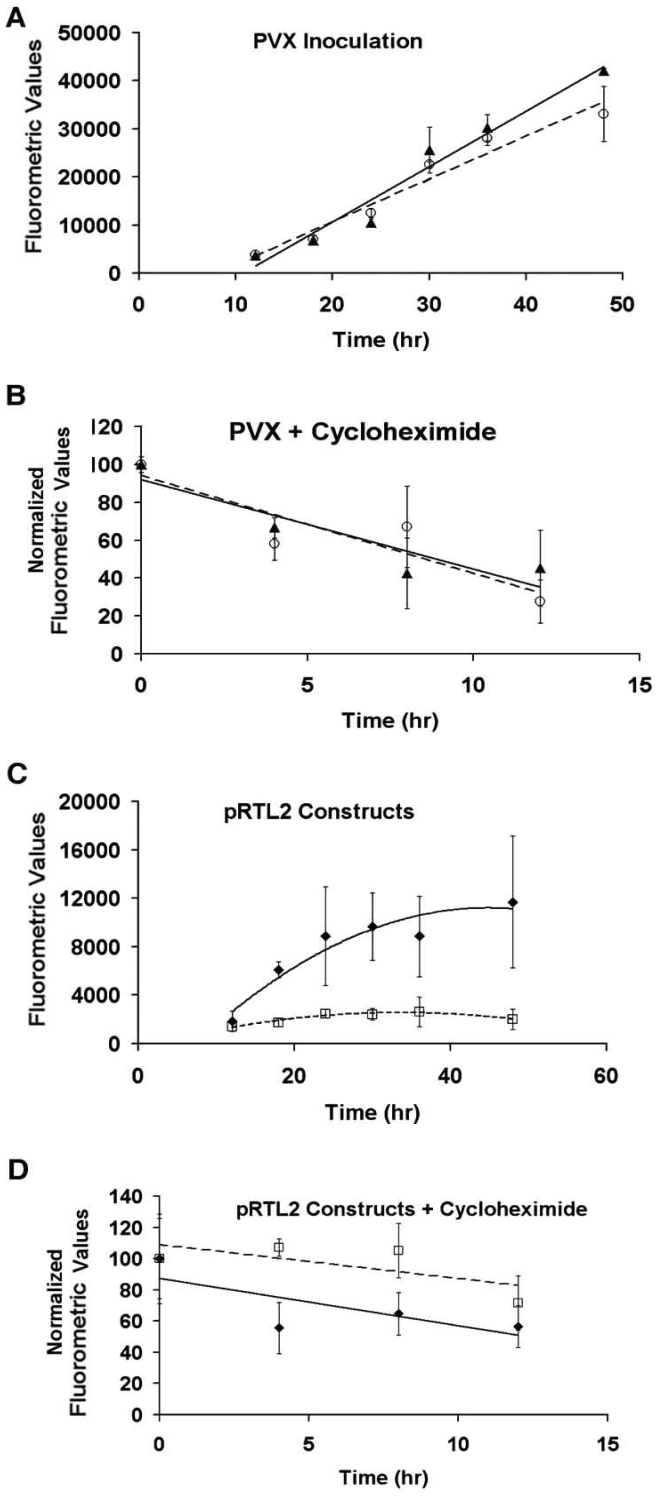
A
PVX Inoculation
Fluorometric Values
50000
40000
30000
20000
10000
0
0
10
20
30
40
50
Time (hr)
B
PVX + Cycloheximide
Normalized Fluorometric Values
120
100
80
60
40
20
0
0
5
10
15
Time (hr)
C
pRTL2 Constructs
Fluorometric Values
20000
16000
12000
8000
4000
0
0
20
40
60
Time (hr)
D
pRTL2 Constructs + Cycloheximide
Normalized Fluorometric Values
140
120
100
80
60
40
20
0
0
5
10
15
Time (hr)

Figure 4. Fluorometric assays measuring GFP fluorescence in BY-2 protoplasts. The averages of three fluorometric values were plotted at each time point. A, PVX-GFP (black triangle) and PVX-GFP:TGBp2 (white circle) infected protoplasts. The average fluorometric values were plotted using linear regression. B, PVX-GFP (black triangles) and PVX-GFP:TGBp2 (white circles) infected protoplasts treated with cycloheximide at 24 hpt. The average fluorometric values were normalized to an average time 0 measurement and then plotted using linear regression. C, pRTL2-GFP (black diamonds) and pRTL2-GFP:TGBp2 (white squares) transfected protoplasts. The average fluorometric values were plotted and a best-fit curve was determined using polynomial regression. D, pRTL2-GFP (black diamonds) and pRTL2-GFP:TGBp2 (white squares) transfected protoplasts were treated with cycloheximide at 24 hpt. The average fluorometric values were normalized to an average time 0 measurement and then plotted using linear regression.

(hpt) as reported for the PVX-GFP- and PVX-GFP:TGBp2-infected protoplasts (compare Fig. 4, A and C). Instead, the fluorometric values obtained for these pRTL2 constructs reached a plateau at approximately 24 hpt (Fig. 4C). The values representing GFP expression were 4-fold greater than the values representing GFP:TGBp2 fluorescence between 24 and 48 hpt (Fig. 4C). This was surprising since the fluorometric values obtained in PVX-GFP- and PVX-GFP:TGBp2-infected protoplasts were not significantly different. Perhaps protein accumulation in these transient assays is different when GFP:TGBp2 is expressed from a DNA or RNA promoter (*Cauliflower mosaic virus* [CaMV] 35S promoter or PVX coat protein subgenomic promoter). Since protein expression reaches a plateau at 24 hpt in protoplasts transfected with pRTL2 constructs but continues to increase in a linear fashion in PVX-inoculated protoplasts, it is possible that nuclear gene expression from a CaMV 35S promoter is more tightly regulated than cytosolic expression of the same gene(s) from a PVX viral promoter. The rate of decrease in GFP fluorescence following cycloheximide treatment was greater than the rate of decrease in GFP:TGBp2 fluorescence. The half-lives calculated for the GFP and GFP:TGBp2 proteins were 12.4 and 27.1 h, respectively. The GFP:TGBp2 fusion protein was more stable than the nonfused GFP protein (Fig. 4D).

Evidence that the GFP and GFP:TGBp2 proteins have shorter half-lives when expressed from the PVX genome than from pRTL2 constructs indicates that protein degradation is stimulated during virus infection. The half-life of the GFP:TGBp2 protein is 8.6 h when expressed from the PVX genome, and this may account for increasing cytosolic fluorescence during the course of infection, representing the last cellular location during degradation. Since the GFP:TGBp2 protein has a 2- to 3-fold longer

half-life when expressed from the pRTL2 plasmid, cytosolic accumulation of fluorescence would be minimal in studies involving these plasmids.

While the cycloheximide chase experiments support the hypothesis that the PVX TGBp2 protein accumulates in the cytosol and nucleus as a result of protein degradation, we could not rule out the possibility that the TGBp2 protein was redirected to the cytosol by other PVX proteins. This hypothesis is also supported by the finding that GFP:TGBp2 is cytosolic when expressed from the PVX genome, but is not cytosolic when expressed from pRTL2 plasmids.

Subcellular Targeting of GFP:TGBp2 and GFP:TGBp3 in Transient Expression Assays

To determine whether the PVX TGBp2 protein itself associates with vesicles in the absence of virus infection, pRTL2-GFP:TGBp2 plasmids were transfected into protoplasts or bombarded to tobacco leaves. For comparison, plasmids expressing GFP, GFP:TGBp3, or mGFP5-ER, which encodes a version of GFP that has an N-terminal basic chitinase signal peptide and a C-terminal HDEL sequence for ER targeting and retention (Siemering et al., 1996), were also used (Fig. 1). The plasmids expressing GFP:TGBp3 or mGFP5-ER were selected because these fusion proteins also associate with the ER and provide a comparison for studying the pattern of GFP:TGBp2 fluorescence. The patterns of green fluorescence in protoplasts and leaves were recorded using confocal microscopy. Ninety-three percent (28/30) of the protoplasts expressed GFP:TGBp2 in vesicles only, and 13% (4/30) of the protoplasts showed fluorescence in the ER as well as in vesicles associated with the ER (Table I).

Table I. *Subcellular accumulation of fluorescence in transiently transfected protoplasts*[a]

Construct	Total Cells	Nucleus	Cytosol	ER	Vesicles	Aggregates
GFP	30	30a	30a	0b	NO	NO
mGFP5-ER	15	0b	0b	15a	NO	1b
GFP:TGBp2	30	0b[b]	0b[b]	4b[b]	28a	30a
GFP:TGBp3	30	0c	0c	24b	NO	30a

[a] BY-2 protoplasts were transfected with four GFP constructs, and fluorescence was analyzed 18 hpt using confocal microscopy. Accumulation of fluorescence in the nucleus, cytosol, ER, vesicles, or aggregates was quantified. Aggregates were defined as those occasions when fluorescence appeared in bright amorphous bodies whose structures were sometimes difficult to describe. The pattern of fluorescence was scored for a random set of 15 or 30 cells. Proportions of cells containing fluorescence in the nucleus, cytoplasm, ER, vesicles, and aggregates are compared pairwise with Fisher's exact test. Numbers within a row with the same letter are not significantly different at a 0.05 significance level.

[b] Comparison of the 0 values for nucleus and cytosol with the value of 4 for ER had a *P* value of 0.0562 and thus is considered biologically significant.

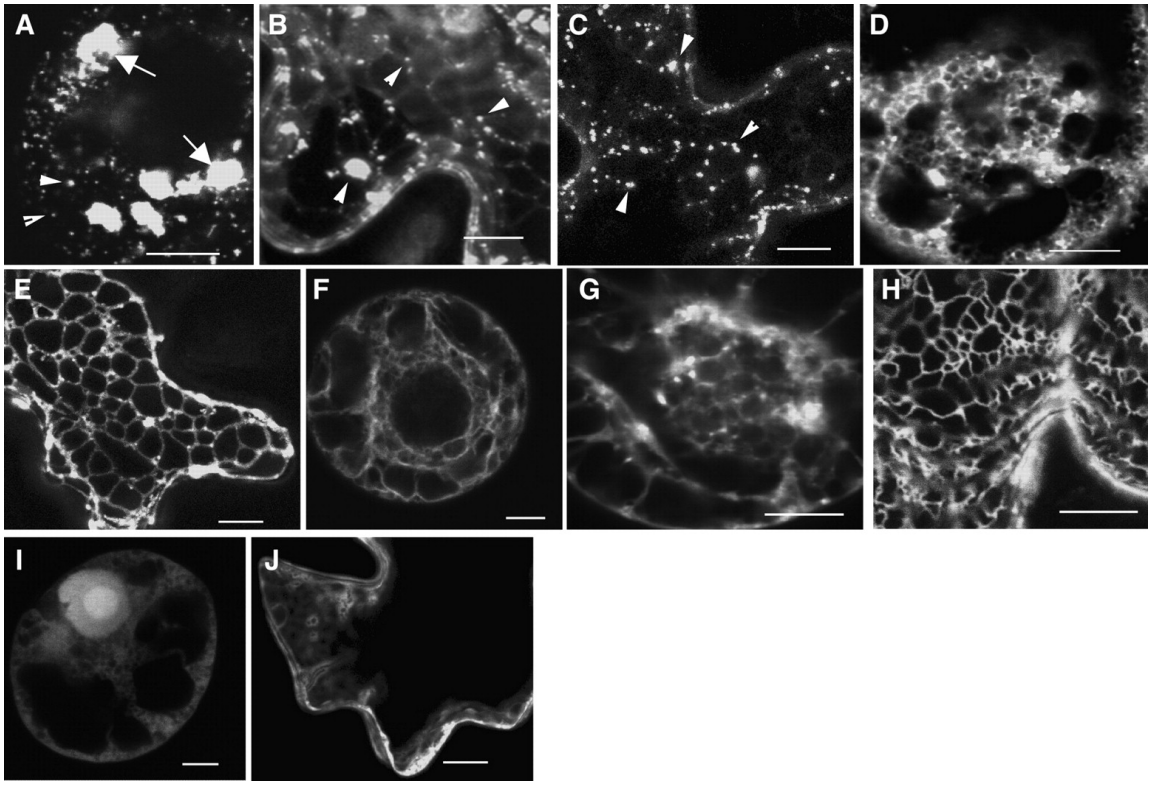

Figure 5. Confocal images showing subcellular accumulation of fluorescent proteins expressed transiently in BY-2 protoplasts and *N. benthamiana* leaves. Arrows point to aggregates and arrowheads point to vesicles in A to C. A, D, F, G, and I, Images of protoplasts. B, C, E, H, and J, Images of tobacco leaf epidermal cells taken by Dr Ruchira Mitra (Ju et al., 2005). A to C, pRTL2-GFP:TGBp2-transfected protoplasts and cells. D and E, pRTL2-GFP:TGBp3-transfected protoplasts and cells. F to H, pBIN-mGFP5-ER-transfected protoplasts and cells. D through H show ER network. I and J, pRTL2-GFP-transfected protoplasts and cells. GFP is cytosolic. Bars represent 10 μm.

All cells contained some aggregates of vesicles (Table I; Fig. 5, A–C). As in the PVX-GFP:TGBp2-infected protoplasts, the vesicles or aggregates were either perinuclear or along the plasma membrane (compare Fig. 2, A and B, with Fig. 5A).

Both GFP:TGBp3 and mGFP5-ER proteins were observed in the ER network in protoplasts and tobacco leaves (Fig. 5, E–H). The tubules and branches of the cortical ER network were shorter in protoplasts (Fig. 5, D–H) than in leaf epidermal cells, making the network in BY-2 protoplasts more difficult to resolve microscopically than in intact leaves. The small volume of the protoplasts cause the ER network to appear more compact than it appears in tobacco leaf epidermal cells. We did not observe fluorescent vesicles in protoplasts or tobacco leaf epidermal cells expressing either the GFP:TGBp3 or mGFP5-ER constructs (Table I). In protoplasts or bombarded leaves expressing only GFP, fluorescence was cytosolic and nuclear (Table I; Fig. 5, I–J).

In comparing the data obtained using GFP:TGBp2, GFP:TGBp3, and mGFP5-ER constructs, it appears that the GFP:TGBp2 proteins have the unique ability to associate with vesicles.

GFP:TGBp2 is in ER-Derived Vesicles and Associated with Actin not Golgi

It is common that viral proteins associating with the endomembrane system cause changes in membrane architecture. The PVX TGBp2 protein may cause invaginations of the ER network similar to those caused by the membrane-binding proteins encoded by TMV, BMV, *Tobacco etch virus* (TEV), and *Peanut clump virus* (PCV; Schaad et al., 1997; Reichel and Beachy, 1998; Dunoyer et al., 2002; Schwartz et al., 2002, 2004; Lee and Ahlquist, 2003). However, we had not eliminated the possibility that the PVX

TGBp2 protein associates with Golgi vesicles. Our collaborators, Drs Ruchira Mitra and Elison Blancaflor, conducted experiments to rule out this (Ju et al., 2005). In a recent publication from our laboratory Ruchira Mitra, who graduated from our laboratory, used immunogold labeling and electron microscopy to show that the GFP:TGBp2 protein associated with ER-derived vesicles that were unrelated to the Golgi apparatus (Ju et al., 2005). Dr. Ruchira Mitra used transgenic tobacco plants expressing GFP:TGBp2 or GFP:TGBp3. She found novel vesicles in GFP:TGBp2 transgenic leaves that were not present in GFP:TGBp3 or nontransgenic samples. Her electron microscopy experiments showed that the TGBp2-related vesicles contain ribosomes and immunolabel with Bip and GFP antisera. Dr. Elison Blancaflor, a collaborator at the Noble Foundation, used DsRed:ST (which targets DsRed to the Golgi) and GFP:TGBp2 expressing plasmids. These plasmids were cobombarded to tobacco leaves, and confocal imaging showed that the GFP:TGBp2 induced vesicles were unrelated to the Golgi apparatus. Furthermore, Elison showed that the GFP:TGBp2-induced vesicles were associated with actin filaments (Ju et al., 2005).

DISCUSSION

There are several reports that the TGBp2 and TGBp3 proteins of PSLV, BNYVV, and PMTV associate with the ER and with peripheral bodies (sometimes called punctate bodies; Erhardt et al., 2000; Solovyev et al., 2000; Cowan et al., 2002; Gorshkova et al., 2003; Morozov and Solovyev, 2003; Zamyatnin et al., 2004; Haupt et al., 2005). Since studies were conducted using confocal microscopy, the nature of the peripheral bodies was a source of speculation. Some have speculated that these peripheral bodies are

vesicles similar to Golgi vesicles (Morozov and Solovyev, 2003). The peripheral bodies observed in studies involving BNYVV, PMTV, and PSLV were sometimes described as twin structures forming on opposite walls of adjacent cells, as seen in this study in PVX-infected cells (Fig. 3, D and E; Erhardt et al., 2000; Solovyev et al., 2000; Cowan et al., 2002; Gorshkova et al., 2003; Morozov and Solovyev, 2003; Zamyatnin et al., 2004; Haupt et al., 2005). This observation has led to the suggestion that these viruses use the secretory pathway to move within the cell toward the plasmodesmata (Morozov and Solovyev, 2003). Here, we demonstrated that the PVX TGBp2 protein induces similar peripheral bodies that could be seen under the confocal microscope (Figs. 2, 3, and 5). This experiment was supported by electron microscopy conducted by Dr. Mitra (Ju et al., 2005). GFP:TGBp2 was observed in the ER and in vesicles in PVX-GFP:TGBp2-infected protoplasts and tobacco plants, in pRTL2-GFP:TGBp2-transfected protoplasts and bombarded tobacco leaves, and in GFP:TGBp2 transgenic tobacco leaves. Vesicles were not observed in mGFP5-ER- or GFP:TGBp3-expressing samples, suggesting that these vesicles were uniquely induced by the GFP:TGBp2 protein.

Using three different experimental systems, new evidence was obtained indicating that the peripheral bodies induced by the PVX TGBp2 protein are vesicles resulting from invagination of the ER network and are unrelated to the Golgi apparatus. In electron microscopy experiments published along with this study, Dr. R. Mitra showed that the vesicles were sometimes studded with ribosomes, suggesting that they were ER derived (Ju et al., 2005). Dr. Elison Blancaflor from Noble Foundation provided further evidence, in the same published study, that these vesicles were not related to the Golgi apparatus was obtained in transient expression studies using the Golgi marker DsRed-ST

(Ju et al., 2005). These combined data provide further evidence that the vesicles were more likely to be derived from the ER network rather than the Golgi apparatus.

The peripheral bodies reported for PSLV were induced by the TGBp3 protein (Solovyev et al., 2000). Similar bodies were reported for PMTV to be induced by both TGBp2 and TGBp3 (Haupt et al., 2005). In this study, the PVX TGBp2 protein, but not the TGBp3 protein, induced similar structures. Differences among the PSLV, PMTV, and PVX TGBp3 proteins in their abilities to induce vesicles might be the result of evolutionary divergence. In fact, amino acid sequence analyses of many triple gene block-containing viruses suggest that the TGBp2 and TGBp3 proteins of potexviruses and hordeiviruses diverge. The hordeivirus and pomovirus TGBp3 proteins have two transmembrane domains, similar to the potexvirus TGBp2 protein. The potexvirus TGBp3 has a single transmembrane domain and has a smaller M_r than the hordeivirus and pomovirus TGBp3 proteins (Morozov and Solovyev, 2003; Verchot-Lubicz, 2005). The amino acid sequences show little conservation among the TGBp2 and TGBp3 proteins of hordei-like and potex-like viruses (Morozov and Solovyev, 2003; Verchot-Lubicz, 2005). While these proteins clearly diverge at the amino acid sequence level, it is also possible that divergence of the potex-like viruses and hordei-like viruses may include differences in their interactions with the cellular endomembrane system.

The association of PVX TGBp2 with the actin cytoskeleton and ER, but not with the Golgi, is consistent with recent results with the PMTV TGBp2/3 complex (Haupt et al., 2005). PMTV TGBp2 and TGBp3 showed early localization with the ER network and eventually induced the formation of motile granules that aligned along actin filaments. Moreover, colocalization of the PMTV TGBp2/3 complex with a variety of

fluorescent markers late in virus infection implicated the endocytic pathway in recycling some of the viral proteins during virus infection (Haupt et al., 2005). Further research is needed to determine whether intracellular movement of PVX, similar to PMTV, uses the endocytotic pathway for protein recycling.

Viral proteins that are known to associate with cellular membranes often cause changes in the endomembrane architecture (Schwartz et al., 2002; Lee and Ahlquist, 2003). As mentioned in the introduction, VRCs reported for bromoviruses, potyviruses, comoviruses, and dianthoviruses are derived from invagination of the cortical ER (Schaad et al., 1997; Carette et al., 2002a, 2002b; Schwartz et al., 2002; Turner et al., 2004). In the case of TMV, the viral movement protein and the 126- and 183-kD proteins are present in these membrane-bound VRCs, which traffic on microfilaments and move to the plasmodesmata (Kawakami et al., 2004; Liu et al., 2005).

The PCV (a pecluvirus) is a triple gene block-containing virus whose replication complex associates with ER-derived vesicles (Dunoyer et al., 2002). These PCV-induced vesicles resemble the vesicles induced by the PVX TGBp2 protein (Dunoyer et al., 2002). While there is no evidence that the PVX TGBp2 protein contributes to virus replication, the TGBp2 protein could potentially colocalize with the viral replicase to mediate transport of membrane-bound PVX VRCs, similar to the TMV VRCs (Kawakami et al., 2004; Liu et al., 2005). Further experiments are needed to determine whether other PVX proteins and PVX RNAs associate with these vesicles.

We observed GFP:TGBp2 in the cytosol and nucleus during PVX infection but not when GFP:TGBp2 was expressed from pRTL2 plasmids. Statistical analysis of the data presented in Figure 2 support the hypothesis that the GFP:TGBp2 protein was

redirected to the cytosol by either viral or cellular factors. It is worthy to mention that the pattern of fluorescence observed in protoplasts expressing GFP:TGBp1 was somewhat similar to the pattern of fluorescence observed in PVX-GFP:TGBp2-infected. Presently, very little is known regarding interactions among the triple gene block proteins. Further research is needed to learn whether protein subcellular targeting is affected by viral protein-protein interactions.

Another explanation for cytosolic and nuclear accumulation of GFP:TGBp2 relates to the increased levels of protein turnover observed in protoplasts infected with PVX (Brandizzi et al., 2003). Both GFP and GFP:TGBp2 proteins had shorter half-lives when they were expressed from the PVX genome than when they were expressed from pRTL2 plasmids (Fig. 4). Either PVX infection, PVX RNA, or other PVX proteins stimulated protein degradation. Since the TGBp3 protein is also linked to the ER, it is possible that either TGBp3 or a combination of viral proteins can stimulate ER stress responses such as protein export from the ER, protein degradation by the 26S proteasome (ER-associated protein degradation), and fluctuations in ER calcium stores (Navazio et al., 2001; Martinez and Chrispeels, 2003; Smalle and Vierstra, 2004; Kirst et al., 2005). The TMV movement protein and the *Turnip yellow mosaic virus* (TYMV) movement proteins are degraded by the 26S proteasome (Reichel and Beachy, 2000; Drugeon and Jupin, 2002; Gillespie et al., 2002). In the case of TMV, protein degradation by the 26S proteasome regulates virus movement across the plasmodesmata (Reichel and Beachy, 2000; Gillespie et al., 2002). In fact, a TMV movement protein that was modified by DNA shuffling showed improved transport functions due to its ability to evade proteasome degradation (Gillespie et al., 2002). Protein degradation by the 26S

proteasome helps to maintain the integrity of the ER and restore homeostasis in the cell (Reichel and Beachy, 2000). Evidence that GFP:TGBp2 has a longer half-life than GFP in pRTL2-transfected protoplasts suggests that TGBp2 has an ability to evade the proteasome or other protein degradation machinery, thereby moving across the plasmodesmata (Reichel and Beachy, 2000). This may account for cytosolic accumulation of TGBp2 late in infection. Evidence that protein translocation out of the ER is independent of proteasomal degradation was presented in a study of ricin A degradation in which cytosolic protein accumulation was detected following treatment of cells with a proteasome inhibitor (Di Cola et al., 2001). Thus, the ER stress response may play a role in plasmodesmata transport by translocating the PVX TGBp2 or viral movement complexes into the cytosol. The viral movement complex might evade degradation by the 26S proteasome by moving across the plasmodesmata (Reichel and Beachy, 2000; Drugeon and Jupin, 2002; Gillespie et al., 2002).

A model was proposed in which the regulation of calcium stores in the ER by calreticulin controls unconventional myosin VIII activities within the plasmodesmata and thereby controls plasmodesmata gating (Baluska et al., 1999; Reichelt et al., 1999). To expand on this model, it is possible that ER stress responses to virus infection cause calreticulin to release calcium stores, thereby modulating plasmodesmata gating (Fig. 6). Formation of TGBp2-induced vesicles might deplete the ER of calcium stores, causing an influx of calcium into the ER as the cell tries to regain homeostasis. If myosin within the plasmodesmata controls plasmodesmata gating, then fluctuations in calcium levels induced by ER stress and virus infection could also regulate virus cell-to-cell movement.

Plasmodesmata gating might allow transport of the TGBp2-induced vesicles across the plasmodesmata. Alternatively, plasmodesmata gating coincides with translocation of PVX proteins out of the ER as a result of ER stress responses. To speculate further, the PVX movement complex might evade 26S proteasome degradation and move across the plasmodesmata (Fig. 6).

To test this model, further research is needed to determine whether PVX infection triggers ER stress responses and whether there is a link between ER stress response and plasmodesmata gating. The ability of virus infection to cause fluctuations in calcium levels across the ER is also worthy of further investigation.

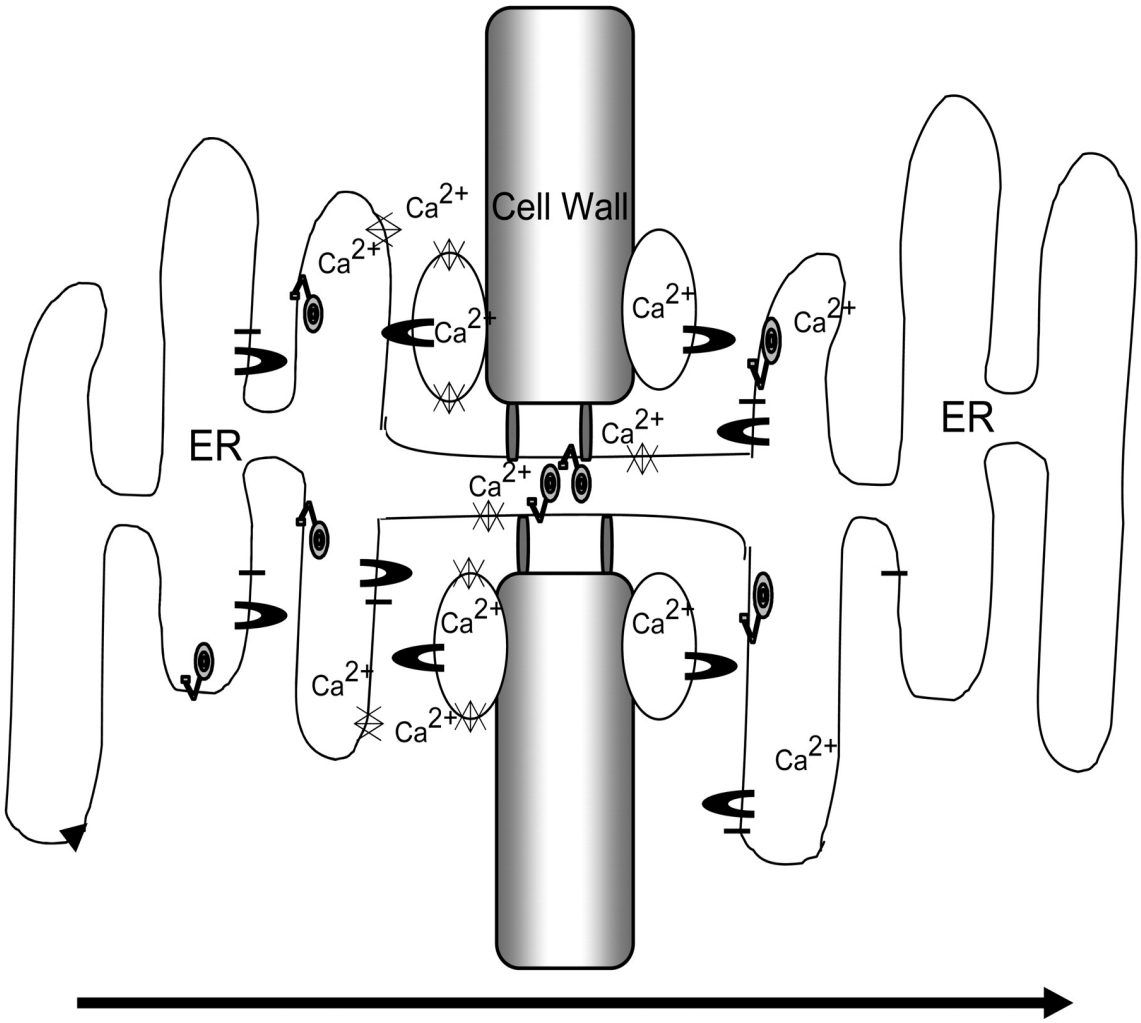

Figure 6. Model linking the ER stress response with virus movement. TGBp2 (black horseshoe) and TGBp3 (black bar) are located in the ER. TGBp2 is also located in ER-derived vesicles located at the periphery of the cell. During PVX infection, TGBp2 is located in vesicles and in the ER in cells located at the infection front and at the center of the infection foci (this study). We do not know whether TGBp3 colocalizes with TGBp2 in the ER-derived vesicles during PVX infection. The ER traverses the plasmodesmata and is a rich store of Ca^{2+} ions. Calmodulin (indicated by gray sphere with a bent arm) is resident in the ER and plasmodesmata and is one example of a factor that controls

fluctuations of Ca^{2+} across the ER. The ER-derived vesicles line the cell wall and may also be Ca^{2+} stores. Unconventional myosin VIII (gray bars) is a component of plasmodesmata that regulates gating. Mobilization of calcium, perhaps as a result of ER stress, controls unconventional myosin VIII activities within the plasmodesmata. ER stress may be caused by TGBp2-induced ER reorganization. We do not yet know whether other PVX proteins associate with the TGBp2-induced vesicles, although it is known that TGBp2 and TGBp3 from PMTV colocalize in vesicles (Haupt et al., 2005). If the viral movement complex is associated with the TGBp2-induced vesicles, then it is possible the vesicles move across the plasmodesmata similar to the TMV VRCs. It is also possible that the viral movement complex is exported from the ER (or vesicles) and then moves across the plasmodesmata. Further research is needed to determine the role of the ER, ER stress, and calcium signaling in virus cell-to-cell transport. Arrow at the bottom indicates direction of virus movement from one cell into the adjacent cell.

MATERIALS AND METHODS

Bacterial Strains and Plasmids

All plasmids were constructed using *Escherichia coli* strain JM109 (Sambrook et al., 1989). The plasmids pPVX-GFP and pPVX12D-GFP are infectious clones of PVX containing the bacteriophage T7 promoter and the enhanced GFP gene inserted into the PVX cDNA(Fig. 1; Verchot et al., 1998; Krishnamurthy et al., 2003; Mitra et al., 2003). The pPVX12D-GFP plasmid lacks the entire coding sequences for the PVX TGBp2 ORF between nucleotide positions 5,170 to 5,423 and was prepared previously (Verchot et al., 1998). The pPVX-GFP:TGBp2 infectious clone was prepared by replacing the GFP gene in the pPVX12D-GFP infectious clone with the GFP:TGBp2-fused genes. This was accomplished in three steps. First, the GFP:TGBp2 fusion was PCR amplified using the pRTL2-GFP:TGBp2 plasmid. A forward GFP primer (CAG CTA GCA TCG ATG GTG AGC AAG GGC GAG GAG CTG) containing a *Cla*I restriction site (underlined) and reverse primer overlapping the TGBp2 (GGC GGT CGA CAT CTA ATG ACT GCT ATG ATT GTT) sequence and containing a *Sal*I restriction site (underlined) were used. The PCR products were ligated to pGEMT plasmids (Promega, Madison, WI). In the second cloning step, the GFP:TGBp2 fusion was introduced into pCXS-GFP constructs, which contain a single *Sal*I site (pPVX-GFP constructs contain two *Sal*I sites). The pGEMT-GFP:TGBp2 and pCXS-GFP plasmids were each digested with *Cla*I and *Sal*I restriction enzymes, gel purified, and then ligated. In the third cloning step, the pCXS-GFP:TGBp2 and pPVX12D-GFP plasmids were digested with *Cla*I and *Spe*I restriction enzymes, gel purified, and then ligated (Fig. 1B).

The plasmids pRTL2-GFP, -GFP:TGBp1, -GFP:TGBp2, and -GFP:TGBp3 were prepared previously (Fig. 1; Yang et al., 2000; Krishnamurthy et al., 2003; Mitra et al., 2003). The pBIN-mGFP5-ER plasmid was obtained from Dr. J. Hasselof (Medical Research Council Laboratory of Molecular Biology, Cambridge, UK; Siemering et al., 1996).

BY-2 Protoplast Preparation and Transfection

Suspension cells of tobacco BY-2 (Nagata et al., 1992) were maintained as described in Qi and Ding (2002) with little change. BY-2 cells were propagated in the BY-2 culture medium (Murashige and Skoog medium [Murashige and Skoog salts; Sigma, St. Louis] supplemented with 30 g L^{-1} Suc, 256 mg L^{-1} KH_2PO_4, 100 mg L^{-1} myoinositol, 1 mg L^{-1} thiamine, and 0.2 mg L^{-1} 2,4-dichlorophenoxyacetic acid, pH 5.5 [w/v]) on a rotary shaker at 120 rpm at 28°C in the dark. Ten milliliters of BY-2 cells were transferred to 50 mL of fresh media weekly.

Protoplasts were isolated from the suspension cells as previously described with slight modifications (Gaire et al., 1999; Qi and Ding, 2002). Three-day-old cells in suspension culture media were collected by centrifugation at 200*g* for 5 min and resuspended in 1.5% cellulose Onozuka RS (w/v; Yakult Pharmaceutical, Tokyo) and 0.2% macerase (w/v; Calbiochem-Novabiochem, La Jolla, CA) in solution 1 [0.5 M mannitol, 3.6 mM MES, pH 5.5 (w/v)], and incubated for 3 to 5 h at 30°C in a water bath with a rotary shaker. The protoplasts were collected by filtration through 41-μm nylon mesh (Spectrum Laboratories, Rancho Dominguez, CA), and were centrifuged and washed twice with solution 1 at 100*g* for 5 min. Finally, protoplasts were resuspended in

solution 2 (solution 1 plus 0.1 mM $CaCl_2$) to a density of about 2 x 10^6 protoplasts mL^{-1} and incubated on ice for 1 h.

Protoplasts were inoculated with infectious viral RNA transcripts. Transcripts were prepared from pPVX-GFP, pPVX12D-GFP, and pPVX-GFP:TGBp2 plasmids described previously (Baulcombe et al., 1995). Five micrograms of transcripts were used to transfect 5 x 10^5 BY-2 protoplasts. Electroporation was carried out at 0.25 kV, 100 Ω, and 125 μF using 0.4-cm gap cuvettes (Bio-Rad Laboratories, Hercules, CA) and a gene pulser (Bio-Rad Laboratories). Following electroporation, protoplasts were immediately transferred into a new tube containing 1 mL of solution 2 and incubated on ice for 30 min, and then at 30°C for 5 min. Protoplasts were collected by centrifugation at 39*g* for 5 min, resuspended in 1 mL of solution 3 (BY-2 culture media plus 0.45 M mannitol), and transferred to 6-well cell culture plates (Corning, Corning, NY) coated with solution 3 plus 1.0% agarose (w/v; pH 5.7). Protoplasts were cultured at 27°C and then collected at 18, 24, 36, and 48 hpi by centrifugation at 39*g* for 5 min.

Protoplasts were also transfected with pRTL2 plasmids by electroporation as described by Gaire et al. (1999) with a few changes. Protoplasts (1 x 10^6 in 0.5 mL) were mixed with 70 to 80 μg of plasmid DNA and 40 μg of sonicated salmon sperm DNA as carrier. The protoplast-DNA mixture was placed in a 0.4-cm gap cuvette (Bio-Rad Laboratories) on ice and then electroporated using a gene pulser (Bio-Rad Laboratories) at 0.18 kV, 100 Ω, and 125 μF with three pulses. Protoplasts were transferred after electroporation into a new tube containing 1 mL of solution 2, incubated on ice for 30 min, and then collected by centrifugation at 59*g* for 5 min. Protoplasts were resuspended in 1.5 mL of solution 3 (BY-2 culture media plus 0.45 M mannitol) and added to 6-well

cell culture plates (Corning) containing solution 3 plus 1.0% agarose (w/v; pH 5.7). Protoplasts were cultured at 27°C for 18 h.

RNA- or DNA-transfected protoplasts were collected, washed with phosphate-buffered saline (PBS), and then fixed with PBS containing 3% paraformaldehyde (v/v) and 5 mM EGTA for 1 h at room temperature, followed by washing twice with PBS. Fixed samples were analyzed by confocal microscopy. Some protoplasts were stained with DAPI. Transfected protoplasts were incubated in 10 μg mL^{-1} DAPI in growth media. Protoplasts were then analyzed by confocal microscopy.

Fluorometric Assays and Cycloheximide Treatment of BY-2 Protoplasts

In some experiments, protoplasts were inoculated with PVX transcripts or transfected with pRTL2 plasmids and fluorescence was monitored fluorometrically at 12, 18, 24, 30, 36, and 48 h as described previously (Howard et al., 2004). The average values from three samples were plotted at each time point. To measure protein turnover, solution 3 was removed at 24 hpt and replaced by solution 3 containing 500 μM cycloheximide (Sigma). Protoplasts were maintained in the 6-well cell culture plates at 27°C for an additional 4, 8, and 12 h. Nontreated protoplast samples were collected at 0 h (24 hpt) and immediately placed in liquid nitrogen. Cycloheximide-treated protoplasts were harvested by centrifugation at 59*g* for 5 min and immediately placed in liquid nitrogen. GFP expression was assayed by fluorometric analyses.

Plant Materials and Plant Inoculations

Tobacco (*Nicotiana benthamiana* and *Nicotiana tabacum*) plants were used for studying the subcellular targeting of most proteins. Transgenic *N. tabacum* plants expressing mGFP5-ER, GFP:TGBp2, or GFP:TGBp3 were prepared previously using Agrobacterium transformation, as previously described (Krishnamurthy et al., 2003; Mitra et al., 2003).

Protoplasts were inoculated with PVX-GFP, PVX12D-GFP, and PVX-GFP:TGBp2 transcripts. Protoplasts were harvested and ground with an equal volume (w/v) of Tris-EDTA. Protoplast extracts were rub inoculated to *N. benthamiana* leaves with carborundum. Two leaves per plant were inoculated. Viruses spread systemically between 5 and 7 dpi. Leaves from systemically infected plants were harvested and used to inoculate further plants for microscopic analysis of virus infection. The leaf inoculum was prepared by grinding leaves 1:5 (w/v) in Tris-EDTA buffer. Two leaves per plant were each inoculated with 20-μL leaf extracts. Systemic spread of GFP expression was checked using a hand-held UV lamp.

Confocal Microscopy

A Leica TCS SP2 (Leica Microsystems, Bannockburn, IL) confocal imaging system was used to study subcellular localization of the GFP fusion proteins in tobacco epidermal cells that were either bombarded with plasmids or inoculated with the PVX viruses. The Leica TCS SP2 system was attached to a Leica DMRE microscopy equipped with epifluorescence and water immersion objectives. For confocal microscopy, a UV laser and a krypton/argon laser were used to examine fluorescence. A 488-nm excitation wavelength was used to view GFP expression, a 358-nm excitation

wavelength was used to view DAPI. In general, 15 to 30 optical sections were taken of each cell at 0.3- to 2-μm intervals. All images obtained by epifluorescence or confocal microscopy were processed using Adobe Photoshop CS version 8.0 software (Adobe Systems, San Jose, CA).

Statistical Analyses

Logistic regression for fluorescence in each subcellular address (vesicle, nucleus, and cytoplasm), with the presence/absence of each address as the response variable and time as the independent variable was performed by Dr. Mark Payton (Statistics Department, OSU) using data presented in Figure 1, J and K (PROC LOGISTIC, PC SAS, version 8.2; SAS Institute, Cary, NC). These regressions were performed for both the PVX-GFP:TGBp2 and PVX-GFP. Slope estimates and *P* values were determined.

Linear and polynomial regressions were used to find the best-fit curve for comparing fluorescence in BY-2 protoplasts before and after cycloheximide treatments in Figure 4. The distribution fluorescence in BY-2 protoplasts recorded in Table I was analyzed with pairwise Fisher's exact tests using PROC FREQ in PC SAS version 8.2. A significance level of 0.05 was used for all comparisons.

ACKNOWLEDGMENTS

I thank Dr. R. Mitra for the supporting material and Dr. M.Payton for the statistical analysis. I appreciate to Dr. T. Sammuel who assists fluorometric assay. I would like to thank Mrs. Phoebe Doss and Mr. Terry Colburn at the Oklahoma State

University Electron Microscopy Center. Further appreciation is extended to Mrs. Barbara Driskel for greenhouse support and to Dr. Biao Ding (Ohio State University) for technical advice and useful discussions. I also thank Dr. J. Fletcher for use of electroporation systems.

LITERATURE CITED

Allison A, Shalla T (1973) The ultrastructure of local lesions induced by *Potato virus X*: a sequence of cytological events in the course of infection. Phytopathology **64:** 784–793

Baluska F, Samaj J, Napier R, Volkmann D (1999) Maize calreticulin localizes preferentially to plasmodesmata in root apex. Plant J **19:** 481–488

Baulcombe DC, Chapman S, Santa Cruz S (1995) Jellyfish green fluorescent protein as a reporter for virus infections. Plant J **7:** 1045–1053

Brigneti G, Voinnet O, Li WX, Ji LH, Ding SW, Baulcombe DC (1998) Viral pathogenicity determinants are suppressors of transgene silencing in *Nicotiana benthamiana.* EMBO J **17:** 6739–6746

Carette JE, Guhl K, Wellink J, Van Kammen A (2002a) Coalescence of the sites of *Cowpea mosaic virus* RNA replication into a cytopathic structure. J Virol **76:** 6235–6243

Carette JE, van Lent J, MacFarlane SA, Wellink J, van Kammen A (2002b) *Cowpea mosaic virus* 32- and 60-kilodalton replication proteins target and change the morphology of endoplasmic reticulum membranes. J Virol **76:** 6293–6301

Cowan GH, Lioliopoulou F, Ziegler A, Torrance L (2002) Subcellular localisation,

protein interactions, and RNA binding of *Potato mop-top virus* triple gene block proteins. Virology **298:** 106–115

Crawford KM, Zambryski PC (2000) Subcellular localization determines the availability of non-targeted proteins to plasmodesmatal transport. Curr Biol **10:** 1032–1040

Crawford KM, Zambryski PC (2001) Non-targeted and targeted protein movement through plasmodesmata in leaves in different developmental and physiological states. Plant Physiol **125:** 1802–1812

Di Cola A, Frigerio L, Lord JM, Ceriotti A, Roberts LM (2001) Ricin A chain without its partner B chain is degraded after retrotranslocation from the endoplasmic reticulum to the cytosol in plant cells. Proc Natl Acad Sci USA **98:** 14726–14731

Ding XS, Liu J, Cheng NH, Folimonov A, Hou YM, Bao Y, Katagi C, Carter SA, Nelson RS (2004) The *Tobacco mosaic virus* 126-kDa protein associated with virus replication and movement suppresses RNA silencing. Mol Plant Microbe Interact **17:** 583–592

Drugeon G, Jupin I (2002) Stability in vitro of the 69K movement protein of *Turnip yellow mosaic virus* is regulated by the ubiquitin-mediated proteasome pathway. J Gen Virol **83:** 3187–3197

Dunoyer P, Ritzenthaler C, Hemmer O, Michler P, Fritsch C (2002) Intracellular localization of the *Peanut clump virus* replication complex in tobacco BY-2 protoplasts containing green fluorescent protein-labeled endoplasmic reticulum or Golgi apparatus. J Virol **76:** 865–874

Erhardt M, Morant M, Ritzenthaler C, Stussi-Garaud C, Guilley H, Richards K, Jonard G, Bouzoubaa S, Gilmer D (2000) P42 movement protein of *Beet necrotic yellow vein virus* is targeted by the movement proteins P13 and P15 to punctate bodies associated with plasmodesmata. Mol Plant Microbe Interact **13:** 520–528

Espinoza AM, Medina V, Hull R, Markham PG (1991) *Cauliflower mosaic virus* gene II product forms distinct inclusion bodies in infected plant cells. Virology **185:** 337–344

Gaire F, Schmitt C, Stussi-Garaud C, Pinck L, Ritzenthaler C (1999) Protein 2A of *Grapevine fanleaf nepovirus* is implicated in RNA2 replication and colocalizes to the replication site. Virology **264:** 25–36

Gillespie T, Boevink P, Haupt S, Roberts AG, Toth R, Valentine T, Chapman S, Oparka KJ (2002) Functional analysis of a DNA-shuffled movement protein reveals that microtubules are dispensable for the cell-to-cell movement of *Tobacco mosaic virus.* Plant Cell **14:** 1207–1222

Gorshkova EN, Erokhina TN, Stroganova TA, Yelina NE, Zamyatnin AA Jr, Kalinina NO, Schiemann J, Solovyev AG, Morozov SY (2003) Immunodetection and fluorescent microscopy of transgenically expressed hordeivirus TGBp3 movement protein reveals its association with endoplasmic reticulum elements in close proximity to plasmodesmata. J Gen Virol **84:** 985–994

Haupt S, Cowan GH, Ziegler A, Roberts AB, Oparka KJ, Torrance L (2005) Two plant-viral movement proteins traffic in the endocytic recycling pathway. Plant

Cell **17:** 164–181

Heinlein M, Epel BL, Padgett HS, Beachy RN (1995) Interaction of tobamovirus movement proteins with the plant cytoskeleton. Science **270:** 1983–1985

Heinlein M, Padgett HS, Gens JS, Pickard BG, Casper SJ, Epel BL, Beachy RN (1998) Changing patterns of localization of the *Tobacco mosaic virus* movement protein and replicase to the endoplasmic reticulum and microtubules during infection. Plant Cell **10:** 1107–1120

Henderson J, Satiat-Jeunemaitre B, Napier R, Hawes C (1994) Brefeldin A-induced disassembly of the Golgi apparatus is followed by disruption of the endoplasmic reticulum in plant cells. J Exp Bot **45:** 1347–1351

Howard AR, Heppler ML, Ju H-J, Krishnamurthy K, Payton ME, Verchot-Lubicz J (2004) *Potato virus X* TGBp1 induces plasmodesmata gating and moves between cells in several host species whereas CP moves only in *N. benthamiana* leaves. Virology **328:** 185–197

Huisman MJ, Linthorst HJ, Bol JF, Cornelissen JC (1988) The complete nucleotide sequence of *Potato virus X* and its homologies at the amino acid level with various plus-stranded RNA viruses. J Gen Virol **69:** 1789–1798

Kawakami S, Watanabe Y, Beachy RN (2004) *Tobacco mosaic virus* infection spreads cell to cell as intact replication complexes. Proc Natl Acad Sci USA **101:** 6291–6296

Kikumoto T, Matsui C (1961) Electron microscopy of intracellular *Potato virus X.* Virology **13:** 294–299

Kirst ME, Meyer DJ, Gibbon BC, Jung R, Boston RS (2005) Identification and

characterization of endoplasmic reticulum-associated degradation proteins differentially affected by endoplasmic reticulum stress. Plant Physiol **138:** 218–231

Kiss JZ, Giddings TH Jr, Staehelin LA, Sack FD (1990) Comparison of the ultrastructure of conventionally fixed and high pressure frozen/freeze substituted root tips of *Nicotiana* and *Arabidopsis.* Protoplasma **157:** 64–74

Kost B, Spielhofer P, Chua N-H (1998) A GFP-mouse talin fusion protein labels plant actin filaments in vivo and visualizes the actin cytoskeleton in growing pollen tubes. Plant J **16:** 393–401

Kozar FE, Sheludko YM (1969) Ultrastructure of potato and *Datura stramonium* plant cells infected with *Potato virus X.* Virology **38:** 220–229

Krishnamurthy K, Heppler M, Mitra R, Blancaflor E, Payton M, Nelson RS, Verchot-Lubicz J (2003) *The potato virus X* TGBp3 protein associates with the ER network for virus cell-to-cell movement. Virology **309:** 135–151

Krishnamurthy K, Mitra R, Payton ME, Verchot-Lubicz J (2002) Cell-to-cell movement of the PVX 12K, 8K, or coat proteins may depend on the host, leaf developmental stage, and the PVX 25K protein. Virology **300:** 269–281

Lee WM, Ahlquist P (2003) Membrane synthesis, specific lipid requirements, and localized lipid composition changes associated with a positive-strand RNA virus RNA replication protein. J Virol **77:** 12819–12828

Liu J-Z, Blancaflor EB, Nelson RS (2005) The *Tobacco mosaic virus* 126-kilodalton protein, a constituent of the virus replication complex, alone or within the complex aligns with and traffics along microfilaments. Plant Physiol **138:** 1853–

1865

Martinez IM, Chrispeels MJ (2003) Genomic analysis of the unfolded protein response in Arabidopsis shows its connection to important cellular processes. Plant Cell **15:** 561–576

Mas P, Beachy RN (1999) Replication of *Tobacco mosaic virus* on endoplasmic reticulum and role of the cytoskeleton and virus movement protein in intracellular distribution of viral RNA. J Cell Biol **147:** 945–958

McCann RO, Craig SW (1997) The I/LWEQ module: a conserved sequence that signifies F-actin binding in functionally diverse proteins from yeast to mammals. Proc Natl Acad Sci USA **94:** 5679–5684

McLean BG, Zupan J, Zambryski PC (1995) *Tobacco mosaic virus* movement protein associates with the cytoskeleton in tobacco cells. Plant Cell **7:** 2101–2114

Mitra R, Krishnamurthy K, Blancaflor E, Payton M, Nelson RS, Verchot-Lubicz J (2003) The *Potato virus X* TGBp2 protein association with the endoplasmic reticulum plays a role in but is not sufficient for viral cell-to-cell movement. Virology **312:** 35–48

Morozov SY, Solovyev AG (2003) Triple gene block: modular design of a multifunctional machine for plant virus movement. J Gen Virol **84:** 1351–1366

Nagata T, Nemoto Y, Hasezawa S (1992) Tobacco BY-2 cell line as the "Hela" cell in the cell biology of higher plants. Int Rev Cytol **132:** 1–31

Navazio L, Mariani P, Sanders D (2001) Mobilization of Ca^{2+} by cyclic ADP-ribose from the endoplasmic reticulum of cauliflower florets. Plant Physiol **125:** 2129–2138

Nelson RS (2005) Movement of viruses to and through plasmodesmata. *In* K Oparka, ed, Plasmodesmata. Blackwell Publishing Ltd, Oxford, pp 188–209

Oparka KJ, Roberts AG, Boevink P, Santa Cruz S, Roberts I, Pradel KS, Imlau A, Kotlizky G, Sauer N, Epel B (1999) Simple, but not branched, plasmodesmata allow the nonspecific trafficking of proteins in developing tobacco leaves. Cell **97:** 743–754

Qi Y, Ding B (2002) Replication of *Potato spindle tuber viroid* in cultured cells of tobacco and *Nicotiana benthamiana*: the role of specific nucleotides in determining replication levels for host adaptation. Virology **302:** 445–456

Reichel C, Beachy RN (1998) *Tobacco mosaic virus* infection induces severe morphological changes of the endoplasmic reticulum. Proc Natl Acad Sci USA **95:** 11169–11174

Rubino L, Russo M (1998) Membrane targeting sequences in tombusvirus infections. Virology **252:** 431–437

Rubino L, Weber-Lotfi F, Dietrich A, Stussi-Garaud C, Russo M (2001) The open reading frame 1-encoded ('36K') protein of *Carnation Italian ringspot virus* localizes to mitochondria. J Gen Virol **82:** 29–34

Sambrook J, Fritsch EF, Maniatis T (1989) Molecular Cloning: A Laboratory Manual, Ed 2. Cold Spring Harbor Laboratory Press, Cold Spring Harbor, NY

Schaad MC, Jensen PE, Carrington JC (1997) Formation of plant RNA virus replication complexes on membranes: role of an endoplasmic reticulum-targeted viral protein. EMBO J **16:** 4049–4059

Schwartz M, Chen J, Janda M, Sullivan M, den Boon J, Ahlquist P (2002) A

positive-strand RNA virus replication complex parallels form and function of retrovirus capsids. Mol Cell **9:** 505–514

Schwartz M, Chen J, Lee WM, Janda M, Ahlquist P (2004) Alternate, virus-induced membrane rearrangements support positive-strand RNA virus genome replication. Proc Natl Acad Sci USA **101:** 11263–11268

Siemering K, Golbik R, Sever R, Haseloff J (1996) Mutations that suppress the thermosensitivity of green fluorescent protein. Curr Biol **6:** 1653–1663

Smalle J, Vierstra RD (2004) The ubiquitin 26S proteasome proteolytic pathway. Annu Rev Plant Biol **55:** 555–590

Solovyev AG, Stroganova TA, Zamyatnin AA Jr, Fedorkin ON, Schiemann J, Morozov SY (2000) Subcellular sorting of small membrane-associated triple gene block proteins: TGBp3-assisted targeting of TGBp2. Virology **269:** 113–127

Spillane C, Verchot J, Kavanagh TA, Baulcombe DC (1997) Concurrent suppression of virus replication and rescue of movement-defective virus in transgenic plants expressing the coat protein of *Potato virus X.* Virology **236:** 76–84

Szecsi J, Ding XS, Lim CO, Bendahmane M, Cho MJ, Nelson RS, Beachy RN (1999) Development of *Tobacco mosaic virus* infection sites in *Nicotiana benthamiana.* Mol Plant Microbe Interact **12:** 143–152

Turner KA, Sit TL, Callaway AS, Allen NS, Lommel SA (2004) *Red clover necrotic mosaic virus* replication proteins accumulate at the endoplasmic reticulum. Virology **320:** 276–290

Verchot J, Angell SM, Baulcombe DC (1998) In vivo translation of the triple gene block of *Potato virus X* requires two subgenomic mRNAs. J Virol **72:** 8316–8320

Verchot-Lubicz J (2005) A new model for cell-to-cell movement of potexviruses. Mol Plant Microbe Interact **18:** 283–290

Yang Y, Ding B, Baulcombe DC, Verchot J (2000) Cell-to-cell movement of the 25K protein of *Potato virus X* is regulated by three other viral proteins. Mol Plant Microbe Interact **13:** 599–605

Zamyatnin AA Jr, Solovyev AG, Savenkov EI, Germundsson A, Sandgren M, Valkonen JP, Morozov SY (2004) Transient coexpression of individual genes encoded by the triple gene block of *Potato mop-top virus* reveals requirements for TGBp1 trafficking. Mol Plant Microbe Interact **17:** 921–930

CHAPTER III

MUTATIONS IN THE CENTRAL DOMAIN OF POTATO VIRUS X TGBp2 ELIMINATE GRANULAR VESICLES AND VIRUS CELL-TO-CELL TRAFFICKING

Published in 2007, Feb Journal of Viology

ABSTRACT

Most RNA viruses remodel the endomembrane network to promote virus replication, maturation, or egress. Rearrangement of cellular membranes is a crucial component of viral pathogenesis. The PVX TGBp2 protein induces granular type vesicles to bud from the ER network. GFP was fused to the PVX TGBp2 coding sequence and inserted into the viral genome and into pRTL2 plasmids to study protein subcellular targeting in the presence and absence of virus infection. Mutations were introduced into the central domain of TGBp2, which contains a stretch of conserved amino acids. Deletion of a 10 amino acid segment (the m2 mutation) overlapping the segment of conserved residues eliminated the granular vesicles and inhibited virus movement. GFP:TGBp2m2 proteins accumulated in enlarged vesicles. Substitution of individual conserved residues in the same region similarly inhibited virus movement and the accumulation of mutant GFP:TGBp2 fusion proteins in enlarged vesicles. These results identify a novel element

in the PVX TGBp2 protein which determines vesicle morphology. In addition, the data indicate that granular type vesicles induced by TGBp2 are necessary for PVX plasmodesmata transport.

INTRODUCTION

Most positive strand RNA viruses cause specific changes in membrane architecture, creating distinct compartments for virus replication complexes. The types of membrane modifications include proliferations, invaginations, novel vesicles or spherules. Proliferations are seen under the electron microscope as an expansion or increase in membrane layers. Invaginations, vesicles, or spherules often derive from ER, nuclear envelope, or organelles. These viral induced compartments protect the replicating virus from host proteases and other defenses.

Poliovirus (PV), *Vaccinia virus* (VV), *Tobacco etch virus* (TEV), *Cowpea mosaic virus* (CPMV), and *Brome mosaic virus* (BMV) are examples of viruses which cause proliferation and invaginations of the ER for replication (Schaad et al., 1997; Restrepo-Hartwig and Ahlquist, 1999; Carette et al., 2000; Suhy et al., 2000; den Boon et al., 2001; Carette et al., 2002; Husain and Moss, 2003; Palacios et al., 2005). The membrane invaginations are containers for the viral replicase, protecting the replication complexes from cellular degrading enzymes. The BMV 1a is responsible for induction of vesicles, while the nature of the structures formed vary with the ratio of 1a:2a proteins (Schwartz et al., 2002; Schwartz et al., 2004). When 2a is expressed at low levels, vesicles are induced. However with increasing 2a concentration, membranes accumulate in stacks rather than vesicles (Schwartz et al., 2004).

The *Tobacco mosaic virus* (TMV) 126-kDa replicase protein induces membranous bodies to form in the absence of other TMV proteins. The TMV movement protein associates with these bodies and transports them along the microfilament network toward the periphery of the cell and, possibly, across the plasmodesmata (Kawakami et al., 2004; Liu et al., 2005). Thus, TMV is the first plant virus that has been reported to involve membrane bound replication complexes in the cell-to-cell transport pathway.

Beyond TMV, many plant viruses involve the endomembrane system in virus intracellular and intercellular movement. Examples of other viruse encoded small hydrophobic movement proteins that associate with the endomembrane system include the carmovirus p9 and p8; panicovirus ORF2 and ORF3 (6.6 and 14.6 kDa); closterovirus p6; potex-, carla-, allexi-, fovea-, hordei-, pomo-, and benyvirus TGBp2 and TGBp3; and sobemovirus p4 (15 kDa) proteins (Memelink et al., 1990; Randles and Rohde, 1990; Gilmer et al., 1992; Meshi et al., 1992; Turner et al., 1993; Ivanov et al., 1994; Martelli and Jelkmann, 1998; Grieco et al., 1999; Turina et al., 2000; Vilar et al., 2002; Zamyatnin et al., 2002; Peremyslov et al., 2004; Zamyatnin et al., 2004; Zamyatnin et al., 2006). Recent studies of *potexvirus* and *pomovirus* provide evidence for endosomal or ER-related vesicles contribute to virus cell-to-cell movement (Mitra et al., 2003; Haupt et al., 2005; Ju et al., 2005).

Research in our laboratory focuses on the potexvirus, *Potato virus X* (PVX). PVX encodes three movement proteins from three overlapping open reading frames (ORFs), termed the triple gene block (TGB). The TGB is conserved among viruses belonging to the genera *Potexvirus, Hordeivirus, Benyvirus, Carlavirus, Allexivirus,*

Foveavirus, and *Pomovirus*. These three proteins, TGBp1, TGBp2, and TGBp3, are required for virus movement.

The PVX TGBp1 protein induces plasmodesmata gating, moves from cell to cell, binds viral RNA, has ATPase activity, and forms inclusion bodies in virus infected cells (Davies et al., 1993; Rouleau et al., 1994; Angell et al., 1996; Donald et al., 1997; Lough et al., 1998; Lough et al., 2000; Yang et al., 2000; Howard et al., 2004). PVX TGBp1 is also a suppressor of RNA silencing and a recent study showed this activity is necessary for virus cell-to-cell movement (Voinnet et al., 2000; Bayne et al., 2005). The PVX TGBp2 and TGBp3 proteins are ER associated (Solovyev et al., 2000; Zamyatnin et al., 2002; Krishnamurthy et al., 2003; Mitra et al., 2003; Ju et al., 2005; Schepetilnikov et al., 2005). PVX TGBp2 has two transmembrane segments and a central domain that is conserved among TGB containing viruses (Mitra et al., 2003). Amino acid sequence analyses of the potexvirus TGBp2 proteins identified two transmembrane segments and a central domain containing conserved amino acids (Mitra et al., 2003) (Fig.1A). The same study introduced two mutations into the TGBp2 coding sequence, named m1 and m3 (Fig.1A), which disrupted the transmembrane domains (Mitra et al., 2003). These mutations inhibited virus cell-to-cell movement, indicating that membrane association of TGBp2 is necessary for virus movement (Mitra et al., 2003). Electron microscopic analysis showed that the PVX TGBp2 protein induces formation of ER-derived vesicles during virus infection (Ju et al., 2005). While some have suggested these are transport vesicles carrying virus from the site of replication to the plasmodesmata, the role of these vesicles in virus movement has not been characterized (Lucas, 2006).

TGBp3 has an N-terminal transmembrane segment and a variable C-terminal domain (Krishnamurthy et al., 2003). Confocal and electron microscopic analysis showed that TGBp3 locates in the ER. Colocalization experiments showed that the TGBp2 and TGBp3 proteins associate with the ER and peripheral bodies that may be ER-derived vesicles(Solovyev et al., 2000; Zamyatnin et al., 2002; Zamyatnin et al., 2004; Haupt et al., 2005; Schepetilnikov et al., 2005). A mutation disrupting the N-terminal transmembrane segment of TGBp3 eliminated ER association and inhibited virus cell-to-cell movement. Thus, membrane association of TGBp2 and TGBp3 is important.

In this study, we asked: Is the granular vesicles induced by TGBp2 specifically needed for virus cell-to-cell movement, or is general remodeling of the ER network important? Here we identified a deletion mutation (m2) in the central domain of the TGBp2 protein (Fig. 1A) that causes TGBp2 to accumulate in enlarged vesicles and in the ER network. The same mutation inhibits virus movement. Further amino acid substitution mutations were used to characterize a segment of the PVX TGBp2 protein which modulates the vesicle phenotype. Single amino acid substitution mutations were enough to cause TGBp2 to associate with enlarged vesicles. These data indicate that specific granular vesicles induced by PVX TGBp2 drive virus cell-to-cell movement.

RESULTS

A Deletion Mutation in the Central Domain of TGBp2 Inhibits Virus Cell-to-Cell Movement

The PVX-GFP:TGBp2 infectious clone was used to study the subcellular accumulation of TGBp2 during virus infection (Mitra et al., 2003; Ju et al., 2005). The

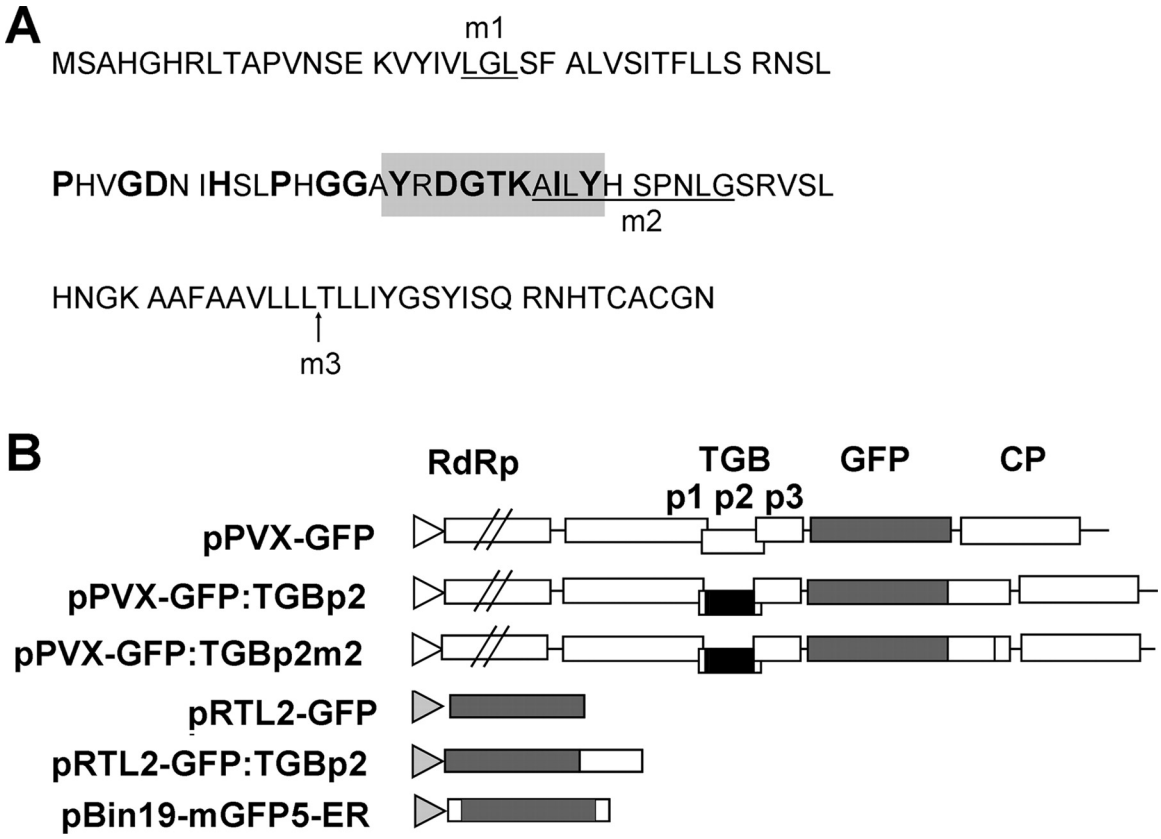

Figure 1. Diagrammatic representation of plasmids used in this work.

A, The PVX TGBp2 amino acid sequence showing conserved residues (bold) and variable residues (unbold). Ten substitution mutations replace six of the seven conserved residues highlighted in the gray box. The m1 mutation replaces a sequence encoding three amino acids, Leu-Gly-Leu (underlined), with a sequence encoding Ser-Arg-Pro. Ten amino acids (underlined) were deleted for the m2 mutation. m3 mutation is an insertion mutation. A, sequence encoding Ser-Arg-Pro was inserted at the position represented by the arrow. B, PVX infection clones and other plasmids used in this study. The name for each plasmid is indicated on the left. Open boxes represent PVX coding regions, gray boxes represent the GFP coding sequence. The PVX genome consists of five open reading frames named at the top of the panel. Abbrev: RdRp, RNA dependent RNA

polymerase; TGB, triple gene block; and CP, coat protein. The pPVX-GFP, pPVX-GFP:TGBp2, and pPVX-GFP:TGBp2m2 plasmids contain bacteriophage T7 promoter (open triangle) and the PVX genomic cDNA. The pPVX-GFP plasmid contains the GFP coding sequence between the TGB and CP coding sequences. The pPVX-GFP:TGBp2 and pPVX-GFP:TGBp2m2 plasmids contain the GFP:TGBp2 and GFP:TGBp2m2 fusions in place of the GFP coding sequence. The black boxes represent deletion mutations in the TGBp2 coding sequences in the pPVX-GFP:TGBp2 and pPVX-GFP:TGBp2m2 plasmids. The pRTL2 constructs have a CaMV 35S promoter (gray triangle).

GFP gene was fused to the 5' end of the TGBp2 coding sequences and inserted into the PVX infectious clone next to the duplicated coat protein subgenomic promoter. Most of the endogenous TGBp2 coding sequence was deleted from the PVX genome and the GFP:TGBp2 fusion was a functional replacement. The PVX-GFP infectious clone expresses GFP alone, and was used as a control (Fig. 1B) (Mitra et al., 2003; Ju et al., 2005). For both PVX-GFP:TGBp2 and PVX-GFP, fluorescence was detected in inoculated tobacco leaves as early as 3 d post inoculation (dpi) and in upper leaves by 6 dpi (Table II).

Infection foci on the inoculated leaves were studied using confocal microscopy to assess changes in subcellular distribution of the fusion protein over time. Each infection focus contains cells representing early and late infection events. The leading edge of infection contains newly infected cells, and should provide insight into where proteins accumulate prior to or during virus transport across plasmodesmata. Cells located at the center of infection represent late stages of infection and should provide insight into where proteins accumulate after virus has moved into adjacent cells.

In PVX-GFP inoculated leaves, fluorescence occurred in the cytoplasm and nucleus in all infected cells (Fig. 2, A and B). Perinuclear inclusion bodies were also observed in PVX-GFP infected cells (Fig. 2, B and C). These are likely X-bodies described in the early literature as masses containing virus particles, ER and ribosomes (Kikumoto and Matsui, 1961; Kozar and Sheludko, 1969; Allison and Shalla, 1974). In previous reports describing the formation of X-bodies, they were often referred to as centers for virus replication, translation, and encapsidation (Kikumoto and Matsui, 1961; Kozar and Sheludko, 1969; Allison and Shalla, 1974; Espinoza et al., 1991). The pattern

Table I. *Oligouncleotides used for mutagenesis of pRTL2-GFP:TGBp2 plasmids*

Plasmids[a]		Oligonucleotide
Y55S	Forward	CACGGAGGAGCT**AGC**AGAGACGGCACC
D57A	Primer	GGAGGAGCTTACAGA**GCC**GGCACCAAAGCAATC
D57E		GGAGGAGCTTACAGA**GAA**GGCACCAAAGCAATC
T59S		GCTTACAGAGACGGC**TCG**AAAGCAATCTTG
T59A		GCTTACAGAGACGGC**GCC**AAAGCAATCTTG
K60A		GCTTACAGAGACGGCACC**GCC**GCAATCTTGTAC
K60R		GCTTACAGAGACGGCACC**CGC**GCAATCTTGTAC
I62A		GGCACCAAAGCA**GCG**TTGTACAACTCCCC
Y64S		CCAAAGCAATCTTG**AGC**AACTCCCCAAATC
Y64A		CCAAAGCAATCTTG**GCC**AACTCCCCAAATC
TGBP2m1		GTA**AGTCGACCA**TCATTTGCTTTAGTTTCAATTACC
TGBP2m2		GAGACGGCACCAA**AT**CACGAGTGAGTCTACACAACGGAAAG
TGBP2m3		TG**AGTCGACCA**ACTTTGCTGATCTATGG
Y55S	Reverse	GGTGCCGTCTCT**GCT**AGCTCCTCCGTG
D57A	Primer	GATTGCTTTGGTGGC**GGC**TCTGATTGCTCCTCC
D57E		GATTGCTTTGGTGGC**TTC**TCTGATTGCTCCTCC
T59S		CAAGATTGCTTT**CGA**GCCGTCTCTGTAAGC
T59A		CAAGATTGCTTT**GGC**GCCGTCTCTGTAAGC
K60A		GTAGAAGATTGC**GGC**GGTGCCGTCTCTGTAAGC
K60R		GTAGAAGATTGC**GCG**GGTGCCGTCTCTGTAGC
I62A		GGGGAGTTGTACAA**CGC**TGCTTTGGTGCC
Y64S		GATTTGGGGAGTT**GCT**CAAGATTGCTTTGG
Y64A		GATTTGGGGAGTT**GGC**CAAGATTGCTTTGG
TGBP2m1		GA**TGGTCGACT**TACTATGTACACTTTTTCAGAATTG
TGBP2m2		**T**TTGGTGCCGTCTCGTAAGCTCCTCC
TGBP2m3		AAAGT**TGGTCGACT**CAGTAGCAAAACGGCAGCAAATGC

[a] Each mutation was separately introduced into pRTL2-GFP:TGBp2 plasmid. All plasmids except for TGBp2m2 or TGBp2m3 have introduced substitution mutations. The m2 mutation is a deletion and the m3 mutation is an insertion mutation

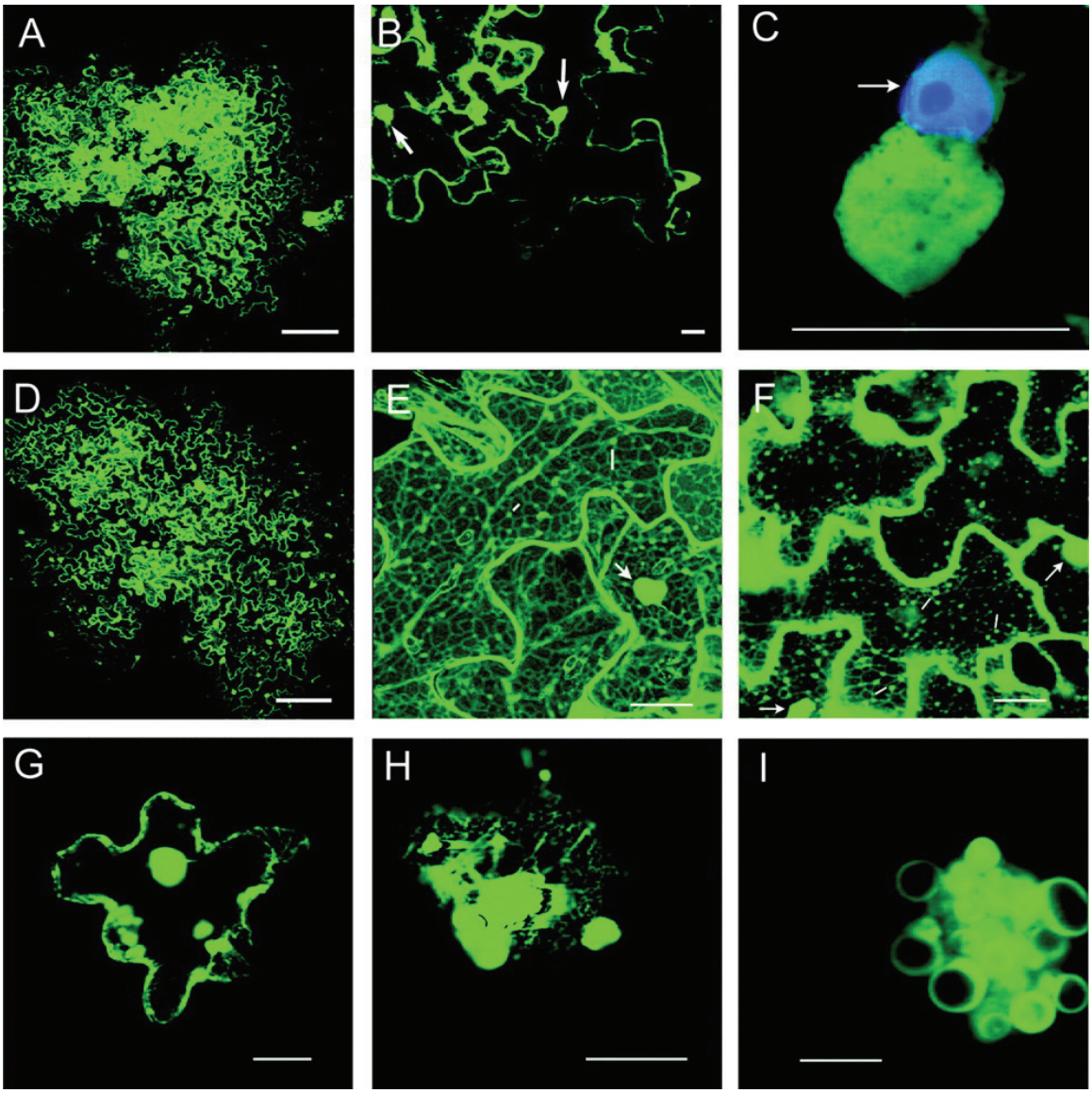

Figure 2. Confocal images of PVX infected tobacco leaves.

A, Image of infection focus on a PVX-GFP inoculated leaf taken roughly 4 dpi. Image was taken in a single optical plane. B, Image taken at 4 dpi of epidermal cells at the leading edge of PVX-GFP infection. Resulting image is a maximum projection of nine serial sections taken at 2.5 m intervals. Fluorescence is mainly cytosolic. Arrows point fluorescences of the perinuclear masses. C, At high magnification, the X-body is seen neighboring the nucleus. Cells were treated with DAPI to differentiate the nucleus

(arrow) from the X-body. D, Image taken at 4 dpi of infection focus on a PVX-GFP:TGBp2 infected leaf. Image taken in a single optical plane. E, Image of epidermal cells located at the center of a PVX-GFP:TGBp2 infection focus. Image is a maximum projection of twelve optical sections taken at 1.3 m steps. Image shows fluorescence in the ER network, in the perinuclear mass, and in granular vesicles. Granules around lines are representative examples of granular vesicles. Arrow points to both nucleus and neighboring inclusion body. F, Image of epidermal cells located at the leading edge of a PVX-GFP:TGBp2 infection focus. Image was taken in a single plane. Cells at the leading edge have mostly granular vesicles (line) and perinuclear masses (arrows). Cells just behind the leading edge show faint ER network. G to I, Images of a single epidermal cell infected with PVX-GFP:TGBp2m2 taken at 6 dpi. Each image was taken of a single plane. G, Image shows fluorescence in ER strands and large fluorescent bodies near the center and periphery of the cell. H, Image taken at high magnification shows fluorescence in the ER. Bright fluorescent bodies are seen. I, Higher magnification shows fluorescent bodies contain enlarged vesicles. For this image the Gain values were lowered to reduce brightness. This improves resolution of the enlarged fluorescent vesicles. When we reduced the Gain to resolve the structure of inclusion bodies in PVX-GFP and PVX-GFP:TGBp2 infected cells we saw an amorphous mass with no real form. We never found enlarged vesicles in X-bodies. Bars in A and D represent 200 m. Bars in B, C, E, F,and G represent 20 m. Bar in H represent 4 m.

of fluorescence seen in PVX-GFP infected cells was similar at the center and leading edge of infection.

In cells located at the center of PVX-GFP:TGBp2 infection foci, we observed fluorescence in perinuclear X-bodies, the ER network and in granular vesicles (Fig. 2, D,E, and F). In cells located at the center of infection, we see a clear ER network, granular vesicles, and perinuclear X-bodies (Fig 2,E). In cells located at the leading edge of infection, GFP:TGBp2 fluorescence was mainly in perinuclear bodies and granular vesicles (Fig. 2,F). Fluorescence was faint in the ER network. A previous study explored fluorescence accumulation in PVX-GFP:TGBp2 infected tobacco protoplasts and found fluorescence in granular vesicles as early as 12 h post inoculation (Ju et al., 2005). These combined studies suggest that the TGBp2 related granular vesicles appear early in virus infection. In a related study we compared the accumulation of GFP:TGBp2 and GFP:TGBp3 in plasmid transfected and transgenic tobacco leaves using confocal and electron microscopy (Ju et al., 2005). GFP:TGBp2 and GFP:TGBp3 were both reported in the ER, however the granular vesicles were seen only in GFP:TGBp2 expressing samples (Ju et al., 2005).

The granular vesicles contained ribosomes and immunolabelling detected BiP (an ER resident protein) in them (Ju et al., 2005). Such granular vesicles accumulate in tobacco leaves infected with PVX-GFP:TGBp2. Thus the granules shown in Fig. 2, E and F are the same granular vesicles induced by TGBp2 that were described in a previous study (Ju et al., 2005).

The m2 mutation is a deletion that eliminates 10 amino acids in the central domain of the TGBp2 protein (Fig. 1A) (Mitra et al., 2003). This mutation overlaps a

segment of highly conserved amino acids. While previous experiments showed the m2 mutation had no effect on ER association of the TGBp2 protein (Mitra et al., 2003), its impact on vesicle formation was unexamined. We introduced the m2 mutation into the PVX-GFP:TGBp2 infectious clone to study the effects of the m2 mutation on virus cell-to-cell movement. Plants inoculated with PVX-GFP:TGBp2m2 were monitored for 3 weeks and fluorescence was restricted to single cells (Fig. 2,E and Table II). Fluorescence in these cells was mainly in the ER network and in bright fluorescent bodies (Fig.2, F, G, and H). The small granular vesicles were rare. When we analyzed the bright fluorescent bodies at highest magnification we discovered they were comprised of enlarged vesicles (Fig. 2H). The X-bodies seen in PVX-GFP or PVX-GFP:TGBp2 infected cells were also "bright fluorescent bodies". However at highest resolution these resembled amorphous masses. We never observe enlarged vesicles in the X-bodies. Thus, these data suggest that the enlarged vesicles, seen in plants inoculated with PVX-GFP:TGBp2m2 transcripts, result from the m2 mutation.

The diameters of 50 granular and 50 enlarged vesicles were measured. The average diameter of the granular vesicles was 0.5 m $\pm$0.1 m and of the enlarged vesicles was 1.4 m $\pm$ 0.5 m. The dimensions of the granular vesicles measured in this study were similar to the dimensions measured previously using electron micrographs (Ju et al., 2005).

Subcellular Localization of Fluorescent Proteins during Virus Infection in Protoplasts

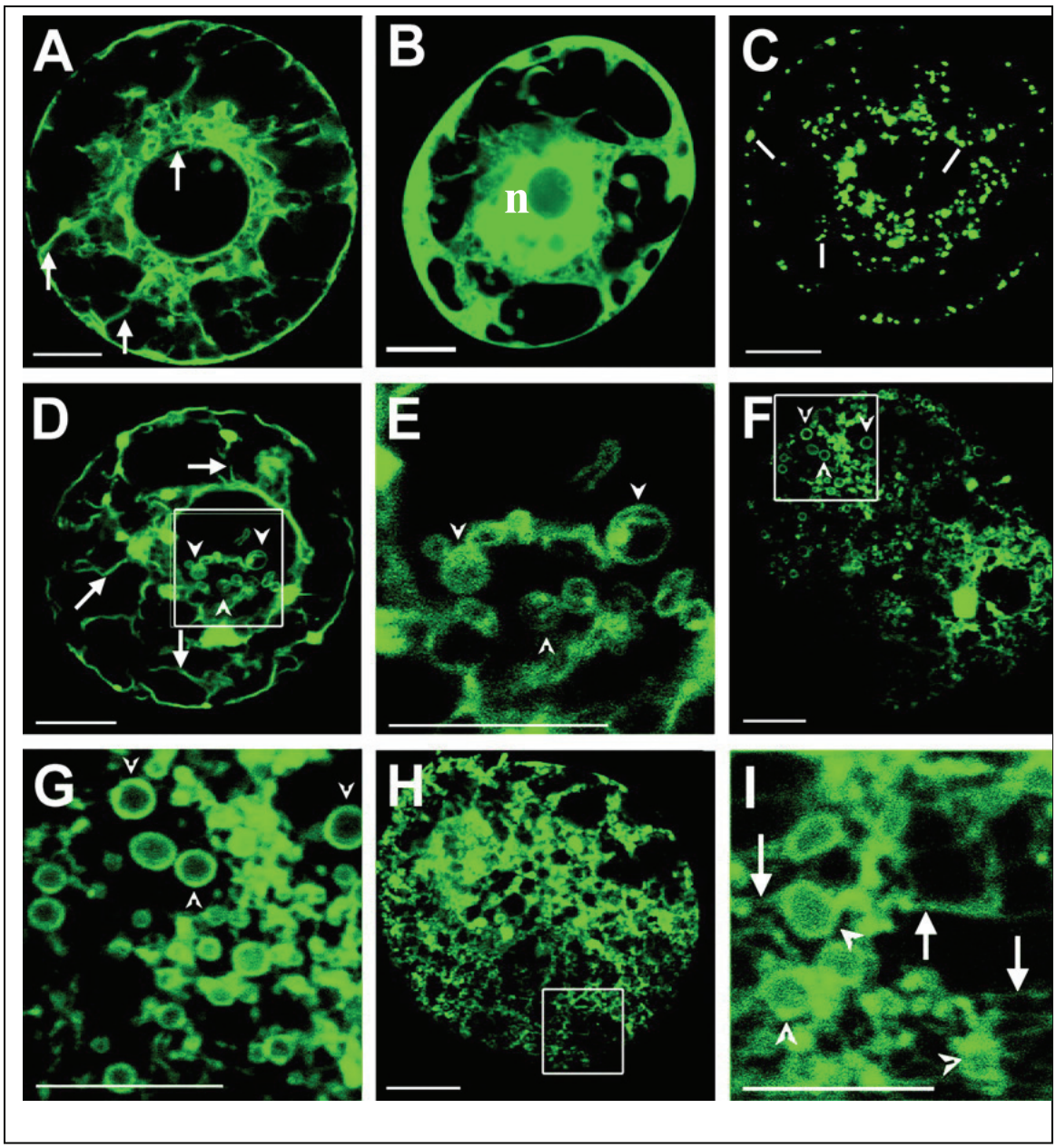

Figure 3. Confocal images show fluorescence patterns in virus infected protoplasts. In each panel arrows point to perinuclear and cortical ER, straight lines point to representative examples of granular vesicles, and arrowheads point to enlarged vesicles. A, Protoplasts expressing mGFP5-ER. B. Protoplast inoculated with PVX-GFP shows fluorescence in the nucleus (n) and cytoplasm. Image was taken at 24 hour post

inoculation (hpi). C, Image of protoplast inoculated with PVX-GFP:TGBp2 at 24 hpi. D and E, Images of PVX-GFP:TGBp2m2 inoculated protoplast at 24 hpi. D, Box highlights enlarged vesicles, which appear to bud from the perinuclear ER. E, View at high magnification of enlarged vesicles seen in the box in panel D. F to I, Images of PVX-GFP:TGBp2m2 inoculated protoplast at 48 hpi. F and H, Images showing condensed ER network. Many enlarged vesicles occur throughout the cortical region of the protoplasts. G and I, View at high magnification of enlarged vesicles seen in the box in panels F and H, respectively. At high magnification the enlarged vesicles seem tethered by strands of ER. These images suggest the budding process might be disrupted by the m2 mutation. Bars in all panels represent 10 μm.

To view early events in virus infection, protoplasts were transfected with PVX-GFP, PVX-GFP:TGBp2, or PVX-GFP:TGBp2m2 transcripts and then analyzed at 18, 24, 36, and 48 h post inoculation (hpi) using confocal microscopy. Protoplasts expressing mGFP5-ER were included for comparison (Fig. 3A). Between 18 and 48 hpi, fluorescence was in the cytoplasm and nucleus of PVX-GFP infected protoplasts, as expected (Fig. 3B).

In PVX-GFP:TGBp2 infected protoplasts, fluorescence was mainly in granular vesicles (Fig. 3C) (Ju et al., 2005). At all time points, PVX-GFP:TGBp2m2 infected protoplasts showed fluorescence mainly in the ER and enlarged vesicles (Fig. 3, D, F, and H). There were fewer granular vesicles (Fig 3D). A strand of ER surrounds the nucleus and can be seen in most protoplasts. At higher magnification, some of the enlarged vesicles appeared to be associated with strands of perinuclear or cortical ER (Fig. 3, D, G, and I).

Subcellular Targeting of Wild-Type and Mutant GFP:TGBp2 Proteins in Leaves

Tobacco leaves were bombarded with pRTL2-GFP:TGBp2 or pRTL2-GFP:TGBp2m2 plasmids and treated with FM4-64 dye. GFP:TGBp2 was seen in granular vesicles and GFP:TGBp2m2 accumulated mainly in the ER and enlarged vesicles (Fig. 4,A and D). Since previous studies indicated that the GFP:TGBp2 related vesicles were novel structures derived from the ER, we conducted further tests to determine if the granular or enlarged vesicles are related to the plasma membrane or endocytic structures. Red fluorescence due to FM4-64 dye is initially seen in the plasma membrane and in endocytic vesicles budding from the plasma membrane. Following

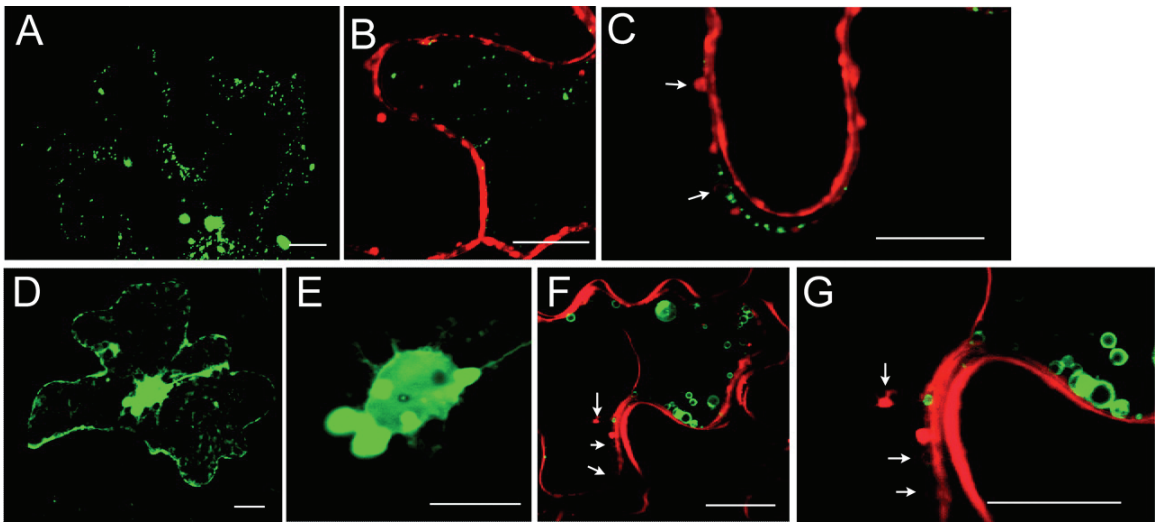

Figure 4. Confocal images of tobacco leaf epidermal cells bombarded with pRTL2-GFP:TGBp2 or –GFP:TGBp2m2 and treated with FM4-64 dye. In each panel, arrows point to endocytic vesicles budding from the plasma membrane. A toC, Images show GFP:TGBp2 fluorescence in granular vesicles. FM4-64 stains the plasma membrane. D to G, Images show GFP:TGBp2m2 in the ER and enlarged vesicles. E, Image shows vesicles budding from the perinuclear ER. F and G, Images of an epidermal cell and the base of a trichome. FM4-64 stains both the epidermal cell and neighboring trichome. Green fluorescent vesicles are neighboring endocytic vesicles along the plasma membrane. Bars represent 10 m.

prolonged incubation, endocytic vesicles carry FM4-64 dye into the Golgi and vacuole. Thus, FM4-64 is used to trace to trace the endocytic pathway from the plasma membrane to the Golgi and vacuole FM-dyes (Bolte et al., 2004). FM4-64 dye does not label the ER or nuclear envelope FM-dyes (Bolte et al., 2004). In Fig. 4, FM4-64 labels the plasma membrane and endocytic vesicles. Leaf samples were incubated with FM4-64 dye between 30 min and 3 hours, and we never detected red fluorescence in the TGBp2 related granular vesicles (Fig. 4, A, B, and C). While the granular and endocytic vesicles were often seen adjacent to one another along the plasma membrane, the red and green signals never appeared to overlap. Similar observations were made in the case of GFP:TGBp2m2. The GFP:TGBp2m2 enlarged vesicles were seen along the perinuclear ER and the plasma membrane (Fig. 4, E and F). Endocytic vesicles seen budding from the plasma membrane were often neighboring GFP:TGBp2m2 related vesicles. However, the red and green signals do not overlap (Fig 4, F and G). Thus the GFP:TGBp2 and GFP:TGBp2m2 induced vesicles were unrelated to the plasma membrane or endocytic pathway(Bolte et al., 2004).

Subcellular Targeting of Wild-Type and Mutant GFP:TGBp2 Proteins in Protoplasts

Five pRTL2 plasmids containing GFP, GFP:TGBp2, GFP:TGBp2m1, GFP:TGBp2m2, or GFP:TGBp2m3 coding sequences were transfected to BY-2 protoplasts. Prior investigations showed that the m1 and m3 mutations lie in the transmembrane domains, while the m2 mutation lies in the central conserved domain (Fig 1A) (Mitra et al., 2003). Since m1, m2, and m3 lie in separate subdomains of TGBp2,

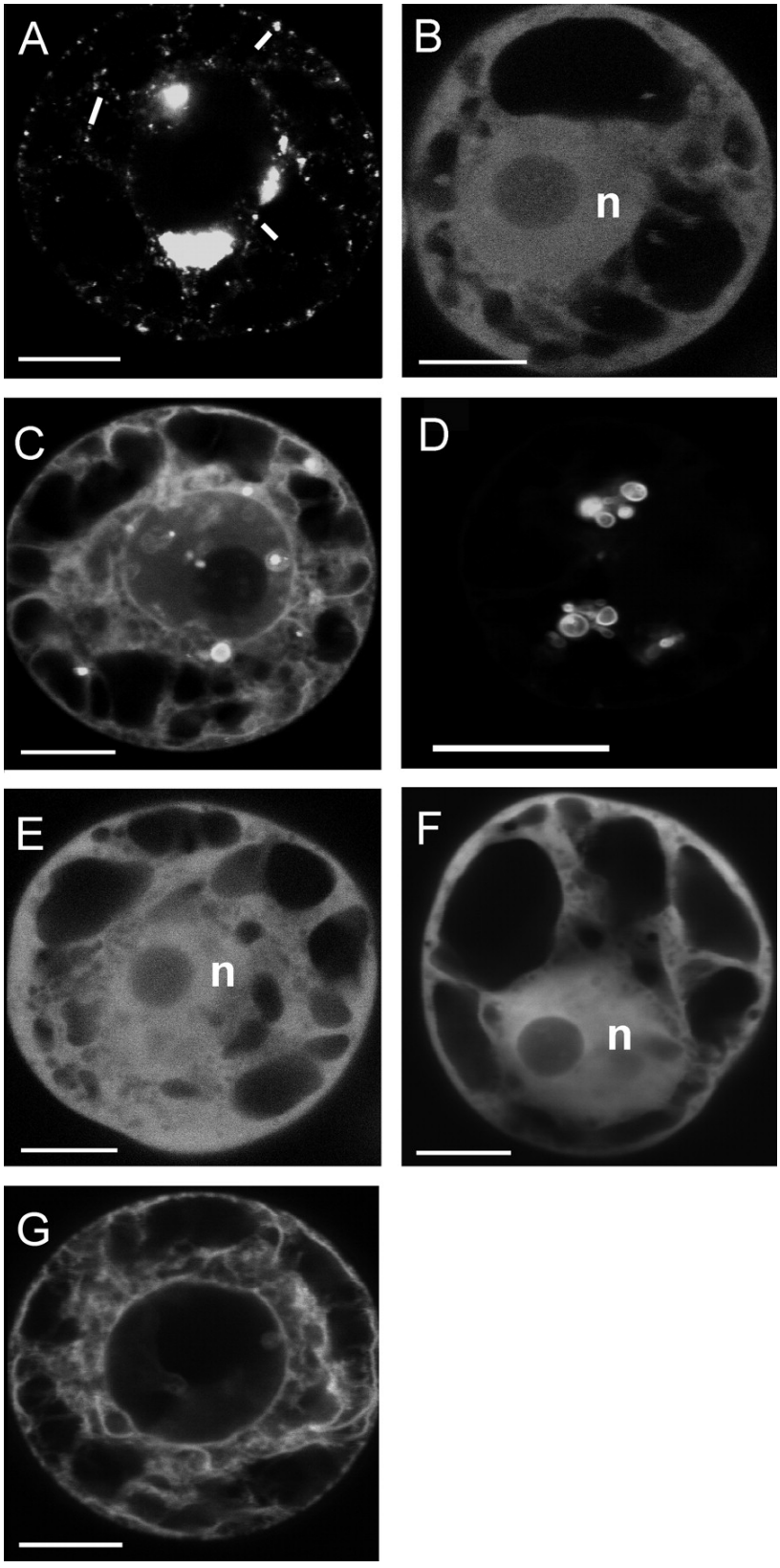
A
B
n
C
D
E
n
F
n
G

Figure 5. Confocal images of protoplasts taken between 18 and 24 h post transfection with pRTL2 plasmids. A, Protoplast transfected with pRTL2-GFP:TGBp2 showing fluorescence in granular vesicles. Some vesicles aggregate in the perinuclear region. White lines point to few representative granular vesicles. B, Protoplast transfected with pRTL2-GFP:TGBp2m1 showing nuclear and cytosolic fluorescence. C and D, Protoplasts transfected with pRTL2-GFP:TGBp2m2 showing ER network and enlarged vesicles. D, Image shows only enlarged vesicles. For this image the Gain values were lowered to reduce brightness and improve resolution. With slightly higher Gain values the ER network is seen in panel C, and resolution of the enlarged vesicles is reduced. E, Protoplast transfected with pRTL2-GFP:TGBp2m3 showing nuclear and cytosolic fluorescence. F, Protoplast transfected with pRTL2-GFP showing nuclear and cytosolic fluorescence. G, Transgenic protoplast expressing mGFP5-ER showing fluorescence in the perinuclear and cortical ER. Abbreviations: n = nucleus. Bars in all images except D represent 10 μm. Bar in D represents 2 m.

these experiments were designed to determine if the central conserved domain of TGBp2 is functionally distinct from the transmembrane domains.

The subcellular accumulation patterns seen here in protoplasts were also confirmed in bombarded leaves (Fig. 4A) (Mitra et al., 2003; Ju et al., 2005). GFP:TGBp2 fluorescence was mainly associated with granular vesicles at 24 h post transfection (Fig. 5A). Sometimes we detected fluorescent aggregates in pRTL2-GFP:TGBp2 transfected protoplasts which were not detected in PVX-GFP:TGBp2 infected protoplasts. These may be aggregates of granular vesicles or artifacts resulting from protein over-expression from a CaMV 35S promoter. GFP:TGBp2m1 and GFP:TGBp2m3 fluorescence accumulated in the cytoplasm and nucleus (Fig. 5, B and E).

The m1 and m3 mutations, which lie in the transmembrane domains of TGBp2, disrupted ER association of GFP:TGBp2, as reported previously (Mitra et al., 2003). GFP:TGBp2m2 fluorescence associated with enlarged vesicles, the perinuclear and cortical ER (Fig. 5,C and D) (Mitra et al., 2003). Granular vesicles were rare in GFP:TGBp2m2 expressing cells. This pattern of fluorescence resembled observations in PVX-GFP:TGBp2m2 inoculated plants and protoplasts. Thus the m2 mutation, disrupting the central conserved domain of TGBp2, caused the protein to accumulate in the ER and in enlarged vesicles.

To determine if the enlarged vesicles were rare or frequent occurrences in GFP:TGBp2 and GFP:TGBp2m2 expressing cells, the presence of fluorescence in the ER network, granular, and enlarged vesicles was quantified (Fig. 6,A and B). For

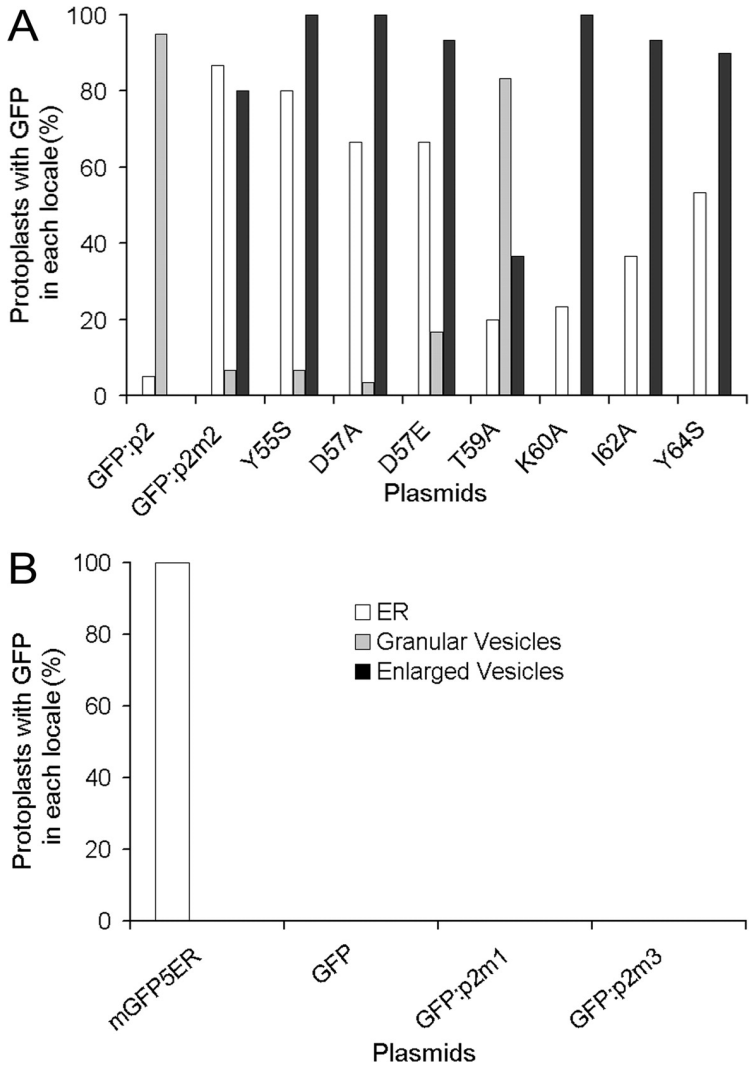

Figure 6. Bar graphs depict the percentage of protoplasts containing fluorescence in the ER network, granular vesicles, and enlarged vesicles following transfection with pRTL2 plasmids. A, Twenty protoplasts expressing GFP:TGBp2 and thirty protoplasts expressing each mutant GFP:TGBp2 protein were scored for fluorescence in each of the three subcellular domains. The percentages were compared statistically to determine a correlation between fluorescence in each subcellular domain. The statistics are provided in the Results. B, Control samples were scored for fluorescence in each of these domains but were not included in the statistical analysis. Fifteen mGFP5-ER and thirty GFP, GFP:TGBp2m1, and GFP:TGBp2m3 expressing protoplasts were scored.

comparison, protoplasts expressing GFP only, or mGFP5-ER were also quantified (Fig. 6B). Plasmids containing mGFP5-ER encode a version of GFP that has an N-terminal basic chitinase signal peptide and a C-terminal HDEL sequence for ER targeting and retention. One hundred percent of protoplasts (30/30) expressing GFP contained fluorescence in the cytosol and nucleus (data not shown). GFP fluorescence was not membrane associated (Fig. 6B).

The data above is in contrast to that of mGFP5-ER, for which 100% (15/15) of the protoplasts contained fluorescence in the ER network. Granular and enlarged vesicles were absent from mGFP5-ER expressing protoplasts (Fig. 6B). Ninety five % of GFP:TGBp2 expressing protoplasts (19/20) contained fluorescence in granular vesicles and 5% showed fluorescence in the ER (1/20; Fig. 6A). As expected, 100% of GFP:TGBp2m1 and GFP:TGBp2m3 expressing protoplasts contained fluorescence in the cytosol and nucleus and not in the ER or vesicles (Fig. 6B). In GFP:TGBp2m2 expressing protoplasts, 86% contained fluorescence in the ER, 80% contained enlarged vesicles, while only 7% contained granular vesicles (Fig. 6A). Since a greater proportion of GFP:TGBp2m2 expressing protoplasts contained enlarged vesicles than granular vesicles, these data indicate that the m2 mutation caused GFP:TGBp2 to accumulate in enlarged vesicles.

Wild-Type and Mutant GFP:TGBp2 Fusion Proteins have Similar Half-Lives

Clearly the m1, m2, and m3 mutations altered the subcellular distribution patterns of GFP:TGBp2 fluorescence. The best explanation is that these mutations disrupt targeting sequences in the PVX TGBp2 protein. However, it is also possible that the

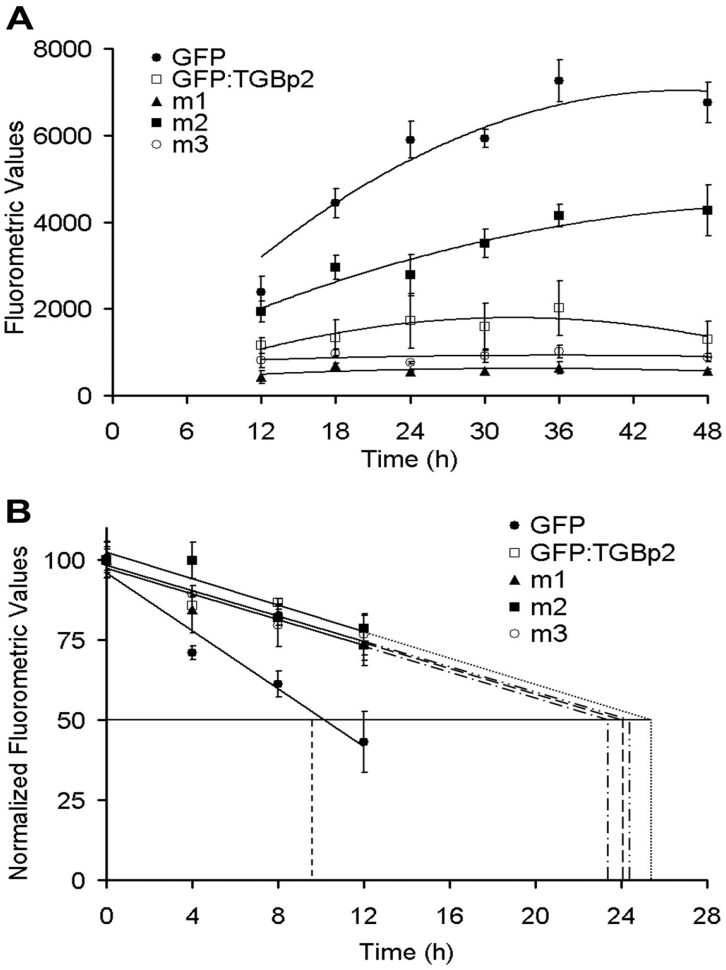

Figure 7. Average fluorometric values in a time course analysis of BY-2 protoplasts transfected with pRTL2 plasmids. Each time point is the average of three fluorometric values.

A, Graph of the average fluorometric values for transfected protoplast between 18 and 48 h post transfection. A best-fit curve was determined using a second-order polynomial regression. B, Transfected protoplasts were treated with cycloheximide at 24 h post transfection. The average fluorometric values were normalized to time 0 (24 h post transfection) and then plotted using a linear regression. The horizontal line at 50 determines the half-life. The dotted lines represent the calculated protein half-lives determined by linear regression.

mutations alter the stability of TGBp2, causing the fusion proteins to be targeted to the cytosol for degradation. Fluorometric assays were used to quantify GFP expression over time as a measure of both protein accumulation and degradation in BY-2 protoplasts (Ju et al., 2005). Transfected protoplasts were chased at 24 h with cycloheximide to halt protein synthesis. Fluorometric values were measured at 0, 4, 8, and 12 h following cycloheximide treatment and the protein half-lives were calculated.

The fluorometric values were normalized to the measurement at 0 h (this value was set at 100%). The data were plotted and linear regression was used to calculate protein half-lives. We predicted that if protein turnover was stimulated as the result of the mutations, then fluorescence would decline more rapidly than in pRTL2-GFP or –GFP:TGBp2 transfected protoplasts.

Fluorescence values measured in protoplasts transfected with pRTL2-GFP were higher than in protoplasts expressing the fusion proteins (Fig. 7A). Between 18 h and 48 h post transfection, GFP values were 3 to 5-fold greater than GFP:TGBp2 values. In general, fluorometric values for all proteins seemed to fluctuate across a plateau between 24 and 48 h post transfection (Fig. 7A) (Ju et al., 2005).

Following addition of cycloheximide, the rate of decrease in GFP fluorescence was greater than the rate of decrease for wild-type and mutant GFP:TGBp2 fluorescence (Fig. 7B). The half-life of GFP was 10.2 h. The GFP:TGBp2, GFP:TGBp2m1, GFP:TGBp2m2, and GFP:TGBp2m3 proteins had similar half lives of 24.5, 23.7, 25.5, and 24.3 h, respectively. The wild-type and mutant GFP:TGBp2 proteins were more stable than the non-fused GFP protein (Fig. 7B). Thus, changes in the subcellular

distribution of mutant GFP:TGBp2 proteins resulted specially from m1, m2, and m3 mutations, rather than from changes in protein stability.

Highly Conserved Amino Acids Regulate Vesicle Phenotype

The m2 deletion mutation overlaps a highly conserved amino acid sequence in the TGBp2 protein (Fig. 1A). The highly conserved amino acids were identified in a prior study by aligning the amino acid sequence of TGBp2 proteins from nine potexviruses (Mitra et al., 2003). If these conserved amino acid residues are essential to form granular vesicles, then single substitution mutations might produce alternative membrane structures. Moreover, if enlarged vesicles were the result of a defect in the ability of TGBp2 to form granular vesicles, then substitution of conserved amino acid residues would result in production of the enlarged vesicles rather than the granular vesicles.

Seven mutations encoding amino acid substitutions were introduced into pRTL2-GFP:TGBp2 plasmids replacing Tyr55 with Ser; Asp57 with Ala or Glu; Thr59 with Ala; Lys60 with Ala; Ile62 with Ala; and Tyr64 with Ser. Protoplasts were transfected with mutant pRTL2-GFP:TGBp2 plasmids and viewed at 24 h post transfection. A random set of 30 protoplasts were scored for the presence of fluorescence in the ER, granular vesicles, and enlarged vesicles. Fluorescence occurred mainly in the ER and enlarged vesicles in protoplasts expressing GFP:TGBp2-Y55S, -D57A, -D57E, -K60A, -I62A, and -Y64S (Fig. 6A and 8). Between 0 and 17% of protoplasts contained a few granular vesicles. The reduction in granular vesicles due to these mutations resembles the reduction due to GFP:TGBp2m2. These data suggest that Tyr55, Asp57, Lys60, Ile62, and Tyr64 modulate the nature of vesicles associated with GFP:TGBp2 fluorescence (Fig. 6A and 8). Replacing Thr59 with Ala increased the proportion of protoplasts

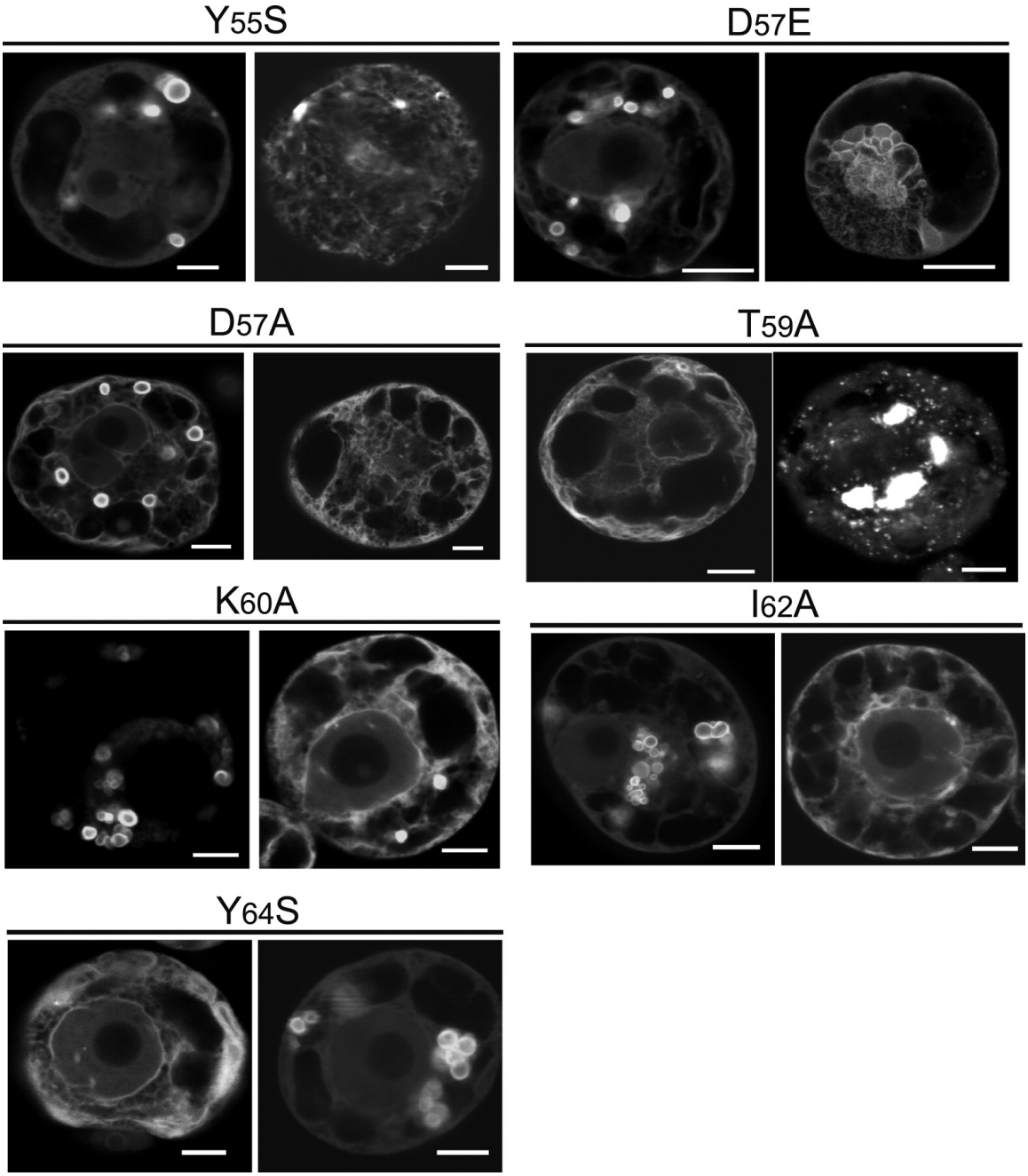

Figure 8. Confocal images show protoplasts transfected with mutant pRTL2-GFP:TGBp2 plasmids at 24 h post transfection. The panels are representative images for each substitution mutation. Each amino acid substitution mutation is identified above the corresponding panels. Bars in all images represent 10 μm.

containing enlarged vesicles, although granular vesicles were not eliminated (Fig. 6,A and 8). The result of substituting Thr59 with Ala was not as significant as substitutions replacing Tyr 55, Asp 57, Ile62, and Tyr64 (Fig. 6,A and 8), indicating that Thr59 is not as important as the other residues for determining the vesicle phenotype.

In comparing GFP:TGBp2, with each of the mutant proteins in Fig. 6A, it seems that deletion and substitution mutations that reduce protein accumulation in granular vesicles also increase accumulation in the ER and enlarged vesicles.

Statistical analysis revealed an inverse correlation between the number of protoplasts showing fluorescence in granular and in enlarged vesicles ($R=-0.96$; $p<0.0001$) and between those in granular and in ER ($R=-0.66$; $p=0.0551$). The number of protoplasts showing fluorescence in enlarged vesicles and those in ER network positively correlate ($R= 0.66$; $p=0.0529$). Thus, a decline in granular vesicles is responsible for an increase in fluorescence in the ER and enlarged vesicles. Since TGBp2 induces vesicles from the ER network, the statistical data indicate that the mutations either cause TGBp2 to be redirected from granular into enlarged vesicles, or alter vesicle morphology causing enlarged vesicles to accumulate.

Substitution Mutations Inhibit PVX Cell-to-Cell Movement

Each substitution mutation was introduced into the PVX-GFP infectious clone to examine the effects of the single amino acid substitution mutations on virus cell-to-cell movement. Transcripts were prepared and inoculated to tobacco leaves to determine if the mutations had any effect on virus movement. GFP expression was used to monitor the

Table II. *Tobacco plants that are systemically infected with modified PVX viruses*

Viruses	Proportion of plant with systemic virus infection[a]
PVX-GFP	15/15
PVX-GFP:TGBp2	15/15
PVX-GFP:TGBP2m2	0/15
PVX-GFP-Y55S	0/12
PVX-GFP-D57A	0/12
PVX-GFP-D57E	0/12
PVX-GFP-T59A	0/12
PVX-GFP-K60A	0/12
PVX-GFP-I62A	1/12[b]
PVX-GFP-Y64S	5/27[b]

[a] Propotions represent the numbers of plants showing fluorescence in upper non-inoculated leaves by 16 dpi relative to the total numbers of plants inoculated with each virus.

[b] RNA was isolated from systemically infected plants, RT-PCR was conducted and PCR products were sequenced. Sequencing results show mutations reverted to wild-type sequence.

spread of infection until 16 dpi. As mentioned previously, PVX-GFP infection was detected in inoculated leaves as early as 3 dpi and in upper leaves by 6 dpi. PVX-GFP-Y55S, -D57A, -D57E, T59A, and K60A were restricted to single cells in inoculated leaves (Table II).

These data indicate: 1) that mutations causing TGBp2 to accumulate in the ER and enlarged vesicles also inhibit virus cell-to-cell movement; and 2) that granular vesicles are important for virus cell-to-cell movement. Between 8 and 18% of plants inoculated with PVX-GFP-I62A and –Y64S showed systemic virus accumulation. In these plants, GFP expression was detected in expanding infection foci on the inoculated leaves by 7 dpi and in upper leaves by 9 dpi.

Virus movement was delayed relative to PVX-GFP. For all plants that showed systemic virus accumulation, RNA was isolated and RT-PCR was conducted to amplify the TGB coding region. PCR products were sequenced and the systemically accumulating virus in plants inoculated with PVX-GFP-I62A and –Y64S did not contain the same mutation. Thus, virus movement was seen only when the mutations reverted to the wild-type sequence. The same mutations causing GFP:TGBp2 to accumulate in enlarged vesicles also inhibited virus cell-to-cell movement (Table II).

The T59A mutation caused GFP:TGBp2 to accumulate in enlarged vesicles and showed a high proportion of protoplasts containing granular vesicles. Since this mutation inhibited PVX cell-to-cell movement (Table II), Thr59 likely contributes to other TGBp2 activities needed for virus movement, beyond regulating granular vesicle morphology.

DISCUSSION

In previous studies we showed that GFP:TGBp2 accumulates in small granular vesicles when the fusion was expressed from the PVX genome in BY-2 protoplasts or infected leaves. We also saw the same granular vesicles when GFP:TGBp2 was expressed from the CaMV 35S promoter in BY-2 protoplasts, bombarded leaves, and transgenic tobacco leaves (Mitra et al., 2003; Ju et al., 2005). Using electron microscopy and cryo-embedded samples, we presented evidence that these granular vesicles consist of ER membranes. These vesicles contain ribosomes and immunolabelling detected BiP, an ER resident protein, in these vesicles (Mitra et al., 2003; Ju et al., 2005). In this study, GFP:TGBp2 expressing cells were treated with FM4-64 dye, which is often used to trace membranes through the endocytic pathway. The red fluorescence observed in the plasma membrane and endocytic vesicles never overlapped with green fluorescence in the GFP:TGBp2 expressing vesicles. These data support previous evidence that the GFP:TGBp2 related vesicles are novel structures derived from the ER and are unrelated to the plasma membrane and endosome.

A study of *Potato mop top virus* (PMTV) showed TGB proteins associate with two types of vesicles: small granular vesicles and endocytic vesicles. The granular vesicles are described as transport vesicles carrying viral RNA to the plasmodesmata (Haupt et al., 2005). In this model these granular vesicles fuse with the plasma membrane (Haupt et al., 2005). Prior studies showed that the PVX TGBp2-induced vesicles associate with the microfilament network (Ju et al., 2005). The PVX TGBp2 induced vesicles might traffic along microfilaments toward the plasmodesmata. For PMTV, evidence indicates that TGBp2 and TGBp3 proteins are recaptured from the plasma membrane by endocytic vesicles, which carry them back to the site of virus

replication (Haupt et al., 2005). While experiments using FM4-64 in this study did not detect PVX TGBp2 associating with the endosome, the results of mutational analysis indicate that the PVX TGBp2 induced granular vesicles are specifically required for virus cell-to-cell movement. Eight mutations were introduced into the central region of the PVX TGBp2 protein. One mutation deleted 10 amino acids, while seven other mutations were substitutions replacing individual residues. Granular vesicles were absent from cells expressing the mutant GFP:TGBp2 proteins. Table 2 shows that these mutations also inhibited virus movement. These data suggest that PVX, similar to PMTV, require these granular vesicles for virus movement.

TGBp2 has three domains: N-terminal and C-terminal transmembrane segments, and a central sequence which lies in the ER lumen (Zamyatnin et al., 2006). The central domain of TGBp2 has a segment of highly conserved amino acid residues between position 40 and 64. In this study we introduced substitution mutations replacing residues between position 55 and 64. These mutations increased GFP:TGBp2 association with the ER and enlarged vesicles, while decreasing its association with granular vesicles. These data suggest that Tyr55, Asp57, Lys60, Iso62, and Tyr64 represent a segment of conserved amino acids which determine the nature of vesicles containing GFP:TGBp2 proteins.

One explanation for the enlarged vesicles is that the mutations had altered the subcellular targeting of GFP:TGBp2 causing the proteins to accumulate in the endosome rather than in the granular vesicles. To test this idea, cells expressing the mutant GFP:TGBp2 proteins were treated with FM4-64. The results indicate that the enlarged vesicles were not related to the endosome. Further evidence that the enlarged vesicles are

not endocytic vesicles was presented in Fig 3. In PVX-GFP:TGBp2 infected protoplasts we observed enlarged vesicles associating with the nuclear envelope. In some instances we observed these vesicles tethered to the cortical ER network (Fig. 3I). The protoplast images in Figs 3G and 3I suggest that the GFP:TGBp2m2 proteins may cause bubbles to form from the perinuclear and cortical ER which become enlarged vesicles. It is worth speculating that the enlarged vesicles result from defects in vesicle formation triggered by TGBp2. However, we cannot be certain whether the enlarged vesicles are the result of mutations that alter the dimensions of the vesicles, cause a defect in the budding process, or cause TGBp2 to be directed into another type of cellular vesicle. Further analysis is needed characterize the identity or origin of these enlarged vesicles.

Since the central domain of TGBp2 lies in the interior of the ER, this sequence may interact with ER lumenal factors, such as small GTPases (ARFs), which regulate vesicle formation. If TGBp2 induced vesicles function as transport vesicles, it is reasonable to consider that they may have features resembling plant transport vesicles. For example, formation of COPI, COPII, or post-Golgi vesicles typically involves ARFs which are involved in the recruitment of coat proteins. These ARFs are crucial for vesicle budding as well as for fusion with target membranes (Nebenfuhr, 2002; Jurgens, 2004; Yang et al., 2005). Perhaps TGBp2 associates with ARFs in the ER lumen to drive vesicle formation. Another possibility is that the central conserved domain of PVX TGBp2 is necessary for oligomeriation of TGBp2 along the membrane surface. TGBp2 oligomers may cause deformation of ER membranes leading to vesicle formation. Perhaps the mutations tested in this study functioned to weaken or inhibit TGBp2 oligomerization and thereby alter vesicle morphology. Further mutational analysis is

needed to define the extent of the conserved sequence which may affect conversion of granular vesicles into enlarged vesicles and to determine if this sequence governs TGBp2 interactions with itself or cellular proteins.

Another explanation for the images in Fig. 3 showing enlarged vesicles tethered to the ER is that these vesicles are fusing with the ER. If the granular vesicles transport viral RNA to the cell surface, they could fuse with the cortical ER releasing their contents into the plasmodesmata for transport into neighboring cells. In this scenario the mutations may cause a defect in vesicles fusing with the ER resulting in the enlarged bubbles that appear to be tethered to the ER network. This model requires that granular vesicles were successfully produced, traffic to the periphery of the cell, associate with the ER network near plasmodesmata, and get stuck while fusing with the ER. This could explain loss of movement for PVX-GFP-T59A. In protoplasts expressing GFP:TGBp2-T59A we saw 83% contained granular vesicles and 37 % contained enlarged vesicles. This mutation had little effect on granular vesicles while causing an increase in enlarged vesicles. Loss of virus movement could occur if the mutation causes vesicles to get stuck and form bubbles while fusing to the ER, and if vesicle fusion with the ER is important for virus movement. Further research is needed to define the origin and target of granular and enlarged vesicles.

Many RNA viruses cause ER modifications to promote virus replication or maturation RNA virus (Schaad et al., 1997; Restrepo-Hartwig and Ahlquist, 1999; Carette et al., 2000; Suhy et al., 2000; den Boon et al., 2001; Carette et al., 2002; Ahlquist et al., 2003; Husain and Moss, 2003; Palacios et al., 2005; Salonen et al., 2005).

These modifications influence protein sorting, secretion, membrane permeability affecting host defense responses, ER stress, and apoptosis (Liu et al., 2005). Real time imaging of TMV have shown that the viral MP binds to membrane bound replication complexes and carries these toward the plasmodesmata for cell-to-cell transport (Kawakami et al., 2004; Liu et al., 2005). We do not yet know if PVX TGBp2 associates with the PVX replicase or, like TMV, moves replication complexes across the plasmodesmata. While evidence of membrane bound bodies contributing to plasmodesmata transport have recently described for TMV and PVX, this study is the first to use mutational analysis to show that viral induced vesicles are necessary for intercellular trafficking.

MATERIALS AND METHODS

Bacterial Strains and Plasmids

The *Escherichia coli* strains JM109, DH5α, and XL10 Gold were used for transformation of all plasmids. Dr. J. Hasselof (Medical Research Council Laboratory of Molecular Biology, Cambridge, UK)(Siemering et al., 1996) provided the pBIN-mGFP5-ER plasmid used here to transform *Agrobacterium tumefaciens* strain LBA4404 to prepare transgenic BY-2 cultures.

The parental and mutant pPVX-GFP, pPVX- GFP:TGBp2, and pPVX-GFP:TGBp2m2 plasmids contain the PVX genome beside a bacteriophage T7 promoter (Baulcombe et al., 1995). The plasmids pPVX-GFP and pPVX-GFP:TGBp2 contain the GFP or GFP:TGBp2 fused genes inserted next to the duplicated coat protein subgenomic promoter, as described previously(Ju et al., 2005). Nt positions 5170 and 5423 were

deleted within the viral genome in both pPVX-GFP:TGBp2 and pPVX-GFP:TGBp2m2 plasmids(Ju et al., 2005). This mutation removes most of the TGBp2 coding sequence within the triple gene block (Fig. 1). The pPVX-GFP:TGBp2m2 plasmid (Fig. 1) is similar to pPVX-GFP:TGBp2 but has 30 nts deleted from the central domain of TGBp2 within the GFP:TGBp2 fused sequences (Fig. 1). The GFP:TGBp2m2 coding sequence was PCR amplified from pRTL2-GFP:TGBp2m2 plasmids using primers containing added *Cla*I and *Sal*I restriction sites(Mitra et al., 2003). The GFP:TGBp2m2 coding sequence was inserted into the PVX genomic cDNA between *Cla*I and *Sal*I sites next to the duplicated coat protein subgenomic promoter (Ju et al., 2005).

The TGBp2 protein has a conserved amino acid sequence: $G_{52}G_{53}XY_{55}XD_{57}G_{58}$ $T_{59}K_{60}XI_{62}XY_{64}$ (Mitra et al., 2003). Substitution mutations were introduced into pPVX-GFP and pRTL2 plasmids using the Quick Change Site-Directed Mutagenesis kit (Stratagene, La Jolla, CA). Three nts encoding S (AGC) replaced Y_{55} (TAC); nts encoding A (GCC) or E (GAA) replaced D_{57} (GAC); nts encoding A (GCC) replaced T_{59} (ACC); nts encoding A (GCC) replaced K_{60} (AAA); nts encoding A (GCG) replaced I_{62} (ATC); and nts encoding S (AGC) replaced Y_{64} (TAC). Mutagenic primers were extended using the prescribed temperature cycling regime. Sequences of the forward and reverse mutagenic primers are detailed in Table 1.

The pRTL2-GFP, -GFP:TGBp2, -GFP:TGBp2m1, -GFP:TGBp2m2, and -GFP:TGBp2m3 were described previously (Mitra et al., 2003). These plasmids contain the *Cauliflower mosaic virus* (CaMV) 35S promoter and *Tobacco etch virus* (TEV) translational enhancer (Carrington and Freed, 1990) upstream of the coding sequences. The pRTL2-GFP:TGBp2 plasmid contains the GFP coding sequence fused to the 5' end

of the PVX TGBp2 coding sequence (Krishnamurthy et al., 2002). The pRTL2-GFP:TGBp2m1 contains a substitution mutations replacing 9 nts, TTAGGTCTA (encoding Leu-Gly-Leu), with AGTCGACCA (encoding Ser-Arg-Pro) between nt positions 61 to 69 within the TGBp2 coding sequence sequence (Mitra et al., 2003). The pRTL2-GFP:TGBp2m2 plasmid has 30 nts deleted from the central domain of TGBp2 coding sequence between nt positions 181 and 210. The pRTL2-GFP:TGBp2m3 has 9 nts, AGTCGACCA, inserted into the TGBp2 coding sequence following nt position 263 within the TGBp2 coding sequence (Mitra et al., 2003).

In Vitro Transcription

In vitro transcription was carried out using the pPVX-GFP, pPVX-GFP:TGBp2, and pPVX-GFP:TGBp2m2 plasmids and the mMESSAGE mMACHINE^{TM} High Yield Capped RNA Transcription kit (Ambion, Inc., Austin, TX). Plasmids were linearized using *Spe*I. Transcripts were used directly to inoculate protoplasts or plants as described previously (Ju et al., 2005).

Inoculation of Plants and RT-PCR Analysis of Mutant Viruses

Nicotiana benthamiana plants were used for studying virus cell-to-cell and systemic movement (Ju et al., 2005). Five µL of parental and mutant PVX-GFP, PVX-GFP:TGBp2, or PVX-GFP:TGBp2m2 transcripts were inoculated to *N. benthamiana* plant dusted with carborundum. A hand held UV lamp was used to monitor virus cell-to-cell and vascular movement. In some plants mutant viruses spread systemically. Total RNA was isolated from upper leaves of systemically infected plants using Triazol

Reagent (Invitrogen, Carlsbad, CA)(An et al., 2003). RT-PCR was conducted using Superscript III One-Step PCR System with Platinum Taq (Invitrogen) to amplify the entire TGB coding sequence. The TGB cDNAs were ligated to pGEM-T Easy plasmids (Promega Corp., Madison, WI) and used to transform JM109 cells. Three colonies were selected, and DNA was isolated and sequenced. Sequencing results for all three colonies were identical for each mutant.

Preparation of Transgenic BY-2 Cells Expressing mGFP5-ER

Transgenic BY-2 suspension cells expressing mGFP5-ER were used as a positive control for experiments studying the relationship of the PVX TGBp2 protein with the ER. Tobacco BY-2 suspension cells were transformed using *Agrobacterium tumefaciens* strain LBA4404 containing pBIN19-mGFP5-ER plasmids according to Hwang and Gelvin (2004). Five mL of three-day-old BY-2 suspension cells and 100 µL *Agrobacterium* suspension were mixed and co incubated on Petri plates containing BY-2 culture medium (4.3 g/L Murashige and Skoog salts [Sigma, St. Louis], 30 g/L Sucrose, 256 mg/L KH_2PO_4, 100 mg/L myo-inositol, 1 mg/L thiamine, and 0.2 mg/L 2,4-dichlorophenoxyacetic acid, pH 5.6) plus 0.8% agar, for two days at 28°C in the dark. The tobacco BY-2 suspension cells were washed twice with 20 mL of BY-2 culture medium, plated onto BY-2 selection medium (BY-2 culture medium plus 0.8% agar, 500 µg/mL carbenicillin, and 300 µg/mL kanamycin) and then maintained for ten days at 28°C in dark. The transgenic tobacco BY-2 suspension cells were then transferred to fresh BY-2 selection medium three times weekly. BY-2 suspension cells were examined with an Olympus SZH-ILLK stereo microscope (Olympus Optical Co., LTD, Japan)

equipped with an excitation mercury lamp and GFP emission filter. Stably transformed BY-2 suspension cells were transferred to 250-mL Erlenmeyer flasks containing 50 mL of liquid BY-2 selection medium (BY-2 culture medium plus 200μg/mL kanamycin).

Nontransgenic and transgenic BY-2 suspension cells (Nagata et al., 1992; Nagata and Kumagai, 1999) were maintained on a rotary shaker at 120 rpm in a growth chamber at 28°C in the dark. Cultures were transferred each week into 250-mL Erlenmeyer flasks containing 50 mL of either fresh BY-2 culture medium or liquid BY-2 selection medium.

BY-2 Protoplast Preparation and Transfection

Protoplasts were prepared from three-day-old BY-2 suspension cells as previously described (Gaire et al., 1999) (Qi and Ding, 2002; Ju et al., 2005). To transfect protoplasts with infectious transcripts, two L (roughly 30 g) transcripts and 5 x 10^5 protoplasts (in 0.5 mL of solution 2 [0.5 M mannitol, 3.6 mM MES0.1 mM $CaCl_2$, pH 5.5 (w/v)]) were mixed and transferred to a 0.4-cm gap cuvette (Bio-Rad Laboratories, Hercules, CA) on ice. To transfect protoplasts with plasmids, 5 μg plasmids, 40 μg sonicated salmon sperm DNA, and 1 x 10^6 protoplasts (in 0.5 mL solution 2) were mixed and transferred to a 0.4-cm gap cuvette on ice. Protoplasts were electroporated using a Gene Pulser (Bio-Rad Laboratories, Hercules, CA) at 0.25 kV, 100 Ω, and 125 μF (Ju et al., 2005)..

After electroporation, protoplasts were immediately transferred into a new tube containing 1 mL solution 2, incubated on ice for 30 min, and then at room temperature for 5 min. Protoplasts were collected by centrifugation at 79*g* for 5 min, resuspended in 1.5 mL of BY-2 culture medium plus 0.45 M mannitol, and transferred to 6-well cell culture

plates (Corning, Corning, NY). The bottom of each well in the culture plates was coated with a solution of BY-2 culture medium plus 0.45 M mannitol and 1.0% agarose (pH 5.7). Transfected protoplasts were cultured at 26°C, collected at various times between 18 and 48 h by centrifugation at 79*g* for 5 min, and then examined using laser scanning confocal microscopy (Ju et al., 2005).

Fluorometric Assays and Cycloheximide Treatment of BY-2 Protoplasts

A VICTOR2D fluorometer (Perkin-Elmer, Boston, MA) was used to measure GFP expression in protoplasts transfected with pRTL2-GFP, -GFP:TGBp2, or GFP:TGBp2m2 plasmids (Ju et al., 2005). Samples of 1 x 10^6 protoplasts were harvested at 18, 24, 30, 36, and 48 h post transfection, and then transferred to liquid nitrogen. To measure protein turnover, the culture medium was removed from transfected protoplasts at 24 h post transfection, and replaced with fresh culture containing 500μM cycloheximide (Sigma, St. Louis, MO). Samples of 1 x 10^6 protoplasts were harvested at 0, 4, 8, and 12 h following addition of the cycloheximide (Ju et al., 2005) and transferred to liquid nitrogen.

One hundred L of protein grinding buffer (10 mM Tris-HCl pH 7.5, 100 mM NaCl, 1 mM $MgCl_2$, and 10 mM DDT) was added to each sample. Samples were vortexed for 1 min, sonicated for 10 min, frozen at -80^{o}C for 10 min, and then thawed at room temperature. Sample vortexing, sonication, freezing, and thawing were repeated. Following centrifugation at 3000g for 10 min, the supernatants of untreated and cycloheximide treated extracts were used for fluorometric analyses. The average values

from three samples at each time point were plotted using Microsoft Office Excel 2003 software (Microsoft Corp., Redmond, WA) (Ju et al., 2005).

Transient Assays in Tobacco Leaves

N. benthamiana leaves were bombarded with pRTL2-GFP:TGBp2 and -GFP:TGBp2m2 transcripts using the PDS1000 He system (Biorad) as described previously (Liu et al., 2005). Leaf segments were treated with FM4-64 dye and analyzed using confocal microscopy (Howard et al., 2004) (Liu et al., 2005).

Microscopy

A Leica TCS SP2 (Leica Microsystems, Bannockburn, IL) confocal laser scanning microscope was used to examine GFP, DAPI, and FM4-64 fluorescence (Molecular Probes Inc., Eugene, OR). The Leica TCS SP2 imaging system is attached to a Leica DMRE upright microscope, UV and Ar/Kr lasers. Images were compiled into figures using Adobe Photoshop CS software (Adobe Systems Inc., San Jose, CA)(Krishnamurthy et al., 2002; Krishnamurthy et al., 2003).

Statistical Analysis

The SAS PROC CORR procedure using SAS 9.1 (SAS Institute, Cary, NC) was used to test correlations between the percentages of protoplasts showing fluorescence in granular vesicles, ER network, and enlarged vesicles in Fig. 5. Tests compared granular vesicles and ER network, enlarged vesicles and ER network, or granular and enlarged vesicles for all mutant pRTL2-GFP:TGBp2 plasmids.

ACKNOWLEDGEMENTS

I appreciate the help of Dr. C.-M. Ye, who made the construction PVX-GFP:TGBp2m2. I thank Drs. J. Fletcher and S. Marek for use of their electroporation systems. I also thank Mr.T. Colberg for training and assistance with the confocal microscope located at the Oklahoma State University Electron Microscopy Center.

LITERATURE CITED

Ahlquist P, Noueiry AO, Lee WM, Kushner DB, Dye BT (2003) Host factors in positive-strand RNA virus genome replication. J Virol **77:** 8181-8186

Allison AV, Shalla TA (1974) Ultrastructure of local lesions induced by *Potato virus X*: a sequence of cytological events in course of infection. Phytopathology **64:** 784-793

An H, Melcher U, Doss P, Payton M, Guenzi AC, Verchot-Lubicz J (2003) Evidence that the 37 kDa protein of *Soil-borne wheat mosaic virus* is a virus movement protein. J Gen Virol **84:** 3153-3163

Angell SM, Davies C, Baulcombe DC (1996) Cell-to-cell movement of *Potato virus X* is associated with a change in the size-exclusion limit of plasmodesmata in trichome cells of *Nicotiana clevelandii*. Virology **216:** 197-201

Baulcombe DC, Chapman S, Santa Cruz S (1995) Jellyfish green fluorescent protein as a reporter for virus infections. Plant J **7:** 1045-1053

Bayne EH, Rakitina DV, Morozov SY, Baulcombe DC (2005) Cell-to-cell movement of *Potato potexvirus X* is dependent on suppression of RNA silencing. Plant J **44:** 471-482

Bolte S, Talbot C, Boutte Y, Catrice O, Read ND, Satiat-Jeunemaitre B (2004) FM-dyes as experimental probes for dissecting vesicle trafficking in living plant cells. J Microsc **214:** 159-173

Carette JE, Stuiver M, Van Lent J, Wellink J, Van Kammen A (2000) *Cowpea mosaic virus* infection induces a massive proliferation of endoplasmic reticulum but not Golgi membranes and is dependent on de novo membrane synthesis. J Virol **74:** 6556-6563

Carette JE, van Lent J, MacFarlane SA, Wellink J, van Kammen A (2002) *Cowpea mosaic virus* 32- and 60-kilodalton replication proteins target and change the morphology of endoplasmic reticulum membranes. J Virol **76:** 6293-6301

Carrington JC, Freed DD (1990) Cap-independent enhancement of translation by a plant potyvirus 5' nontranslated region. J Virol **64:** 1590-1597

Davies C, Hills G, Baulcombe DC (1993) Sub-cellular localization of the 25-kDa protein encoded in the triple gene block of *Potato virus X*. Virology **197:** 166-175

den Boon JA, Chen J, Ahlquist P (2001) Identification of sequences in *Brome mosaic virus* replicase protein 1a that mediate association with endoplasmic reticulum membranes. J Virol **75:** 12370-12381

Donald RG, Lawrence DM, Jackson AO (1997) The *Barley stripe mosaic virus* 58-kilodalton beta(b) protein is a multifunctional RNA binding protein. Journal Of Virology **71:** 1538-1546

Espinoza AM, Medina V, Hull R, Markham PG (1991) *Cauliflower mosaic virus* gene II product forms distinct inclusion bodies in infected plant cells. Virology **185:** 337-344

Gaire F, Schmitt C, Stussi-Garaud C, Pinck L, Ritzenthaler C (1999) Protein 2A of *Grapevine fanleaf nepovirus* is implicated in RNA2 replication and colocalizes to the replication site. Virology **264:** 25-36

Gilmer D, Bouzoubaa S, Hehn A, Guilley H, Richards K, Jonard G (1992) Efficient cell-to-cell movement of *Beet necrotic yellow vein virus* requires 3' proximal genes located on RNA 2. Virology **189:** 40-47

Grieco F, Castellano MA, Di Sansebastiano GP, Maggipinto G, Neuhaus JM, Martelli GP (1999) Subcellular localization and in vivo identification of the putative movement protein of *Olive latent virus* 2. J Gen Virol **80 (Pt 5):** 1103-1109

Haupt S, Cowan GH, Ziegler A, Roberts AG, Oparka KJ, Torrance L (2005) Two plant-viral movement proteins traffic in the endocytic recycling pathway. Plant Cell **17:** 164-181

Howard AR, Heppler ML, Ju HJ, Krishnamurthy K, Payton ME, Verchot-Lubicz J (2004) *Potato virus X* TGBp1 induces plasmodesmata gating and moves between cells in several host species whereas CP moves only in *N. benthamiana* leaves. Virology **328:** 185-197

Husain M, Moss B (2003) Evidence against an essential role of COPII-mediated cargo transport to the endoplasmic reticulum-Golgi intermediate compartment in the formation of the primary membrane of *Vaccinia virus*. J Virol **77:** 11754-11766

Hwang HH, Gelvin SB (2004) Plant proteins that interact with VirB2, the *Agrobacterium tumefaciens* pilin protein, mediate plant transformation. Plant Cell **16:** 3148-3167

Ivanov KI, Ivanov PA, Timofeeva EK, Dorokhov YL, Atabekov JG (1994) The immobilized movement proteins of two tobamoviruses form stable ribonucleoprotein complexes with full-length viral genomic RNA. FEBS Lett **346:** 217-220

Ju HJ, Samuels TD, Wang YS, Blancaflor E, Payton M, Mitra R, Krishnamurthy K, Nelson RS, Verchot-Lubicz J (2005) The *Potato virus X* TGBp2 movement protein associates with endoplasmic reticulum-derived vesicles during virus infection. Plant Physiol **138:** 1877-1895

Jurgens G (2004) Membrane trafficking in plants. Annu Rev Cell Dev Biol **20:** 481-504

Kawakami S, Watanabe Y, Beachy RN (2004) *Tobacco mosaic virus* infection spreads cell to cell as intact replication complexes. Proc Natl Acad Sci U S A **101:** 6291-6296

Kikumoto T, Matsui C (1961) Electron microscopy of intracellular *Potato virus X*. I. Virology **13:** 294-299

Kozar FE, Sheludko YM (1969) Ultrastructure of potato and *Datura stramonium* plant cells infected with *Potato virus X*. Virology **38:** 220-229

Krishnamurthy K, Heppler M, Mitra R, Blancaflor E, Payton M, Nelson RS, Verchot-Lubicz J (2003) The *Potato virus X* TGBp3 protein associates with the ER network for virus cell-to-cell movement. Virology **309:** 135-151

Krishnamurthy K, Mitra R, Payton ME, Verchot-Lubicz J (2002) Cell-to-Cell Movement of the PVX 12K, 8K, or coat proteins may depend on the host, leaf developmental stage, and the PVX 25K protein. Virology **300:** 269-281

Liu JZ, Blancaflor EB, Nelson RS (2005) The *Tobacco mosaic virus* 126-kilodalton protein, a constituent of the virus replication complex, alone or within the complex aligns with and traffics along microfilaments. Plant Physiol **138:** 1853-1865

Liu Y, Schiff M, Czymmek K, Talloczy Z, Levine B, Dinesh-Kumar SP (2005) Autophagy regulates programmed cell death during the plant innate immune response. Cell **121:** 567-577

Lough TJ, Netzler NE, Emerson SJ, Sutherland P, Carr F, Beck DL, Lucas WJ, Forster RL (2000) Cell-to-cell movement of potexviruses: evidence for a ribonucleoprotein complex involving the coat protein and first triple gene block protein. Mol Plant Microbe Interact **13:** 962-974

Lough TJ, Shash K, Xoconostle-Cazares B, Hofstra KR, Beck DL, Balmori E, Forster RLS, Lucas WJ (1998) Molecular dissection of the mechanism by which potexvirus triple gene block proteins mediate cell-to-cell transport of infectious RNA. Molecular Plant-Microbe Interactions **11:** 801-814

Lucas WJ (2006) Plant viral movement proteins: Agents for cell-to-cell trafficking of viral genomes. Virology **344:** 169-184

Martelli GP, Jelkmann W (1998) *Foveavirus*, a new plant virus genus. Arch Virol **143:** 1245-1249

Memelink J, van der Vlugt CI, Linthorst HJ, Derks AF, Asjes CJ, Bol JF (1990) Homologies between the genomes of a carlavirus (*Lily symptomless virus*) and a potexvirus (*Lily virus X*) from lily plants. J Gen Virol **71:** 917-924

Meshi T, Hosokawa D, Kawagishi M, Watanabe Y, Okada Y (1992) Reinvestigation of intracellular localization of the 30K protein in tobacco protoplasts infected with *Tobacco mosaic virus* RNA. Virology **187:** 809-813

Mitra R, Krishnamurthy K, Blancaflor E, Payton M, Nelson RS, Verchot-Lubicz J (2003) The *Potato virus X* TGBp2 protein association with the endoplasmic reticulum plays a role in but is not sufficient for viral cell-to-cell movement. Virology **312:** 35-48

Nagata T, Kumagai F (1999) Plant cell biology through the window of the highly synchronized tobacco BY-2 cell line. Methods Cell Sci **21:** 123-127

Nagata T, Nemoto Y, Hasezawa S (1992) Tobacco BY-2 cell line as the "Hela" cell in the cell biology of higher plants. Internat. Rev. of Cytol **132**

Nebenfuhr A (2002) Vesicle traffic in the endomembrane system: a tale of COPs, Rabs and SNAREs. Curr Opin Plant Biol **5:** 507-512

Palacios S, Perez LH, Welsch S, Schleich S, Chmielarska K, Melchior F, Locker JK (2005) Quantitative SUMO-1 modification of a vaccinia virus protein is required for its specific localization and prevents its self-association. Mol Biol Cell **16:** 2822-2835

Peremyslov VV, Pan YW, Dolja VV (2004) Movement protein of a *closterovirus* is a type III integral transmembrane protein localized to the endoplasmic reticulum. J Virol **78:** 3704-3709

Qi Y, Ding B (2002) Replication of *Potato spindle tuber viroi*d in cultured cells of tobacco and *Nicotiana benthamiana*: the role of specific nucleotides in determining replication levels for host adaptation. Virology **302:** 445-456

Randles JW, Rohde W (1990) *Nicotiana velutina mosaic virus*: evidence for a bipartite genome comprising 3 kb and 8 kb RNAs. J Gen Virol **71:** 1019-1027

Restrepo-Hartwig M, Ahlquist P (1999) *Brome mosaic virus* RNA replication proteins 1a and 2a colocalize and 1a independently localizes on the yeast endoplasmic reticulum. J Virol **73:** 10303-10309

Rouleau M, Smith RJ, Bancroft JB, Mackie GA (1994) Purification, properties, and subcellular localization of *Foxtail mosaic potexvirus* 26-kDa protein. Virology **204:** 254-265

Salonen A, Ahola T, Kaariainen L (2005) Viral RNA replication in association with cellular membranes. Curr Top Microbiol Immunol **285:** 139-173

Schaad MC, Jensen PE, Carrington JC (1997) Formation of plant RNA virus replication complexes on membranes: role of an endoplasmic reticulum-targeted viral protein. Embo J **16:** 4049-4059

Schepetilnikov MV, Manske U, Solovyev AG, Zamyatnin AA, Jr., Schiemann J, Morozov SY (2005) The hydrophobic segment of *Potato virus X* TGBp3 is a major determinant of the protein intracellular trafficking. J Gen Virol **86:** 2379-2391

Schwartz M, Chen J, Janda M, Sullivan M, den Boon J, Ahlquist P (2002) A positive-strand RNA virus replication complex parallels form and function of retrovirus capsids. Mol Cell **9:** 505-514

Schwartz M, Chen J, Lee WM, Janda M, Ahlquist P (2004) Alternate, virus-induced membrane rearrangements support positive-strand RNA virus genome replication. Proc Natl Acad Sci U S A **101:** 11263-11268

Siemering KR, Golbik R, Sever R, Haseloff J (1996) Mutations that suppress the thermosensitivity of green fluorescent protein. Curr Biol **6:** 1653-1663

Solovyev AG, Stroganova TA, Zamyatnin AA, Jr., Fedorkin ON, Schiemann J, Morozov SY (2000) Subcellular sorting of small membrane-associated triple gene block proteins: TGBp3-assisted targeting of TGBp2. Virology **269:** 113-127

Suhy DA, Giddings TH, Jr., Kirkegaard K (2000) Remodeling the endoplasmic reticulum by *Poliovirus* infection and by individual viral proteins: an autophagy-like origin for virus-induced vesicles. J Virol **74:** 8953-8965

Turina M, Desvoyes B, Scholthof KB (2000) A gene cluster encoded by P*anicum mosaic virus* is associated with virus movement. Virology **266:** 120-128

Turner RL, Mills PR, Foster GD (1993) Nucleotide sequence of the 7 K gene of *Helenium virus S.* Acta Virol **37:** 523-528

Vilar M, Sauri A, Monne M, Marcos JF, von Heijne G, Perez-Paya E, Mingarro I (2002) Insertion and topology of a plant viral movement protein in the endoplasmic reticulum membrane. J Biol Chem **277:** 23447-23452

Voinnet O, Lederer C, Baulcombe DC (2000) A viral movement protein prevents spread of the gene silencing signal in *Nicotiana benthamiana*. Cell **103:** 157-167

Yang Y, Ding B, Baulcombe DC, Verchot J (2000) Cell-to-cell movement of the 25K protein of *Potato virus X* is regulated by three other viral proteins. Mol Plant Microbe Interact **13:** 599-605

Yang YD, Elamawi R, Bubeck J, Pepperkok R, Ritzenthaler C, Robinson DG (2005) Dynamics of COPII vesicles and the Golgi apparatus in cultured *Nicotiana tabacum* BY-2 cells provides evidence for transient association of Golgi stacks with endoplasmic reticulum exit sites. Plant Cell **17:** 1513-1531

Zamyatnin AA, Jr., Solovyev AG, Bozhkov PV, Valkonen JP, Morozov SY, Savenkov EI (2006) Assessment of the integral membrane protein topology in living cells. Plant J **46:** 145-154

Zamyatnin AA, Jr., Solovyev AG, Sablina AA, Agranovsky AA, Katul L, Vetten HJ, Schiemann J, Hinkkanen AE, Lehto K, Morozov SY (2002) Dual-colour imaging of membrane protein targeting directed by *Poa semilatent virus* movement protein TGBp3 in plant and mammalian cells. J Gen Virol **83:** 651-662

Zamyatnin AA, Jr., Solovyev AG, Savenkov EI, Germundsson A, Sandgren M, Valkonen JP, Morozov SY (2004) Transient coexpression of individual genes encoded by the triple gene block of *Potato mop-top virus* reveals requirements for TGBp1 trafficking. Mol Plant Microbe Interact **17:** 921-930

CHAPTER IV

MUTATIONS IN TGBp3 DELAY VIRUS CELL-TO-CELL MOVEMENT AND INHIBIT VASCULAR TRANSPORT

ABSTRACT

Potato virus X (PVX) requires TGBp1, TGBp2, TGBp3, and coat protein (CP) for cell-to-cell and systemic movement. PVX TGBp3 has a single N-terminal transmembrane domain and a C-terminal cytosolic domain. TGBp3 was shown previously to associate with the ER in transgenic tobacco plants. In this study the GFP gene was fused to the 3' end of the TGBp3 gene in the PVX genome to study subcellular accumulation of the TGBp3 protein during virus infection. TGBp3:GFP fluorescence was seen in the endoplasmic reticulum (ER), granular bodies, nucleus, and perinuclear masses. Four mutations were introduced into the TGBp3 coding sequence to study their effects on virus movement and TGBp3:GFP subcellular targeting. Each mutation reduced virus cell-to-cell movement and eliminated systemic virus movement. The m1* mutation disrupted the N-terminal transmembrane segment of TGBp3 and hampered TGBp3:GFP association with the ER and granular bodies. The Dm2 and Dm3 mutations deleted sequences near the 3' end of the TGBp3 coding sequence. These mutations increased TGBp3:GFP fluorescence in the cytoplasm, reduced virus cell-to-cell movement, and

eliminated systemic virus movement. Combined, these data suggest that TGBp3 association with the ER and granular bodies is necessary for optimal cell-to-cell and systemic movement of PVX. The m2 mutation is a substitution in the cytosolic domain of TGBp3 that has no effect on TGBp3 association with the ER and granular bodies although it negatively effects virus cell-to-cell movement. These data suggest that the C-terminal cytosolic domain of TGBp3 plays a role in virus movement beyond regulating membrane association.

INTRODUCTION

Potato virus X (PVX) is the type member for the genus *Potexvirus* and has five open reading frames (ORFs) (Huisman et al., 1988; Skryabin et al., 1988). The 5' most ORF encodes replicase, which is responsible for virus replication (Huisman et al., 1988). Potexviruses contain a genetic module that is termed the "triple gene block" (TGB), which encodes three proteins named TGBp1 (25kDa), TGBp2 (12kDa), and TGBp3 (8kDa). The TGB proteins are required for virus cell-to-cell and vascular movement (Beck et al., 1991; Verchot et al., 1998). The last ORF encodes the viral coat protein (CP), which is essential for RNA encapsidation and virus movement (Forster et al., 1992; Chapman et al., 1992a; SantaCruz et al., 1998).

The PVX TGBp1 induces plasmodesmata gating for virus cell-to-cell movement (Angell et al., 1996; Yang et al., 2000; Howard et al., 2004), has RNA helicase/ATPase activity (Gorbalenya and Koonin, 1989; Kalinina et al., 1996; Kalinina et al., 2002; Leshchiner et al., 2006), promotes translation of virion derived RNAs (Atabekov et al., 2000; Rodionova et al., 2003), and suppresses RNA silencing (Voinnet et al., 2000;

Bayne et al., 2005). The current model describing Potexvirus cell-to-cell movement suggest that the PVX TGBp1, CP, and vRNA form a ribonucleoprotein complex that is transported across plasmodesmata (Lough et al., 2000; Lough et al., 2006).

PVX TGBp2 has two transmembrane domains and TGBp3 has one transmembrane domain located near the N-terminus (Krishnamurthy et al., 2003; Mitra et al., 2003). GFP was fused to the TGBp2 and TGBp3 coding sequences to study protein subcellular targeting using confocal microscopy. GFP:TGBp2 was detected in the ER and in vesicles associated with the ER (Mitra et al., 2003; Ju et al., 2005). Mutations in TGBp2 disrupting ER or vesicle association also disrupted virus movement (Mitra et al., 2003; Ju et al., 2007). GFP:TGBp3 was reported to accumulate in the ER network (Krishnamurthy et al., 2003; Ju et al., 2005). Mutations disrupting the ER association of GFP:TGBp3 also inhibited virus movement (Krishnamurthy et al., 2003).

Microinjection and bombardment studies show that TGBp2 and TGBp3 do not gate PD but associated with ER (Lough et al., 1998; Lough et al., 2000; Krishnamurthy et al., 2002), indicating that these proteins are involved in intracellular movement of viral components by ER association. ER-rich bodies were found at the periphery of the cell which in *Potato mop top virus* (PMTV), *Beet necrotic yellow vein virus* (BNYVV), and *Poa semilatent virus* (PSLV) infected plants. Studies indicate that, in PVX, PMTV and PSLV, TGBp3 plays a role in transporting TGBp2 from small granular vesicles to the peripheral bodies (Solovyev et al., 2000; Haupt et al., 2005). Some have suggested that TGBp3 plays a role in guiding TGBp2 to the plasma membrane and PD (Lawrence and Jackson, 2001; Zamyatnin et al., 2004). Most studies to examine the subcellular distribution of the PVX TGBp3 protein have fused GFP to the 5' end of TGBp3. The

GFP:TGBp3 fusion has been linked to the CaMV 35S promoter and most studies have reported subcellular targeting of the fusion either expressed transiently or co-delivered with PVX to plant cells. These studies showed that GFP:TGBp3 associates primarily with the ER (Krishnamurthy et al., 2002; Krishnamurthy et al., 2003; Schepetilnikov et al., 2005). However, when the GFP:TGBp3 fusion was introduced into the PVX genome to study protein subcellular targeting during virus infection, the recombinant virus was not infectious. These results suggest that the fusion may have hampered TGBp3 function or subcellular targeting necessary to promote virus infection.

In this study we fused GFP to the 3' end of the TGBp3 coding sequence in the PVX genome and showed the recombinant virus to be infectious. GFP fluorescence was used to study the subcellular distribution of TGBp3 during virus infection. As in previous report (Krishnamurthy et al., 2003), TGBp3 associated with the ER. In addition, we also detected the fusion protein in ER related vesicles. Mutations were introduced into the TGBp3 coding sequence to determine if ER association or the cytosolic domain of TGBp3 is necessary for virus movement. Mutations did not block virus cell-to-cell movement completely, allowing movement within limited distant viruses moved. TGBp3 protein was localized on the ER during virus infection regardless of mutation. Protein stability was influenced by mutation. GFP fluorescence was used to visualize subcellular distribution of TGBp3 in the epidermal cells in the absence or presence of virus. Previous work used pRTL2-GFP:TGBp3 to study PVX TGBp3 association with ER network (Krishnamurthy et al., 2003), however when we introduced the GFP:TGBp3 fusion into the PVX genome, the recombinant virus was not infectious. Therefore, we fused GFP to the 3' end of TGBp3 in the PVX genome and this recombinant virus was infectious. This

study showed that TGBp3:GFP accumulates in previously undescribed subcellular compartments.

RESULTS

TGBp3:GFP Associates with ER Network and Granular Bodies

Two methods were used to study the subcellular accumulation of the PVX TGBp3 in tobacco leaves. First, pRTL2 plasmids expressing GFP fused to the 3' end of the TGBp3 coding sequence (Fig. 1) were biolistically delivered to tobacco leaves. GFP fluorescence was visualized using confocal microscopy. The pattern of fluorescence was analyzed by confocal microscopy and representative examples of images obtained are shown in Fig. 2. A fluorescent polygonal network, resembling the ER network, was observed in bombarded *N. tabacum* leaves expressing TGBp3:GFP (Fig. 1). Fluorescence was also seen in the perinuclear ER and found a fluorescent halo around the nucleus. There were also ER-associated granular bodies, which were not previously described in studies using the GFP:TGBp3 fusion.

For controls, tobacco leaves were also bombarded with pBin19-mGFP5-ER or pRTL2-GFP (Fig 2). The mGFP5-ER coding sequence includes ER targeting and retention signals (Haseloff et al., 1997), and therefore shows GFP fluorescence in the ER network. The network seen in TGBp3:GFP expressing cells resembled the network seen in cells expressing mGFP5-ER (Krishnamurthy et al., 2003, Ju et al., 2005, Zamyatnin, 2002). Granular bodies seen in TGBp3:GFP expressing cells were not seen in mGFP5-ER expressing cells, suggesting that these granules are specific to TGBp3:GFP. Cells expressing GFP alone, show fluorescence in the cytoplasm and nucleus. Thus the pattern of TGBp3:GFP fluorescence was due to subcellular targeting by TGBp3.

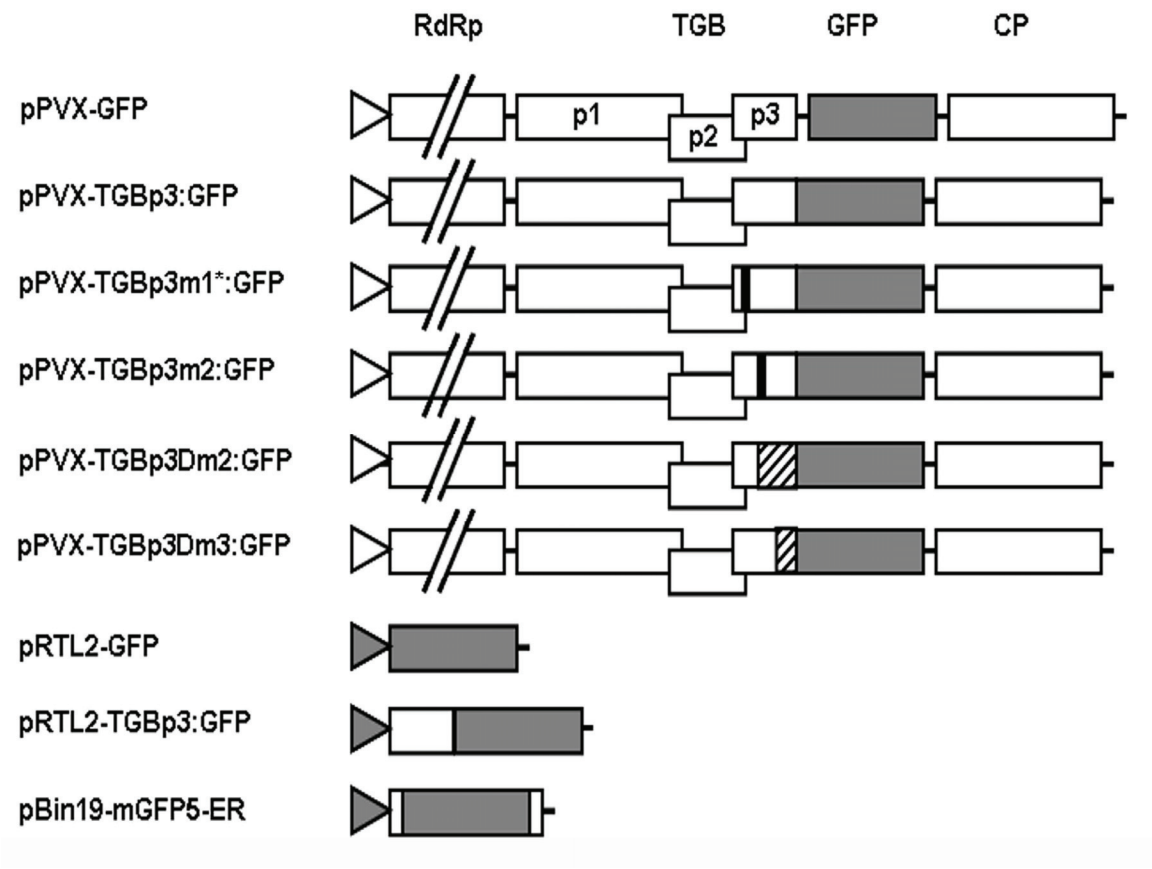

Figure 1. Diagrammatic representation of PVX infectious clones and other plasmids used in this study. Plasmids beginning with the name pPVX contain the PVX genome inserted next to bacteriophage T7 promoters (open triangle). The names of each PVX coding sequence is indicated at the top of the panel above the pPVX plasmids. Open boxes represent PVX coding sequences and gray boxes represent GFP coding sequences. Open boxes representing the PVX RNA dependent RNA polymerase (RdRp) are interrupted by double lines indicating that the coding sequences are drawn shorter than to

scale. The remaining PVX coding sequences are drawn to scale. The horizontal lines on each side of the open boxes indicate non translated sequences within the PVX genome. For all pPVX-TGBp3:GFP plasmids the GFP coding sequence is fused to the TGBp3 coding sequence. The black boxes within the TGBp3 coding sequence represent the m1* and m2 substitution mutations (Krishnamurthy et al., 2003). The hatched boxes represent sequences deleted from the TGBp3 coding sequence (Krishnamurthy et al., 2003). Plasmids beginning with the name pRTL2 or pBIN19 contain the CaMV 35S promoter (gray triangle). The pBin-mGFP5-ER plasmid contains sequences encoding ER-targeting and retention signals fused to the 5'- and 3'-ends of the GFP gene (gray box) (Haseloff et al., 1997).

In a second set of experiments, plants were inoculated with PVX-TGBp3:GFP. Infection foci on inoculated leaves were studied using confocal microscopy between 5 and 7 days post inoculation (dpi). As a control, plants were also inoculated with PVX-GFP, which expresses GFP alone from a duplicated CP subgenomic promoter. As expected, fluorescence in PVX-GFP infected leaves was in the cytoplasm and nucleus (Fig. 2, A and E). There was also a large fluorescent mass (Fig. 2, E and H-J) surrounding the nucleus, which was not detected in the cells bombarded with pRTL2-GFP (Fig. 2A). The fluorescent masses are likely X-bodies, described in early literature to contain virus particles, ER, and ribosomes (Kikumoto and Matsui, 1961; Kozar and Sheludko, 1969; Allison and Shalla, 1973). Based on previous reports describing the formation of X-bodies (Kikumoto and Matsui, 1961; Kozar and Sheludko, 1969; Allison and Shalla, 1973; Espinoza et al., 1991), we postulate the strands extending from these X-bodies to the plasma membrane (Fig 2F) to be ER derived. In a recent report we treated PVX-TGBp3:GFP infected protoplasts with ER-tracker dye. We found that the perinuclear masses containing GFP fluorescence also labeled with ER-tracker dye, indicating that the perinuclear masses are membrane rich bodies (Samuels et al., submitted).

Fluorescence due to PVX-TGBp3:GFP was in seen a polygonal network resembling the ER network. We also observed granular bodies associated with the ER network (Fig. 2, F and G). This pattern was similar to the pattern seen in pRTL2-TGBp3:GFP expressing cells (Fig. 2, B and C). In addition, PVX-TGBp3:GFP fluorescence was also detected in the nucleus and perinuclear masses (Fig. 2, F and K-M) of all infected cells.

Mutations in PVX TGBp3 Disrupt Virus Systemic Movement

Five mutations were separately introduced into the PVX-TGBp3:GFP genome to study their effects on TGBp3 subcellular targeting and virus cell-to-cell movement. These mutations, named m1*, m2, Dm2, Dm3, were first introduced into pRTL2-GFP:TGBp3 plasmids to study the requirements for membrane association of the PVX TGBp3 protein (Krishnamurthy et al., 2003). The m1 and m2 mutations are substitution mutations replacing 9 nts within the TGBp3 coding sequence with 9 nts encoding Ser-Arg-Pro (Krishnamurthy et al., 2003). The Dm2 and Dm3 mutations delete 96 and 39 nucleotides near the 3' end of TGBp3, respectively. We previously reported that the m1 mutation disrupts a transmembrane domain of TGBp3, inhibiting GFP:TGBp3 association with the ER (Krishnamurthy et al., 2003).

The m2, Dm2, and Dm3 mutations (Fig. 1) were determined to lie in the cytosolic domain of TGBp3 (Krishnamurthy et al., 2003). When the same mutations were introduced into pPVX204, virus movement was inhibited by m1, m2, Dm2, and Dm3 (Krishnamurthy et al., 2003). The pPVX204 infectious clone expresses the PVX genome from a CaMV35S promoter and contains the GFP coding sequence next to the duplicated CP subgenomic promoter (Krishnamurthy et al., 2003). In this current study we found that the TGBp3 mutations that were deleterious to PVX204 had different effects when they were introduced into the PVX-TGBp3:GFP infectious clones. The PVX-GFP and PVX-TGBp3:GFP infectious clones contain the PVX genome fused to a bacteriophage T7 promoter. We found that PVX-GFP and PVX-TGBp3:GFP transcripts synthesized *in vitro* were more infectious than the PVX204 plasmids when rub inoculated to tobacco leaves or electroporated into protoplasts (data not shown).

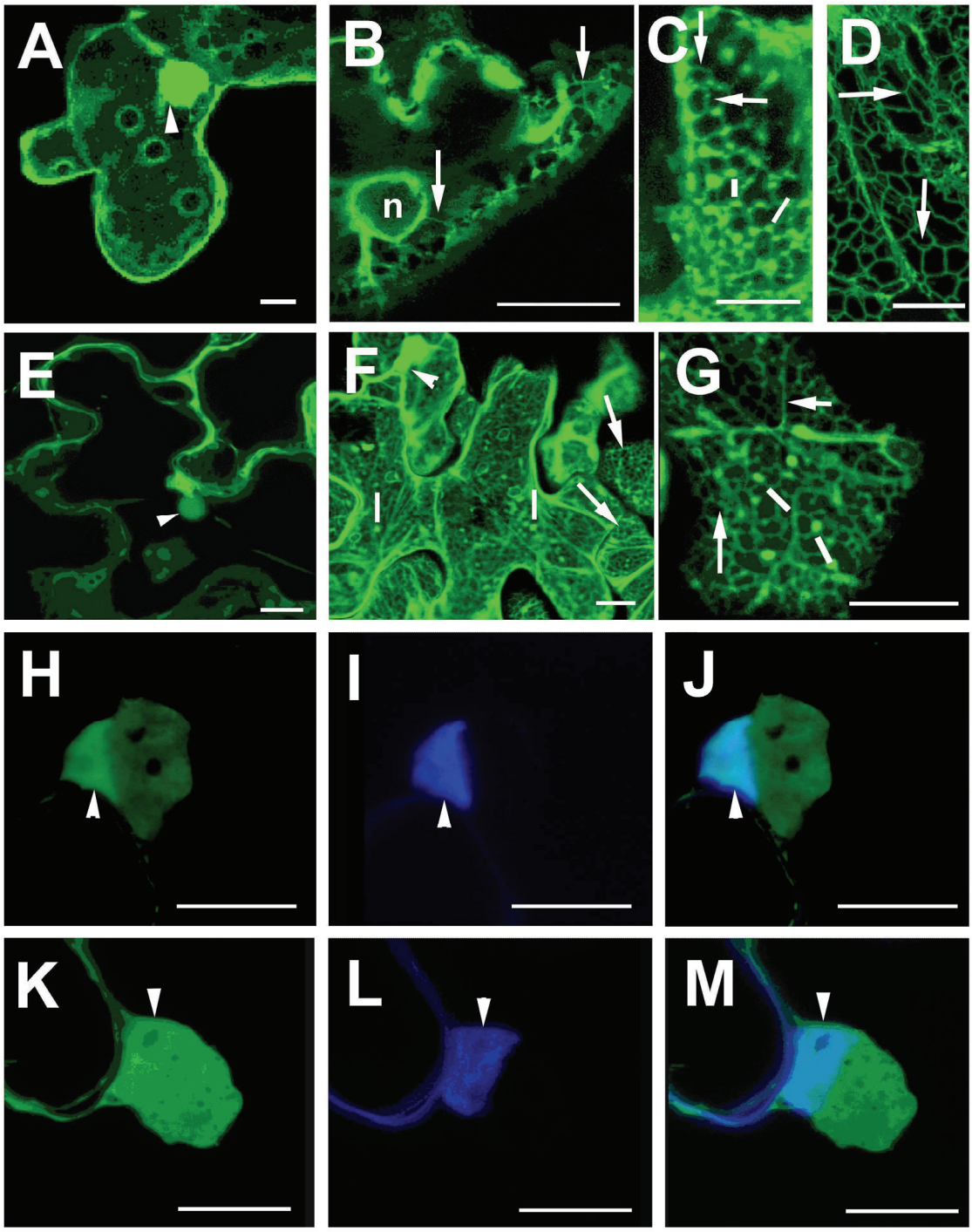

Figure 2. Confocal images of tobacco leaf epidermal cells showing subcellular accumulation of TGBp3:GFP. A, Epidermal cell expressing pRTL2-GFP shows fluorescence in cytoplasm and nucleus. B and C, Epidermal cells bombarded with pRTL2-TGBp3:GFP show fluorescence in tubular ER network (arrows), and granular

bodies (lines) associated with the tubular ER network. Fluorescence is also seen in ER surrounding the nucleus (n). D, Epidermal cell bombarded with pBin19-mGFP5-ER plasmids shows fluorescence in tubular ER network. E, PVX-GFP infected epidermal cells show fluorescence in the cytoplasm and nucleus. F, PVX-TGBp3:GFP infected epidermal cells show fluorescence in tubular ER network, granular bodies, nucleus (arrowhead), and perinuclear inclusion body. G, High magnification of PVX-TGBp3:GFP infected epidermal cells. TGBp3:GFP fluorescence was associated with tubular ER network and granular bodies. H to J, High magnification images showing nucleus and perinuclear inclusion body in PVX-GFP infected epidermal cells. K to M, High magnification images showing nucleus and perinuclear inclusion body in PVX-TGBp3:GFP infected epidermal cells. Cells were treated with DAPI (blue) to differentiate the nucleus from the green fluorescent inclusion body. Bars in all images represent 20 μm.

In plants, 'more infectious" means that we see GFP fluorescent infection sites earlier on inoculated leaves, using lower quantities of transcripts than plasmids. Thus, for this study we introduced the same TGBp3 mutants into the PVX-TGBp3:GFP infectious clone and found that the mutations limited virus cell-to-cell and systemic movement (Fig 1, Table 1). We also inoculated plants using a sap inoculum derived from protoplasts that were transfected with parental or mutant PVX-TGBp3:GFP. The infectious transcripts and infected sap produced similar results (data not shown), verifying that the deleterious effects of the mutations were the same regardless of whether plants were inoculated with infectious transcripts or virus. Since TGBp3:GFP accumulates in multiple subcellular compartments, we used confocal microscopy to determine if the mutations alter the ability of TGBp3:GFP to reach any of its typical subcellular destinations during virus infection.

Infectious transcripts were directly inoculated to tobacco leaves and GFP expression was monitored until 14 dpi. Either 19 or 20 plants were inoculated with each recombinant virus. Green fluorescent infection foci were first seen on PVX-GFP and PVX-TGBp3:GFP inoculated plants 3 and 4 dpi, respectively. One hundred percent of plants inoculated with either PVX-GFP and PVX-TGBp3:GFP were systemically infected between 5 and 6 dpi, respectively (Table I). Each mutant PVX-TGBp3:GFP was first detected in expanding infection foci around 7 dpi. Each of the four mutants were restricted to the inoculated leaves, and did not spread systemically by 21 dpi (Table. I).

The diameters of PVX infection foci were measured at 7 dpi to compare the extent of virus spread on the inoculated leaves. For each of the mutant PVX-TGBp3:GFP viruses a microscope was employed to measure the infection foci diameters.

Table I. *Number of plants showing systemic and cell-to-cell movement of recombinant PVX viruses*

Virus	Systemic accumulation of GFP expression[a]	Diameter of infection sites on inoculated leaves[b]
PVX-GFP	20/20	>3 mm
PVX-TGBp3:GFP	20/20	>3mm
PVX-TGBp3m1*:GFP	0/19	0.69±0.12
PVX-TGBp3m2:GFP	0/19	1.47±0.12
PVX-TGBp3Dm2:GFP	0/19	1.35±0.25
PVX-GBp3Dm3:GFP	0/19	1.39±0.15

[a] The total number of plants showing GFP fluorescence in upper non inoculated leaves by 14 dpi.

[b]Green fluorescence in plants inoculated with PVX-GFP and PVX-TGBp3:GFP spread beyond the initial infection site into the vasculature, while fluorescence due to mutant PVX-TGBp3:GFP were restricted to microscopic sites. Values represent the average diameters of infection foci measured in inoculated leaves at 7 dpi. PVX-GFP and PVX-TGBp3:GFP sites expanded beyond the view of the objective at 7 dpi.

PVX-TGBp3:GFP spread beyond the microscopic view and the infection foci diameters were greater than 3 mm (Fig. 3A). The average diameter of PVX-TGBp3m1*:GFP infection foci was at least 4-fold smaller than the remaining PVX-TGBp3:GFP. The diminished ability of TGBp3m1* to move from cell-to-cell supports previous reports indicating that the same mutation disrupts TGBp3 association with the ER, which is necessary for virus movement (Krishnamurthy et al., 2003). The average diameters of PVX-TGBp3m2:GFP, -TGBp3Dm2:GFP, and –TGBp3Dm3:GFP containing infection foci were at least half the size of PVX-TGBp3:GFP. Mutants altering the C-terminal cytosolic domain of TGBp3 showed reduced ability to move from cell-to-cell and were unable to spread systemically. These data indicate that the cytosolic domain is essential for optimal virus cell-to-cell and vascular transport.

Mutations in TGBp3:GFP Coding Sequence Affect Subcellular Localization during Virus Infection

Confocal microscopy was used to study the effects of the TGBp3 mutations on protein subcellular targeting during virus infection. A single infection focus contains cells that represent both early and late stages of virus infection. Cells located at the center of the infection site represent late stages of infection and show a pattern of fluorescence seen after virus has moved out of the cells. Cells located at the infection front represent earlier stages of infection and show a pattern of fluorescence seen when virus has recently entered the cell and has not yet moved into neighboring cells. The intracellular fluorescence patterns located at the leading edge and at the center of infection foci were compared to determine whether the subcellular distribution of

fluorescence changed as infections developed. Since tobacco leaf cells are not synchronously infected, we could not use statistical methods to assess changes in the distribution of GFP, TGBp3:GFP, or mutant TGBp3:GFP proteins over time.

Infection foci in leaves inoculated with PVX-TGBp3:GFP or PVX-GFP were examined at 5 dpi (Fig. 3, A-E), while infection sites produced by mutant PVX-TGBp3:GFP viruses were examined at 7 dpi (Fig. 3, F-Y). PVX-GFP infection sites showed fluorescence in the cytoplasm, nucleus, and perinuclear inclusions (Fig. 2E). Fluorescence due to PVX-TGBp3:GFP, or -TGBp3m2:GFP infection was distributed in the polygonal ER network, ER associated granular bodies, perinuclear masses, and the nucleus. The patterns of GFP (data not shown), TGBp3:GFP (Fig. 3,B-E), and TGBp3m2:GFP (Fig. 3, L-O) fluorescence were the same in cells located at the leading edge and center of infection foci (Samuels et al., submitted).

PVX-TGBp3m1*:GFP (Fig. 3, G-J), -TGBp3Dm2:GFP (Fig. 3Q-T), or –TGBp3Dm3:GFP (Fig. 3, V-Y) showed novel fluorescence accumulation patterns when compared to PVX-TGBp3:GFP infection sites (Fig. 3B-E). For PVX-TGBp3m1*:GFP, fluorescence seen in cells located at the infection front was in the cytoplasm, nucleus, and perinuclear masses (Fig. 3, G and H). However in cells located toward the center of infection foci, fluorescence was evident in the ER network, granular bodies associated with the ER, perinuclear masses, and nucleus (Fig. 3, I and J). These data suggest that the m1* mutation inhibited TGBp3 association with the ER and granular bodies early in infection, which may have reduced virus cell-to-cell movement. Evidence of TGBp3m1*:GFP in the ER and granular bodies late in infection was surprising. Perhaps interactions with TGBp2 may have restored membrane targeting of TGBp3.

We saw two different fluorescence patterns in cells infected with PVX-TGBp3Dm2:GFP or PVX–TGBp3Dm3:GFP. Both mutant viruses produced the same two fluorescence patterns and Fig 3 shows representative examples of each pattern. PVX-TGBp3Dm2:GFP or PVX-TGBp3Dm3:GFP infection sites showed two patterns of fluorescence at both the infection fronts and infection centers. Neighboring cells did not contain the same patterns of fluorescence regardless of whether the cells were located at the infection front or infection center. Thus, we did not see temporal changes in protein distribution, rather we saw two fluorescence patterns randomly distributed among neighboring cells. Some cells showed fluorescence in the polygonal ER network, granular bodies, perinuclear masses, and nucleus (Fig. 3, Q-T and data not shown). Other PVX-TGBp3Dm2:GFP or PVX-TGBp3Dm3:GFP cells showed fluorescence in the cytoplasm, granular bodies, perinuclear masses, perinuclear ER, and nucleus, but not in polygonal ER network (Fig. 3, V-Y and data not shown). The granular bodies, seen in cells showing the latter fluorescence pattern, were often along the periphery of the cell. The inconsistent distribution of fluorescence in PVX-TGBp3Dm2:GFP and –TGBp3Dm3:GFP infected cells led us to speculate that the mutations may have reduced the ability of TGBp3 to stably interact with specific subcellular targets or to reach specific subcellular destinations, thereby hampering virus cell-to-cell movement. Considering the effects of m1*, Dm2, and Dm3 on TGBp3:GFP association with the ER, these data suggest that the reduced ability of mutant TGBp3 to interact with the ER correlates with reduced virus cell-to-cell movement.

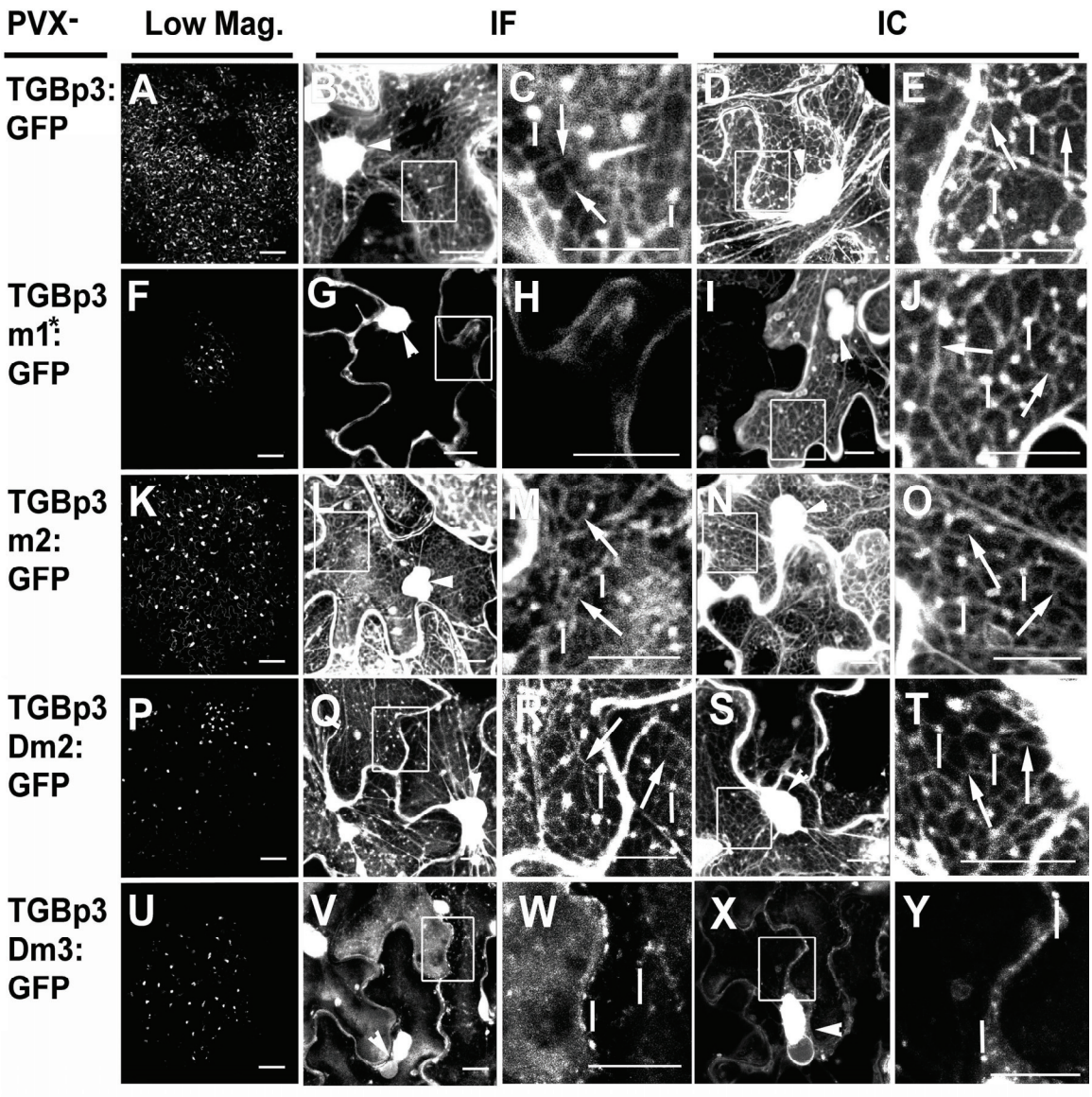

Figure 3. Confocal images of infection foci in tobacco leaves. Names of each recombinant PVX virus are identified on the left. Low magnification (Low Mag.) images of infection sites are shown in the second column. The central two panels represent cells at the infection front (IF) and the two right hand panels represent images of cells at the infection center (IC). All images are projections of serial sections. PVX-TGBp3:GFP infection sites at 5 dpi while the mutant PVX-TGBp3:GFP infection sites were imaged at 7 dpi. Cells located at the IF and IC of PVX-TGBp3:GFP and -TGBp3m2-GFP

infection sites show similar fluorescdence patterns. Images show polygonal ER network (arrows), granular bodies (lines), and inclusion body surrounding the nucleus (arrowheads). While cells located at the IF of an PVX-TGBp3m1*:GFP infection site show fluorescence in the cytoplasm and in inclusion body surrounding the nucleus, cells located at the IC of PVX-TGBp3m1*:GFP infection site show fluorescence in the ER network, granular bodies, and the inclusion body surrounding the nucleus. Among the images at the IF, white boxes in B, G, L, Q, and V indicate subcellular regions magnified in panels C, H, M, R, and W, respectively. Among the images at the IC, white boxes in D, I, N, S, and X indicate subcellular regions magnified in panels E, J, O, T, and Y, respectively. The magnified images clearly show tubular ER network and granular bodies, while the original images better display the inclusion bodies and nuclear fluorescence. Q to T, Representative images of PVX-TGBp3Dm2:GFP which resemble the patterns shown for PVX-TGBp3:GFP at the IF and IC. In some infection sites PVX-TGBp3Dm2:GFP, produced a fluorescence pattern similar to PVX-TGBp3Dm3:GFP. V to Y, Representative images of PVX-TGBp3Dm3:GFP. Images at the IF and IC are similar. Fluorescence occurs in the cytoplasm, granular bodies, and perinuclear inclusion bodies. X, Shows a halo around the nucleus indicating TGBp3Dm3:GFP in perinuclear ER. W and Y, Shows granular bodies along the cell wall. In some infection sites PVX-TGBp3Dm3:GFP produced a fluorescence pattern similar to PVX-TGBp3:GFP at the IF and IC. Bars in the A, F, K, P, and U represent 200 μm. Bars B, D, G, I, L, N, Q, S, V, and X represent 20 μm. Bars in C, E, H, J, M, O, R, T, W, and Y represent 10 μm.

Fluorescence Declines in PVX-Infected BY-2 Protoplasts Following Cycloheximide Treatment

In a recent study of the PVX TGBp2 protein, the GFP gene was fused to the 5' end of the TGBp2 gene and the fusion was introduced into the PVX genome or into pRTL2 plasmids. In protoplasts inoculated with PVX-GFP:TGBp2, fluorescence was redistributed from the vesicles into the cytosol. However, we did not detect cytosolic accumulation of GFP:TGBp2 when it was expressed from pRTL2 plasmids (Ju et al., 2005). We hypothesized that ER retention of viral proteins and/or ER reorganization by the TGBp2 protein triggers ER-associated protein degradation (ERAD) as a result of ER stress (Brandizzi et al., 2003; Martinez and Chrispeels, 2003; Smalle and Vierstra, 2004; Kirst et al., 2005). Typically, misfolded proteins present in the ER are exported to the cytosol and degraded by the 26S proteasome. We reported that the half life of GFP:TGBp2 was significantly shorter when it was expressed from the PVX genome than when it was expressed from pRTL2 plasmids, suggesting that virus infection might have triggered ER export and degradation of GFP:TGBp2 (Ju et al., 2005). Evidence of enhanced GFP:TGBp2 turnover during virus infection, along with an increase in cytosolic fluorescence, provided support for the assertion that ERAD may be involved in GFP:TGBp2 degradation (Ju et al., 2005). This led to a model speculating that ER stress responses might be linked to virus cell-to-cell movement (Ju et al., 2005).

In this study, we found that the fluorescence pattern due to PVX-TGBp3Dm2:GFP or PVX–TGBp3Dm3:GFP varied between infection sites. Some infection sites showed fluorescence in the ER and granular bodies, while other sites showed fluorescence in the cytoplasm as well as granular bodies. Similar to

GFP:TGBp2, an increase of cytosolic fluorescence seen in PVX-TGBp3Dm2:GFP or -TGBp3Dm3:GFP infected cells may reflect changes in the steady state levels of TGBp3Dm2:GFP and TGBp3Dm3:GFP.

Fluorometric assays were used to quantify GFP expression over time as a measure of both protein accumulation and degradation in BY-2 protoplasts. We then compared the rates of protein turnover in protoplasts inoculated with each of the PVX viruses. Inoculated protoplasts were chased at 24 h with cycloheximide to halt protein synthesis. Fluorometric values were obtained at 0, 4, 8, and 12 h following treatment with cycloheximide and the protein half-lives were calculated. The fluorometric values were normalized to a time 0 measurement. The data were plotted and protein half-lives were calculated from the trend lines (Fig 4). We predicted that if protein turnover was stimulated as the result of the Dm2 and Dm3 mutations, then PVX-TGBp3Dm2:GFP and PVX-TGBp3Dm3 fluorescence would decline more rapidly than that of PVX-GFP, PVX-TGBp3:GFP, or the remaining PVX-TGBp3:GFP mutants in virus-infected protoplasts.

In all virus inoculated protoplasts, there was a steady increase in fluorescence between 12 and 48 hpi (Fig. 4A). For PVX-GFP the fluorescence values obtained at 48 hpi were 13-fold higher than the values obtained at 12 hpi. For each of the recombinant PVX-TGBp3:GFP viruses, the fluorescence values obtained at 48 hpi were between 1.7 and 4-fold higher than the values obtained at 12 hpi. The plotted fluorometric values for PVX-GFP infected protoplasts were significantly higher thanthose of the wild-type and mutant PVX-TGBp3:GFP infected protoplasts (Fig. 4A).

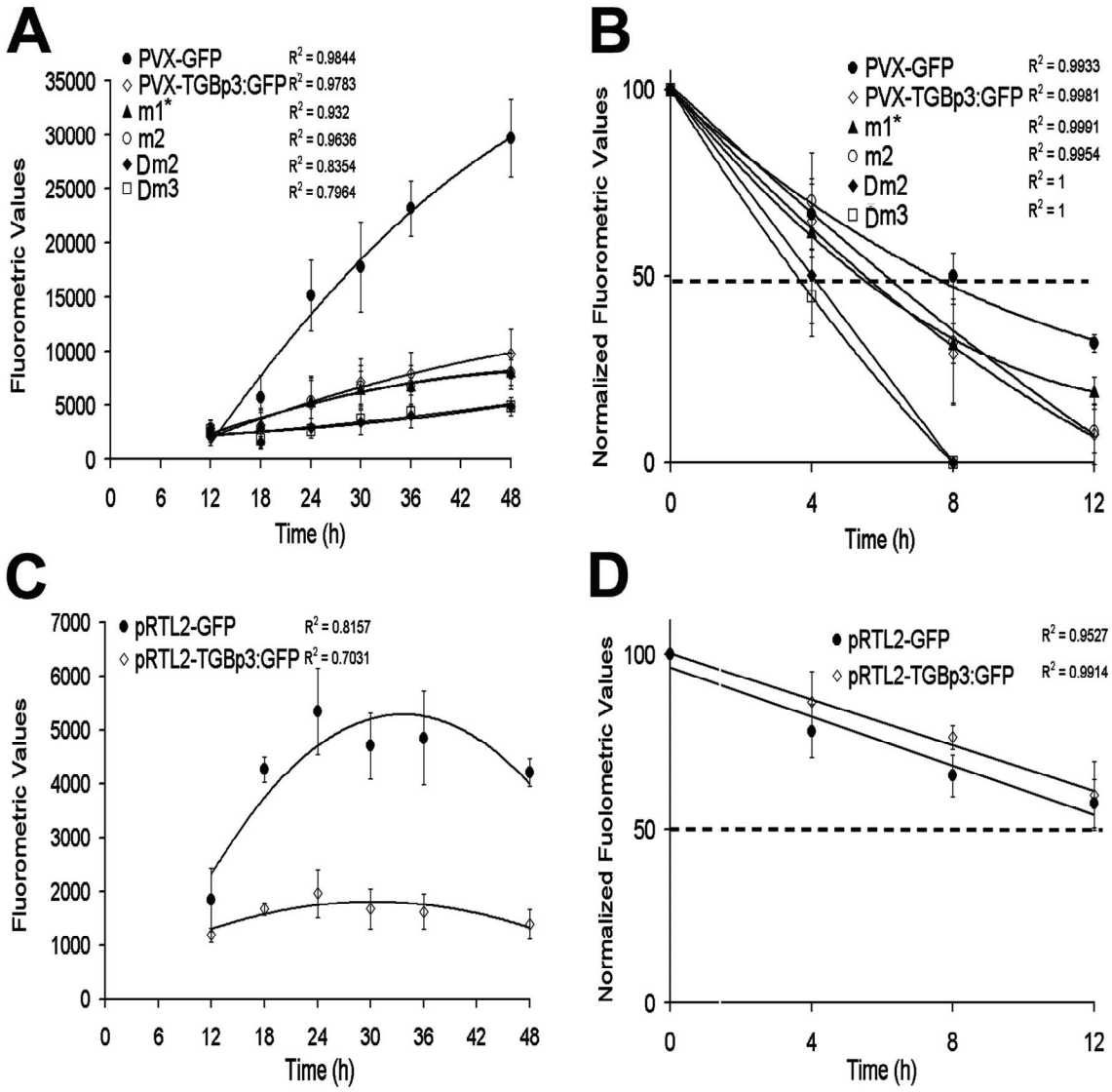

Figure 4. Fluorometric values of the GFP fluorescence in BY-2 protoplasts. Plots at each time point present the averages of three fluorometric values. Names of the viruses and pRTL2 plasmids were indicated in each graph. R^2 values for each trend line are provided. A, The GFP fluorescence values were measure in protoplasts between 18 and 48 h after viral transcription electroporation. Best fit graphs were drawn using polynomial or linear regression (R^2). B, Viral transcription electroporated protoplasts were treated with cycloheximide at 24 hpt considering time 0. The fluorometric values

were normalized to the fluorometric value acquired at time 0 and then plotted to estimate protein half-lives. C, The GFP fluorescence values were measure in protoplasts between 18 and 48 h after pRTL2 plasmids were electroporated. D, pRTL2 plasmid electroporated protoplasts were treated with cycloheximide at 24 hpt considering time 0. The fluorometric values were normalized to fluorometric value acquired at time 0 and then plotted to estimate protein half-lives.

This result is expected because the two viruses express GFP from different viral promoters, which produce significantly different levels of subgenomic RNAs. In PVX-GFP the GFP coding sequence is expressed from a monocistronic RNA synthesized from the CP subgenomic promoter, while the TGBp3:GFP fusion is expressed from the bicistronic subgenomic RNA2, which is synthesized by an alternative subgenomic promoter. Subgenomic RNA2 accumulates to significantly lower levels than does subgenomic RNA derived from the CP subgenomic promoter (Chapman et al., 1992b; Kim and Hemenway, 1996; Verchot et al., 1998). TGBp3:GFP is expressed by leaky ribosomal scanning through the TGBp2 coding sequence (Verchot et al., 1998).

Following cycloheximide treatment, the decrease related fluorescence was somewhat different in PVX-GFP and PVX-TGBp3:GFP, suggesting that the stability of GFP is slightly altered by fusion to the TGBp3 protein (Fig. 4B). The half-lives of GFP and TGBp3:GFP proteins were 7.4 and 5.5 h, respectively. The calculated half-lives of TGBp3m1*:GFP and TGBp3m2:GFP were 5.3 and 6.1 h, respectively. The endpoints of the GFP, TGBp3:GFP, TGBp3m1*:GFP, TGBp3:m2:GFP trend lines stretched beyond 12h. By comparing the half lives for PVX-TGBp3m1*:GFP and PVX-TGBp3m2:GFP with the half lives for PVX-GFP and PVX-TGBp3:GFP, it appears that the m1* and m2 mutations did cause a reduction in the steady state level of TGBp3:GFP. The trend lines for PVX-TGBp3Dm2:GFP and –TGBp3Dm3:GFP declined more rapidly than those of PVX-GFP or PVX-TGBp3:GFP. TGBp3Dm2:GFP and TGBp3Dm3:GFP fluorescence was negligible at 8h. The calculated half-lives of TGBp3Dm2:GFP and TGBp3Dm3:GFP were 4.0 and 3.6 h, respectively. Thus the Dm2 and Dm3 mutations were responsible for reduced steady state levels of TGBp3:GFP during virus infection. It

is possible that changes in TGBp3 steady state levels during virus infection may be a factor delaying PVX cell-to-cell and vascular movement.

We also transfected protoplasts with pRTL2-GFP and –TGBp3:GFP. Previous studies of GFP:TGBp2 showed that protein turnover was enhanced by PVX infection when we compared the half-lives of the GFP and GFP:TGBp2 proteins expressed from the PVX genome with the half lives calculated for proteins expressed from pRTL2 plasmids. In this study we found that GFP and TGBp3:GFP expression increased between 12 and 24 h. The fluorescence values reached a plateau or declined somewhat after 24 h (Fig 4C). Samples were treated with cycloheximide at 24 h and fluorometric values were measured at 0, 4, 8, 12 h after cycloheximide treatment. The calculated half lives of GFP and TGBp3:GFP were 13 and 15 h. In this study the half life of GFP, when expressed from pRTL2 plasmids, was almost twice the calculated half life when expressed from the PVX genome. The half-life of TGBp3:GFP, when expressed from pRTL2 plasmids ,was 2.7-fold greater than the calculated half-life when expressed from the PVX genome. These data suggest that, as in the previous study of PVX TGBp2, PVX infection enhanced TGBp3:GFP turnover (Ju et al., 2005). Since both TGBp2 and TGBp3 associate with ER membranes it is reasonable to consider that both proteins are targeted by ERAD for degradation.

DISCUSSION

This study explores subcellular accumulation of TGBp3 during virus infection. In this study GFP gene was fused to the 3' end of the endogenous TGBp3 coding sequence and the recombinant virus was inoculated to plants. TGBp3:GFP fluorescence was

reported to accumulate in the ER, granular bodies associated with the ER, perinuclear masses, and the nucleus. Previous reports used CaMV 35S containing plasmids to express a GFP:TGBp3 fusion in which GFP was fused to the 5' end of the PVX TGBp3 coding sequence. Subcellular accumulation of the fusion was first studied in the absence of virus infection using confocal and electron microscopy (Krishnamurthy et al., 2003, Ju et al., 2005). In the absence of virus infection GFP:TGBp3 was seen in the ER. When PVX and pRTL2-GFP:TGBp3 plasmids were codelivered to tobacco leaves, the fusion was also seen in large peripheral bodies accumulating along the cell wall (Schepetilnikov et al., 2005). These peripheral bodies were shown in recent studies of PVX and BNYVV to be cytopathic structures that are contain short fragments of ER membranes (Erhardt et al., 2005; Schepetilnikov et al., 2005). The complex pattern of TGBp3:GFP accumulation during virus infection suggests that TGBp3 may provide activities for different steps of the PVX infection cycle, or its role in promoting PVX cell-to-cell movement may involve directing viral RNA between multiple subcellular compartments.

When TGBp3:GFP was expressed from pRLT2 plasmids or the PVX genome, fluorescence was seen in the ER and granular bodies associated with the ER (compare Fig 2,B, C and 2,F, G). A similar subcellular accumulation pattern was reported for PVX-GFP:TGBp2, suggesting that these two proteins colocalize during virus infection (Ju et al., 2005, Samuels et al., submitted). When CFP:TGBp2 and TGBp3:GFP were co-expressed in tobacco leaves, the two fusion proteins colocalize in the same granular bodies (Samuels et al., submitted). We previously showed that TGBp2 induces these granular bodies to bud from the ER in the absence of virus infection. When we compare tobacco protoplasts expressing pRTL2-GFP:TGBp2 and -TGBp3:GFP the granular

bodies are abundant in GFP:TGBp2 expressing cells, while we see fewer granular bodies in TGBp3:GFP expressing cells (Samuels et al., submitted). Thus both proteins may have the ability to target to the same granular vesicles although TGBp2 has the particular ability to stimulate abundant vesicle formation.

The m1* mutation used in this study was similar to the m1 mutation reported by Krishnamurthy et al., 2003, except that in the earlier study the m1 mutation also eliminated the TGBp2 stop codon (replacing TAG with AAG) when it was introduced into the PVX genome. GFP:TGBp3m1, when expressed from pRTL2 plasmids, was cytosolic and PVX-GFP-TGB3m1 was restricted to single cells (Krishnamurthy et al., 2003). In this study the m1* mutation replaced 9 TGBp3 nucleotides without impacting the TGBp2 stop codon (see Materials and Methods). To our surprise the m1* mutation did not completely eliminate PVX-TGBp3:GFP cell-to-cell movement. The m1* eliminated TGBp3:GFP accumulation in the ER and granular bodies, but did not affect fluorescence accumulation in the nucleus and perinuclear masses in cells located at the front of PVX-TGBp3m1*:GFP infection foci. However, we detected fluorescence in the cortical ER, granular bodies, perinuclear masses, and nucleus in cells at the center of the infection site. The negative effect of the m1 mutation reported by Krishnamurthy et al. (2003) on PVX cell-to-cell movement might have been the result of its effects on TGBp2 and TGBp3 expression. Although we cannot rule out that the m1* mutation may have impacted both TGBp2 and TGBp3, the results of this mutation were slightly different from the m1 mutation reported previously (Krishnamurthy et al., 2003). The m1* mutation caused a delay in TGBp3:GFP accumulation in the cortical ER and granular bodies but did not impact fluorescence accumulation in the nucleus and perinuclear

masses. These data suggest that TGBp3:GFP targets the nucleus and perinuclear masses first during virus infection and later associates with the cortical ER and granular bodies. Fluorescence in PVX-TGBp3m1*:GFP was seen 3 d later than PVX-TGBp3 or PVX-GFP in inoculated leaves. The delay in fluorescence accumulation in the cortical ER and granular bodies correlates with a delay in virus movement, suggesting that TGBp3 association with these two subcellular compartments is necessary for optimal cell-to-cell movement. The delay in TGBp3m1*:GFP association with the cortical ER and granular bodies may explain the reduce diameter of the infection foci seen at 7 dpi. The m1* mutation did not reduced the steady state levels of TGBp3:GFP during PVX infection (Fig 4) indicating the m1* mutation specifically affects protein subcellular targeting.

The m2, Dm2, and Dm3 mutations introduced into the PVX-TGBp3:GFP gene were shown here and in a prior study to inhibit virus systemic movement (Krishnamurthy et al., 2003). Each mutation lies in the C-terminal cytosolic domain of TGBp3. The m2 mutation is a substitution mutation near the center of the protein and has little effect on the subcellular targeting or steady state level of TGBp3:GFP during virus infection. The TGBp3Dm2:GFP and TGBp3Dm3:GFP lack32 and 13 amino acids from the C-terminal domain of TGBp3 and have much shorter half-lives than wild-type TGBp3:GFP during virus infection. TGBp3Dm2:GFP and TGBp3Dm3:GFP fluorescence was negligible by 8 hpi, while TGBp3:GFP fluorescence remained measurable at 12 hpi. PVX-TGBp3Dm2:GFP and PVX-TGBp3Dm3:GFP infection sites were at least half the diameter of PVX-TGBp3:GFP infection sites measured at 7 dpi (Table 1). Changes in TGBp3:GFP stability due to the Dm2 and Dm3 mutations correlate with reduced virus movement, suggesting that protein stability might impact the extent of virus spread.

PVX-TGBp3Dm2:GFP or PVX-TGBp3Dm3:GFP infection sites showed two patterns of fluorescence at both the infection fronts and infection centers. The two fluorescent patterns were randomly distributed among neighboring cells providing no evidence of temporal changes in TGBp3:GFP accumulation. Some cells showed fluorescence in the polygonal ER network, granular bodies, perinuclear masses, and nucleus while other cells showed fluorescence in the cytoplasm, granular bodies, perinuclear masses, perinuclear ER, and nucleus (Fig. 3). The uncertain distribution of fluorescence in PVX-TGBp3Dm2:GFP and –TGBp3Dm3:GFP infected cells led us to speculate that the mutations may reduced the ability of TGBp3 to stably interact with the ER. If we compare the results of the m1*, Dm2, and Dm3 mutations, the results presented in this study show that mutations altering the ability of TGBp3 to associate with the ER also delay or reduce the ability of PVX-TGBp3:GFP to move from cell-to-cell.

With respect to PVX-TGBp3Dm2:GFP and –TGBp3Dm3:GFP, the presence of fluorescence in the cytoplasm and inconsistent pattern of fluorescence in the ER in some cells might be the result of reduced protein stability caused by these mutations. We previously reported cytoplasmic fluorescence in PVX-GFP:TGBp2 infected cells which was not detected in pRTL2-GFP:TGBp2 expressing cells. When we compared protein-turnover in PVX-GFP:TGBp2 and pRTL2-GFP:TGBp2 transfected protoplasts following cycloheximide treatment, we found that the half-life of GFP:TGBp2 was reduced 3-fold as the result of PVX infection (Ju et al., 2005). These data led us to speculate that PVX infection triggered ER associated protein degradation (ERAD). In this model GFP:TGBp2 was exported from the ER into the cytoplasm for degradation during virus

infection (Ju et al., 2005). Since TGBp3Dm2:GFP and TGBp3Dm3:GFP were sometimes cytosolic and showed reduced half-lives in comparison to TGBp3:GFP during virus infection, it is possible that the mutant TGBp3:GFP proteins were degraded by ERAD. Furthermore, comparing protein-turnover in PVX-TGBp3:GFP and pRTL2-TGBp3:GFP transfected protoplasts following cycloheximide treatment, we found that the half-life of TGBp3:GFP was reduced 3-fold as the result of PVX infection. Thus it is reasonable to speculate that ERAD may also play a role in TGBp3:GFP turnover. In this case the Dm2 and Dm3 mutations may have exacerbated protein turnover causing an increase in cytosolic fluorescence as well as reduced protein half-lives.

In a related study, we reported evidence of cytosolic and nuclear accumulation of GFP:TGBp2 during virus infection and suggested that this relates to the increased levels of protein turnover observed in protoplasts infected with PVX (Ju et al., 2005, Brandizzi et al., 2003). Both GFP and GFP:TGBp2 proteins had shorter half-lives when they were expressed from the PVX genome than when they were expressed from pRTL2 plasmids. We proposed that either PVX infection, PVX RNA, or other PVX proteins stimulated protein degradation. Since TGBp3:GFP also has a shorter half-life when expressed from the PVX genome then when expressed from pRTL2 plasmids, it is likely that TGBp3 is not the factor triggering protein turnover. It is more likely that other viral factors, or combinations of viral proteins can stimulate ER stress responses such as protein export from the ER and protein degradation by the 26S proteasome (ER-associated protein degradation) (Navazio et al., 2001; Martinez and Chrispeels, 2003; Smalle and Vierstra, 2004; Kirst et al., 2005).

The TMV movement protein and the *Turnip yellow mosaic virus* (TYMV) movement proteins are degraded by the 26S proteasome (Reichel and Beachy, 2000; Drugeon and Jupin, 2002; Gillespie et al., 2002). In the case of TMV, protein degradation by the 26S proteasome regulates virus movement across the plasmodesmata (Reichel and Beachy, 2000; Gillespie et al., 2002). In fact, a TMV movement protein that was modified by DNA shuffling showed improved transport functions due to its ability to evade proteasome degradation (Gillespie et al., 2002). Protein degradation by the 26S proteasome helps to maintain the integrity of the ER and restore homeostasis in the cell (Reichel and Beachy, 2000). In a prior study we reported evidence that GFP:TGBp2 has a longer half-life than GFP in pRTL2-transfected protoplasts suggests that TGBp2 has an ability to evade the proteasome or other protein degradation machinery, thereby moving across the plasmodesmata (Reichel and Beachy, 2000). This was suggested to account for cytosolic accumulation of TGBp2 late in infection. Since we do not detect TGBp3:GFP in the cytoplasm in PVX infected cells, it may not have the same ability to evade the proteasome. In addition, Figure 4 shows that TGBp3:GFP and GFP have similar half-lives in pRTL2-transfected protoplasts, suggesting that it may not have the same ability as TGBp2 to evade the hosts degradation machinery. Thus, TGBp2 and TGBp3 may be differently affected by ER stress.

If both TGBp2 and TGBp3 are components of the movement complex trafficking across the plasmodesmata, results of this study do not support the model that the viral movement complex evades degradation by the 26S proteasome by moving across the plasmodesmata (Reichel and Beachy, 2000; Drugeon and Jupin, 2002; Gillespie et al., 2002).

MATERIALS AND METHODS

Bacterial Strains and Plasmids

All plasmids (Fig. 1) were prepared from *Escherichia coli* strains JM 109, DH5α, and XL10Gold, transformed using standard cloning techniques (Sambrook et al., 1989). The pPVX-GFP, pPVX-TGBp3:GFP, - TGBp3m1*:GFP, - TGBp3m2:GFPP, -Dm2:GFP, and -Dm3:GFP plasmids contain the PVX genome and enhanced GFP (eGFP) gene with the bacteriophage T7 promoter (Baulcombe et al., 1995). The plasmid pPVX-GFP contains the intact PVX genome and the eGFP coding sequence (Clontech, Palo Alto, CA) next to a duplicated coat protein subgenomic promoter described by Ju et al.,(2005). The plasmid pPVX-TGBp3:GFP and its mutant plasmids contain the eGFP coding sequence fused to the 3' end of the TGBp3 or TGBp3 mutant coding sequences, respectively.

The plasmid pPVX-TGBp3:GFP was constructed by removal of the non-coding sequences between the TGBp3 and EGFP gene in pPVX-GFP (Fig. 1). A forward 25K primer (CTT AGA GAT TTG AAT AAG ATG GAT ATT CTC ATC AC) overlapping the TGBp1 start codon (underlined), a reverse 8K primer (CAT GAT CGA TGC TAG ATG GAA ACT TAA CCG TTC) overlapping the 3' end of TGBp3 and containing a *Cla*I restriction site (underlined), and pPVX-GFP were used to PCR amplify the TGB coding sequence. pGEM-TGB was made by ligating the gel purified PCR products with pGEM-T Easy Vector (Promega, Madison, WI). The pGEM-TGB and pPVX-GFP plasmids were digested using *Apa*I and *Cla*I restriction enzymes and then ligated to make pPVX-TGBp3:GFP.

The plasmids pPVX-TGBp3m1*:GFP and –TGBp3m2:GFP have separate substitution mutations. Nine nts between positions 5483 and 5493 (GCA GTC ATT), coding Ala-Val-Ile, were replaced with 9 nts (AGT CGA CCT) coding Ser-Arg-Pro to make pPVX-TGBp3m1:GFP and 9 nts between positions 5531 and 5541 (ATT ACT GGG), encoding Ile-Thr-Gly, were replaced with 9 nts (AGT CGA CCA) encoding Ser-Arg-Pro to make pPVX-TGBp3m2:GFP (Krishnamurthy et al., 2003). To prepare pPVX-TGBp3m1:GFP and –TGBp3m2:GFP the 25K forward and 8K reverse primers, described above, were used to PCR amplify the TGB coding sequence. The PCR products and pPVX-TGBp3:GFP plasmids were digested using *Apa*I and *Cla*I restriction enzymes and then ligated. The initial m1 mutation reported by Krishnamurthy et al., (2003) (AGT CGA CCA AG) also eliminated the TGBp2 stop codon (underlined). The m1* mutation was prepared to restore the TGBp2 stop codon (AGT CGA CCT AG) and retain the Ser-Arg-Pro coding sequences. The QuickChange II XL Site-Directed Mutagenesis Kit, M1 forward primer (GTA ACA ATC ATA AGT CGA CCT AGC ACT TCC TTA) and M1 reverse primer (TAA GGA AGT GCT AGG TCG ACT TAT GAT TGT TAC) were used to replace A with T (Stratagene, La Jolla, CA) (Chapter 3).

For the pPVX-TGBp3Dm2:GFP, sequences between nt position 5531 and 5637 were deleted in pPVX-TGBp3:GFP and 9 nts (AGT CGA CCA), encoding Ser-Arg-Pro were inserted (Krishnamurthy et al., 2003). The sequences between nt position 5588 and 5637 were deleted in pPVX-TGBp3:GFP and 9 nts (AGT CGA CCA), encoding Ser-Arg-Pro, were inserted (Krishnamurthy et al., 2003). To prepare PVX-TGBp3Dm2:GFP and -TGBp3Dm3:GFP, the DM2 reverse primer (CATGAT CGA TGC TAG TGG TCG ACT CTT GAT GAC ACA AGG TTC AG) or DM3 reverse primer (CAT GAT CGA

TGC TAG TGG TCG ACT CCT TAT GGT TTC TGC ATC TA) containing *Cla*I restriction sites (underlined) were used to amplify the mutant TGB coding sequences, respectively. The PCR products and pPVX-TGBp3:GFP plasmids were digested using *Apa*I and *Cla*I restriction enzymes and then ligated.

The plasmid pRTL2-TGBp3:GFP has sequences encoding fusion GFP, which was fused to the 3' end of the TGBp3 gene with the *Cauliflower mosaic virus* (CaMV) 35S promoter and *Tobacco etch virus* (TEV) translational enhancer region (Carrington and Freed, 1990). The TGBp3:GFP coding sequences were PCR amplified using pPVX-TGBp3:GFP plasmid, a forward primer overlapping the 5' end of TGBp3 (GCG CCG CCA TGG AAG TAA ATA CAT AT), and a reverse primer overlapping the 3' end of GFP (GGC CGG ATC CTT ACT TGT ACA GCT CG). The forward primer contains an additional *Nco*I restriction site while the reverse primer contains an additional *Bam*HI restriction site (underlined). The PCR products and the pRTL2 plasmid were digested using *Nco*I and *Bam*HI restriction enzymes, gel purified, and ligated to create the pRTL2-TGBp3:GFP plasmid (Samuels et al., submitted). The pBIN-mGFP5-ER plasmid containing *Cauliflower mosaic virus* (CaMV) 35S promoter and coding sequences for ER-targeting and retention signals was provided by Dr. J. Hasselof (Medical Research Council Laboratory of Molecular Biology, Cambridge, UK) (Haseloff et al., 1997).

***In Vitro* Transcription**

The pPVX-GFP, pPVX-TGBp3:GFP, -m1*:GFP, -m2:GFP, -Dm2:GFP, and -Dm3:GFP plasmids were linearized using *Spe*I restriction enzyme. One µg linearized plasmids were transcribed using the mMESSAGE mMACHINE^{TM} High Yield Capped

RNA Transcription Kit (Ambion, Inc., Austin, TX). Transcripts were directly used to inoculate either BY-2 protoplasts or tobacco plants dusted with carborundum.

Inoculation of Plants

Five µL of the PVX-GFP, PVX-TGBp3:GFP, -m1*:GFP, -m2:GFP, -Dm2:GFP, and -Dm3:GFP transcripts were inoculated on *Nicotiana benthamiana* plants dusted with carborundum to study virus movement. Virus movement for each infectious construct was obserbed with a hand held UV lamp and with laser scanning confocal microscopy. Leaf segments inoculated with PVX-GFP and PVX-TGBp3:GFP were treated with DAPI to visualize the nuclear regions and analyzed using laser scanning confocal microscopy (Ju et al., 2007).

Biolistic Bombardment of Tobacco Leaves

Biolistic bombardments were conducted for the transient expression of the pRTL2-GFP, -TGBp3:GFP, and, Bin-mGFP5-ER plasmids. DNA/gold mixtures were prepared by mixing 1µg plasmids mixed with 0.75mg of 1 µm gold particles (Bio-Rad Laboratories, Hercules, CA). DNA/gold mixtures were bombarded to detached *N. benthamiana* leaves using the PDS1000 He system (Bio-Rad Laboratories, Hercules, CA) (Krishnamurthy et al., 2003; Ju et al., 2005).

BY-2 Protoplast Preparation and Transfection

Transgenic BY-2 cells expressing mGFP5-ER were transformed using *Agrobacterium tumefaciens* strain LBA4404 containing pBIN19-mGFP5-ER plasmids and protoplasts from this cell line were used as a positive control for studying the TGBp3 association with ER (Hwang and Gelvin, 2004; Ju et al., 2007).

To isolate BY-2 protoplasts, 3 to 5 -day-old BY-2 suspension cells were collected and resuspended in an enzyme solution as previously described (Gaire et al., 1999; Qi and Ding, 2002; Ju et al., 2005; Ju et al., 2007).

Protoplasts were transfected with either infectious transcripts or pRTL2 plasmids (Gaire et al., 1999; Qi and Ding, 2002; Ju et al., 2005; Ju et al., 2007). Between 2 and 5 µl of transcripts or, 40 µg of plasmids plus 40 µg sonicated salmon sperm DNA were mixed with 0.5 mL of protoplasts (5 x 10^5 or 1 x 10^6 protoplasts) in a 0.4-cm gap cuvette (Bio-Rad Laboratories, Hercules, CA) on ice. Protoplasts were electroporated using a Gene Pulser (Bio-Rad Laboratories) with 0.25 kV, 100, and 125 µF (Gaire et al., 1999; Qi and Ding, 2002; Ju et al., 2005; Ju et al., 2007). Protoplasts cultured at 26°C were observed using laser scanning confocal microscopy or collected at various time intervals for fluorometric assays (Gaire et al., 1999; Qi and Ding, 2002; Ju et al., 2005; Ju et al., 2007).

Microscopy and Image Processing

A Leica TCS SP2 imaging system attached to a Leica DMRE upright microscope (Leica Microsystems, Bannockburn, IL) was used. UV and krypton/argon lasers were used to observe fluorescence due to DAPI staining or GFP expression (Molecular Probes Inc., Eugene, OR). Images were processed and compiled using Adobe Photoshop CS software (Adobe Systems Inc., San Jose, CA) (Krishnamurthy et al., 2002; Krishnamurthy et al., 2003; Ju et al., 2005; Ju et al., 2007).

Fluorometric Assays and Cycloheximide Treatment of BY-2 Protoplasts

For the fluorometric assay, 1 x 10^6 transfected protoplasts were collected at 12, 18, 24, 30, 36, and 48 h post transfection by centrifugation at 59g for 5 min as described

by Ju et al., (2005). Cycloheximide (500 μM; Sigma, St. Louis, MO) was added to the protoplast medium at 24 h post electroporation. Protoplasts were collected at 4, 8, and 12 h following the cycloheximide treatment by centrifugation at 59g for 5 min. Collected protoplasts were ground using 100 μL of protein grinding buffer (10 mM Tris-HCl pH 7.5, 100 mM NaCl, 1 mM MgCl2, and 10 mM DDT), repeating twice, vortexing for 1 min, sonicating for 10 min, freezing at -80^{o}C for 10 min, and thawing at room temperature. By centrifugation at 3000g for 10 min, protoplast debris was removed. Fluorescence values of the supernatants were measured using a VICTOR2D fluorometer (Perkin-Elmer, Boston, MA) and the average values at each time point were plotted using Microsoft Office Excel 2003 software (Microsoft Corp., Redmond, WA) (Ju et al., 2005; Ju et al., 2007).

ACKNOWLEDGEMENTS

I appreciate the assistance of Dr. T. Samuel, who made PVX-TGBp3:GFP. I thank Drs. J. Fletcher and S. Marek for use of their electroporation systems and Dr. J. Malayer for use of fluorometer. I also thank Mr. T Colberg for training and assistance with the confocal microscope located at the Oklahoma State University Electron Microscopy Center.

LITERATURE CITED

Angell SM, Davies C, Baulcombe DC (1996) Cell-to-cell movement of *Potato virus X* is associated with a change in the size-exclusion limit of plasmodesmata in trichome cells of *Nicotiana clevelandii*. Virology **216:** 197-201

Atabekov JG, Rodionova NP, Karpova OV, Kozlovsky SV, Poljakov VY (2000) The movement protein-triggered in situ conversion of *Potato virus X* virion RNA from a nontranslatable into a translatable form. Virology **271:** 259-263

Baulcombe DC, Chapman S, Santa Cruz S (1995) Jellyfish green fluorescent protein as a reporter for virus infections. Plant J **7:** 1045-1053

Bayne EH, Rakitina DV, Morozov SY, Baulcombe DC (2005) Cell-to-cell movement of *Potato virus X* is dependent on suppression of RNA silencing. Plant J **44:** 471-482

Beck DL, Guilford PJ, Voot DM, Andersen MT, Forster RL (1991) Triple gene block proteins of *White clover mosaic potexvirus* are required for transport. Virology **183:** 695-702

Brandizzi F, Hanton S, DaSilva LL, Boevink P, Evans D, Oparka K, Denecke J, Hawes C (2003) ER quality control can lead to retrograde transport from the ER lumen to the cytosol and the nucleoplasm in plants. Plant J **34:** 269-281

Carrington JC, Freed DD (1990) Cap-independent enhancement of translation by a plant potyvirus 5' nontranslated region. J Virol **64:** 1590-1597

Chapman S, Hills G, Watts J, Baulcombe D (1992a) Mutational analysis of the coat protein gene of *Potato virus X*: Effects on virion morphology and viral pathogenicity. Virology **191:** 223-230

Chapman S, Kavanagh T, Baulcombe D (1992b) *Potato virus X* as a vector for gene expression in plants. Plant J **2:** 549-557

Drugeon G, Jupin I (2002) Stability in vitro of the 69K movement protein of *Turnip yellow mosaic virus* is regulated by the ubiquitin-mediated proteasome pathway. J Gen Viol*:* **83** 3187-3197

Erhardt M, Vetter G, Gilmer D, Bouzoubaa S, Richards K, Jonard G, Guilley H (2005) Subcellular localization of the Triple Gene Block movement proteins of *Beet necrotic yellow vein virus* by electron microscopy. Virology **340:** 155-166

Forster RLS, Beck DL, Guilford PJ, Voot DM, Van Dolleweerd CJ, Andersen MT (1992) The coat protein of *White clover mosaic potexviru*s has a role in facilitating cell-to-cell transport in plants. Virology **191:** 480-484

Gaire F, Schmitt C, Stussi-Garaud C, Pinck L, Ritzenthaler C (1999) Protein 2A of *Grapevine fanleaf nepovirus* is implicated in RNA2 replication and colocalizes to the replication site. Virology **264:** 25-36

Gillespie T, Boevink P, Haupt S, Roberts AG, Toth R, Valentine T, Chapman S, Oparka KJ (2002) Functional analysis of a DNA-shuffled movement protein reveals that microtubules are dispensable for the cell-to-cell movement of *Tobacco mosaic virus*. Plant Cell **14:** 1207-1222

Gorbalenya AE, Koonin EV (1989) Viral proteins containing the purine NTP-binding sequence pattern. Nucleic Acids Res **17:** 8413-8440

Haseloff J, Siemering KR, Prasher DC, Hodge S (1997) Removal of a cryptic intron and subcellular localization of green fluorescent protein are required to mark transgenic Arabidopsis plants brightly. Proc Natl Acad Sci U S A **94:** 2122-2127

Haupt S, Cowan GH, Ziegler A, Roberts AG, Oparka KJ, Torrance L (2005) Two plant-viral movement proteins traffic in the endocytic recycling pathway. Plant Cell **17:** 164-181

Howard AR, Heppler ML, Ju HJ, Krishnamurthy K, Payton ME, Verchot-Lubicz J (2004) *Potato virus X* TGBp1 induces plasmodesmata gating and moves between cells in several host species whereas CP moves only in *N. benthamiana* leaves. Virology **328:** 185-197

Huisman MJ, Linthorst HJ, Bol JF, Cornelissen JC (1988) The complete nucleotide sequence of *Potato virus X* and its homologies at the amino acid level with various plus-stranded RNA viruses. J Gen Virol **69** 1789-1798

Hwang HH, Gelvin SB (2004) Plant proteins that interact with VirB2, the A*grobacterium tumefacien*s pilin protein, mediate plant transformation. Plant Cell **16:** 3148-3167

Ju HJ, Brown JE, Ye CM, Verchot-Lubicz J (2007) Mutations in the Central Domain of *Potato virus X* TGBp2 Eliminate Granular Vesicles and Virus Cell-to-Cell Trafficking. J Virol **81:** 1899-1911

Ju HJ, Samuels TD, Wang YS, Blancaflor E, Payton M, Mitra R, Krishnamurthy K, Nelson RS, Verchot-Lubicz J (2005) The *potato virus X* TGBp2 movement protein associates with endoplasmic reticulum-derived vesicles during virus infection. Plant Physiol **138:** 1877-1895

Kalinina NO, Fedorkin ON, Samuilova OV, Maiss E, Korpela T, Morozov SY, Atabekov JG (1996) Expression and biochemical analyses of the recombinant *Potato virus X* 25K movement protein. FEBS Letters **397:** 75-78

Kalinina NO, Rakitina DV, Solovyev AG, Schiemann J, Morozov SY (2002) RNA Helicase Activity of the Plant Virus Movement Proteins Encoded by the First Gene of the Triple Gene Block. Virology **296:** 321-329

Kim KH, Hemenway C (1996) The 5' nontranslated region of *Potato virus X* RNA affects both genomic and subgenomic RNA synthesis. J Virol **70:** 5533-5540

Kirst ME, Meyer DJ, Gibbon BC, Jung R, Boston RS (2005) Identification and characterization of endoplasmic reticulum-associated degradation proteins differentially affected by endoplasmic reticulum stress. Plant Physiol **138:** 218-231

Krishnamurthy K, Heppler M, Mitra R, Blancaflor E, Payton M, Nelson RS, Verchot-Lubicz J (2003) The *Potato virus X* TGBp3 protein associates with the ER network for virus cell-to-cell movement. Virology **309:** 135-151

Krishnamurthy K, Mitra R, Payton ME, Verchot-Lubicz J (2002) Cell-to-cell Movement of the PVX 12K, 8K, or coat proteins may depend on the host, leaf developmental stage, and the PVX 25K protein. Virology **300:** 269-281

Lawrence DM, Jackson AO (2001) Interactions of the TGB1 protein during cell-to-cell movement of Barley stripe mosaic virus. J Virol **75:** 8712-8723

Leshchiner AD, Solovyev AG, Morozov SY, Kalinina NO (2006) A minimal region in the NTPase/helicase domain of the TGBp1 plant virus movement protein is responsible for ATPase activity and cooperative RNA binding. J Gen Virol **87:** 3087-3095

Lough TJ, Lee RH, Emerson SJ, Forster RLS, Lucas WJ (2006) Functional analysis of the 5' untranslated region of potexvirus RNA reveals a role in viral replication and cell-to-cell movement. Virology **351:** 455-465

Lough TJ, Netzler NE, Emerson SJ, Sutherland P, Carr F, Beck DL, Lucas WJ, Forster RL (2000) Cell-to-cell movement of potexviruses: evidence for a ribonucleoprotein complex involving the coat protein and first triple gene block protein. Mol Plant Microbe Interact **13:** 962-974

Lough TJ, Shash K, Xoconostle-Cazares B, Hofstra KR, Beck DL, Balmori E, Forster RLS, Lucas WJ (1998) Molecular dissection of the mechanism by which potexvirus triple gene block proteins mediate cell-to-cell transport of infectious RNA. Mol Plant Microbe Interact **11:** 801-814

Martinez IM, Chrispeels MJ (2003) Genomic analysis of the unfolded protein response in Arabidopsis shows its connection to important cellular processes. Plant Cell **15:** 561-576

Mitra R, Krishnamurthy K, Blancaflor E, Payton M, Nelson RS, Verchot-Lubicz J (2003) The *Potato virus X* TGBp2 protein association with the endoplasmic reticulum plays a role in but is not sufficient for viral cell-to-cell movement. Virology **312:** 35-48

Navazio L, Mariani P, Sanders D (2001) Mobilization of Ca2+ by cyclic ADP-ribose from the endoplasmic reticulum of cauliflower florets. Plant Physiol **125:** 2129-2138

Qi Y, Ding B (2002) Replication of Potato spindle tuber viroid in cultured cells of tobacco and *Nicotiana benthamiana*: the role of specific nucleotides in determining replication levels for host adaptation. Virology **302:** 445-456

Reichel C, Beachy RN (2000) Degradation of *Tobacco mosaic virus* movement protein by the 26S proteasome. J Virol **74:** 3330-3337

Rodionova NP, Karpova OV, Kozlovsky SV, Zayakina OV, Arkhipenko MV, Atabekov JG (2003) Linear remodeling of helical virus by movement protein binding. J Mol Biol **333:** 565-572

Sambrook J, Fritch EF, Mantiatis T (1989) Molecularcloning: A laboratory mamual, 2nd ed. Cold Spring Horbor Press, Cold Spring Horbor, NY

Samuels TD, Ju, H-J, Ye, C-H, Howard, A, Blancaflor, E, Verchot-Lubicz, J (2007) The Potato virus X TGBp1protein accumulaton independent of TGBp2 and TGBp3 to promote virus cell-to-cell (Summitted)

SantaCruz S, Roberts AG, Prior DA, Chapman S, Oparka KJ (1998) Cell-to-cell and phloem-mediated transport of *Potato virus X*. The role of virions. Plant Cell **10:** 495-510

Schepetilnikov MV, Manske U, Solovyev AG, Zamyatnin AA, Jr., Schiemann J, Morozov SY (2005) The hydrophobic segment of *Potato virus X* TGBp3 is a major determinant of the protein intracellular trafficking. J Gen Virol **86:** 2379-2391

Skryabin KG, Morozov S, Kraev AS, Rozanov MN, Chernov BK, Lukasheva LI, Atabekov JG (1988) Conserved and variable elements in RNA genomes of potexviruses. FEBS Lett **240:** 33-40

Smalle J, Vierstra RD (2004) The ubiquitin 26S proteasome proteolytic pathway. Annu Rev Plant Biol **55:** 555-590

Solovyev AG, Stroganova TA, Zamyatnin AA, Jr., Fedorkin ON, Schiemann J, Morozov SY (2000) Subcellular sorting of small membrane-associated triple gene block proteins: TGBp3-assisted targeting of TGBp2. Virology **269:** 113-127

Verchot J, Angell SM, Baulcombe DC (1998) In vivo translation of the triple gene block of *Potato virus X* requires two subgenomic mRNAs. J Virol **72:** 8316-8320

Voinnet O, Lederer C, Baulcombe DC (2000) A viral movement protein prevents spread of the gene silencing signal in *Nicotiana benthamiana*. Cell **103:** 157-167

Yang Y, Ding B, Baulcombe DC, Verchot J (2000) Cell-to-cell movement of the 25K protein of *Potato virus X* is regulated by three other viral proteins. Mol Plant Microbe Interact **13:** 599-605

Zamyatnin AA, Jr., Solovyev AG, Savenkov EI, Germundsson A, Sandgren M, Valkonen JP, Morozov SY (2004) Transient coexpression of individual genes encoded by the triple gene block of *Potato mop-top virus* reveals requirements for TGBp1 trafficking. Mol Plant Microbe Interact **17:** 921-930

VITA

HO-JONG JU

Candidate for the Degree of

Doctor of Philosophy or Other

Thesis: SUBCELLULAR LOCALIZATION AND ROLE OF POTATO VIRUS X (PVX) TGBp2 AND TGBp3 IN VIRUS MOVEMENT

Major Field: Plant Pathology

Biographical:

Personal Data: Born in Cheonbook, Republic of Korea on May 25, 1969, the son of Jaenam Ju and Soonduck Kim. Married to Soogyeong Oh on November 9, 1997. Have three children, Seoyeon, Seungyeon, and Chungyeon

Education: Received a Bachelor of Science degree in Agronomy from Kon-Kuk University, Seoul, Republic of Korea in Febrary 1995. Received a Master of Science degree in Agronomy from Kon-Kuk University, Seoul, Republic of Korea in Febrary 1997. Received a Master of Science degree in Crop and Soil Sciences from University of Georgia, Athens, Georgia in August 2003. Completed the requirements for the degree of Doctor of Philosophy in Plant Pathology at Oklahoma State University in May 2007.

Experience: Worked as a graduate research assistant in Department of Crop Scinece, Kon-Kuk University from 1993 to 1998. Worked as a graduate research assistant in Department of Crop and Soil Sciences, University of Georgia from 1999 to 2003. Worked as a graduate research assistant in Department of Entomology and Plant Pathology, Oklahoma State University from 2003 to 2006.

Professional Memberships: Member of American Society for Virology.

Name: Ho-Jong Ju Date of Degree: May, 2007

Institution: Oklahoma State University Location: Stillwater, OK

Title of Study: SUBCELLULAR LOCALIZATION AND ROLE OF *POTATO VIRUS X* (PVX) TGBp2 AND TGBp3 IN VIRUS MOVEMENT

Pages in Study: 163 Candidate for the Degree of Doctor of Philosophy

Major Field: Plant Pathology

Scope and Method of Study: The objectives of this research were to explore the functions of *Potato virus X* (PVX) TGBp2 and TGBp3. The green fluorescent protein (GFP) was fused to the PVX TGBp2 or TGBp3 coding sequences and the fusions were inserted into PVX genomes or plasmids. Confocal microscopy was then used to study subcellular accumulation patterns of the fusion proteins in the presence and absence of virus infection. Mutations were introduced into the TGBp2 and TGBp3 coding sequences to identify domains controlling protein subcellular targeting. During the course of this thesis I established a system for studying PVX infection using BY-2 tobacco suspension cells. I also developed a fluorometric assay to measure turnover of GFP containing fusion proteins.

Findings and Conclusions: Novel TGBp2 induced vesicles were identified. These are ER-derived structures which are important for virus cell-to-cell movement. A central conserved amino acid sequence in PVX TGBp2 was shown to modulate vesicle morphology. Substitution of only a single amino acid was sufficient to change vesicle morphology, increase TGBp2 association with the ER, and inhibit PVX movement. A single mutation disrupting ER association of TGBp3, inhibited PVX cell-to-cell movement. Mutations near the C-terminus of TGBp3 delayed PVX cell-to-cell movement and inhibited vascular transport. These data indicate that the C-terminal cytosolic domain plays a role in virus movement that has not been previously described. Degradation of GFP:TGBp2 and TGBp3:GFP is stimulated by virus infection. These observations led to a model suggesting that viral induced ER stress and protein degradation may be linked to virus cell-to-cell movement.

ADVISER'S APPROVAL: Dr. Jeanmarie Verchot-Lubicz